IDENTIFICATION AND CHARACTERIZATION OF PATHWAYS REGULATED BY KDM4B IN OVARIAN CANCER

BY

Cailin Wilson

Submitted to the graduate degree program in Pathology and Laboratory Medicine and the Graduate Faculty of the University of Kansas in partial fulfillment of the requirements of the degree of Doctor of Philosophy

_____

Co-chair: Adam J. Krieg, Ph.D.

_____

Co-chair: Jeremy Chien, Ph.D.

_____

Co-chair: Soumen Paul, Ph.D.

_____

Michael J. Soares, Ph.D.

_____

Katherine F. Roby, Ph.D.

_____

Nikki Cheng, Ph.D.

_____

Kenneth R. Peterson, Ph.D.

Date Defended: 10/4/2016

The Dissertation Committee for Cailin Wilson certifies that this is the approved version of the following dissertation:

IDENTIFICATION AND CHARACTERIZATION OF PATHWAYS REGULATED BY KDM4B IN OVARIAN CANCER

_____

Co-chair: Adam J. Krieg, Ph.D.

_____

Co-chair: Jeremy Chien, Ph.D.

_____

Co-chair: Soumen Paul, Ph.D.

Date Approved: 10/4/2016

ABSTRACT

KDM4B is a hypoxia-inducible, histone lysine demethylase responsible for primarily demethylating H3K9 and H3K36. This enzyme has been implicated in the literature as a contributor to tumorigenesis in many solid tumor models. Multiple factors contribute to the aggressiveness of ovarian cancer, including hypoxia-induced mechanisms. Establishing the tumorigenic mechanisms regulated by KDM4B provide novel epigenetic links between the hypoxic tumor microenvironment and Epithelial Ovarian Cancer (EOC) progression. This body of work established the *in vitro* and *in vivo* relevance of KDM4B in EOC, connecting expression to increased tumorigenesis. KDM4B is expressed in patient primary and metastatic tumors, correlating with hypoxic regions identified by CA-IX. Additionally, KDM4B is robustly induced in EOC cell lines exposed to hypoxia. KDM4B regulates expression of metastatic genes in a demethylase-dependent manner, including *LOXL2*, *LCN2*, and *PDGFB.* KDM4B expression correlates with increased ovarian cancer cell invasion, migration and attachment-free growth *in vitro*. Intraperitoneal xenograft models demonstrated KDM4B expression corresponded with increased peritoneal dissemination *in vivo*. Further mechanistic analysis has identified a possible link between KDM4B expression and another epigenetic regulator ARID5B. Functional analysis demonstrates KDM4B participates in secretion of factors contributing to metastasis and tumor progression. 3-Dimensional *in vitro* functional analysis suggests KDM4B contributes to increased spheroid invasion on Type I Collagen. This project highlights some of the first studies demonstrating that a Jumonji-domain histone demethylase regulates cellular processes required for peritoneal dissemination of EOC. The following observations provide additional knowledge regarding KDM4B activity and its influence in EOC models. These findings provide a better understanding of KDM4B, its activity, and the role it plays in regulating the epigenetic landscape in tumors. The mechanistic and functional pathways regulated by KDM4B may present novel opportunities to develop combinatorial therapies to improve existing therapies for EOC patients.

ACKNOWLEDGEMENTS

Undergoing a graduate education as involved as a PhD program would not be possible without guidance, support, camaraderie, and time from many people. I would like to thank my family for their unconditional love and support. My father and mother, Lee and Beth Wilson are my role models. Growing up on a farm in a tiny unincorporated town in southeast Kansas, they made sure I had every opportunity to succeed academically in an environment with limited resources. They have taught me the importance of hard work and never giving up. Because of them, I have developed the mentality that to achieve any goal, you must put in the time and hard work. I believe the world owes you nothing without effort in return. These instilled beliefs and work ethic have made a positive impact on my life and have driven me to become the best version of myself. I would also like to thank my sister Haley Wilson. She is one of my best friends. No matter how hard things got during my PhD, she was always there for me to make me see the good in each situation. Not to mention, she is a wizard at Adobe Photoshop and Illustrator as an architect and has provided me with assistance on this front. I also would like to thank my brother Tristan Wilson, my sister-in-law Andi Wilson, my niece Ruby, and nephews Miles and Ashton. They have always been there for me and I appreciate having their smiling faces in my life. I would also like to thank all of my Scottish community friends, including: Anna Oyler, Kyle Womelduff, Sarah McKee, Jarrod Wood, Matt Kline, and Neil Womelduff. We have grown very close through the years and without you, I would never have been able to get through this process. I could also not have gone through this process without my Pathology Department classmates, especially Wei Wang. She has been a good listening ear and friend for me during this process. I wish everyone I have depended on in my personal life nothing but happiness and success in the future.

I would like to thank my primary mentor Dr. Adam Krieg for supporting me and shaping my development as a scientist and an academic. He has challenged me to think critically and independently about science. He is a great teacher and always puts the needs of his students ahead of his own. Without his good nature and selflessness, I would not have been able to finish my PhD and I am forever grateful for this. I hope to carry his admirable qualities of a good teacher and scientist into my future research and

teaching endeavors. I want to thank my adoptive KU mentor, Dr. Jeremy Chien. He welcomed me into his lab group with open arms and provided a home for me during my last year of my PhD. I have learned a great deal from him and his lab members and I am forever grateful for his kindness. Special thanks to Dr. Mike Werle, Dr. Soumen Paul, and Dr. Diane Durham for stepping up to help me in my desperate time of need when Dr. Krieg left KU Med. Truly without their fortitude and student-first approach to academia, I would not have been able to complete our manuscript and my PhD project. I also want to thank all of my committee members for their support and understanding through this difficult experience.

As I have learned from Dr. Krieg, science does not happen in a bubble of isolation. Science will only drive forward as a team effort. My heartfelt thanks go out to the past members of the Krieg lab at KU Med, Dr. Lei Qiu and Yan Hong. This project would not have been possible without the time and scientific efforts of Dr. Krieg's former student Lei. She spent much time working on many aspects of this project as well as with the rest of our lab. Without her contributions, our manuscript would not have been possible. I would also like to thank Yan for her efforts and contributions to our project. Her knowledge of immunohistochemistry and animal work are second-to-none at KU Med and I am honored to have learned and worked with her. I would also like to thank the OBGYN department for providing me with resources and a space to work day in and day out. Our scientific progress would also not be possible without the support of Norma Turner. She has been a great resource and I am forever grateful for her help.

My gratitude also extends to our many collaborators on our central manuscript and otherwise. From the efforts of the KU Med Pathology department to Dr. Adam Krieg's collaborators and friends, I am forever grateful for your time, insight, and scientific contributions. There are too many people to name here, but they include Dr. Michael J. Soares, Dr. Damayanti Chakraborty, Dr. Osaama Tawfik, and Dr. Katherine Roby. Without your contributions, we would not be able to complete our initial paper. Lastly, I would like to thank Dr. Krieg's funding sources, including the KU COBRE grant, KU Cancer Biology Department, and the American Cancer Society and the many core facilities at KU med that made my education and project possible.

TABLE OF CONTENTS

LIST OF FIGURES

List of Figures

Chapter 3: INVESTIGATING MECHANISMS REGULATED BY KDM4B IMPLICATED IN EOC METASTASIS AND PERIOTONEAL DISSEMINATION *IN VITRO*

CHAPTER 1:

GENERAL INTRODUCTION

Epigenetic changes are well-established contributors to cancer progression. Aberrant epigenetic changes are potentially reversible and targetable for the fight against cancer progression. In this project, focus is on the role of the hypoxia-inducible, histone demethylase KDM4B in ovarian cancer progression and peritoneal dissemination. KDM4B provides a novel link between ovarian cancer tumorigenesis and the hypoxic tumor microenvironment. Until this project, KDM4B had not been studied in ovarian cancer progression and explains its mechanistic role in this tumor type. Understanding the role of KDM4B in ovarian cancer progression will help explain another facet of hypoxia-induced epigenetic changes.

Epigenetics

Epigenetics and Chromatin Structure

Epigenetics encapsulates mitotically and/or meiotically heritable changes that are reversible and do not alter the genetic code (Hancock, Dunne et al. 2015; Schuebel, Gitik et al. 2016). Epigenetic modifications can include methylation and hydroxymethylation of cytosines and other nucleotides, the shortening and lengthening of telomeres, and chromatin compacting and opening through histone modifications (Schuebel, Gitik et al. 2016). Chromatin is the complex of DNA and proteins that form chromosomes (Kouzarides 2007; Schuebel, Gitik et al. 2016). The nucleosome is the basic unit of chromatin (Fig 1.1). A single nucleosomes is composed of an octamer of the four core histone proteins (H3, H4, H2A, H2B) and is wrapped 1.6 times by 147 base pairs of DNA (Kouzarides 2007). The linker histone, H1 is also sits on top of each nucleosome to orient and guide compaction of higher order chromatin structures (Schuebel, Gitik et al. 2016). Core and linker histone proteins are globular except for their N-terminal tails, which have a large number of possible residue modifications (Kouzarides 2007; Shmakova, Batie et al. 2014; Hancock, Dunne et al. 2015). Histone modifications influence the compaction state of chromatin. The modifications are very dynamic and can change chromatin quickly between heterochromatin (silenced state) and euchromatin (active state) (Shmakova, Batie et al. 2014). The types and locations of histone modifications are numerous, each providing a different alteration to chromatin compaction and gene expression. These post-translational histone modifications include:

acetylation, methylation, phosphorylation, ubiquitination, sumoylation, ADP ribosylation, deamination, and proline isomerization (Kouzarides 2007). Methylation is of particular interest for this body of work, focused on the study of the histone demethylase, KDM4B.

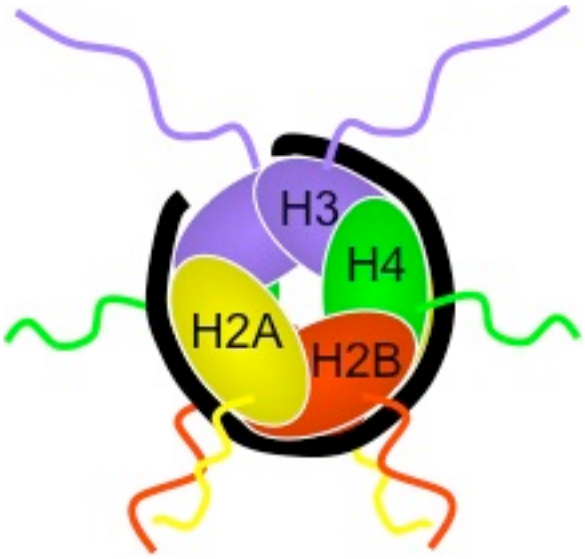
H3
H4
H2A
H2B

Figure 1.1 Histone Protein Structure

Histones are proteins that organize DNA within the nucleus. Two copies of each core histone, H2A, H2B, H3, and H4 form an octamer. This octamer is wrapped 1.6 times by 146 bp of DNA (not shown), forming a nucleosome. (Figure adapted from Adam Krieg Lab diagram.)

Histone methylation is one of many epigenetic modifications that play an important role in chromatin compaction and gene expression. Numerous sites of modification are possible, each contributing to the expression level of marked genes. Arginines may be modified in H3, H4, and H2A histone proteins (Di Lorenzo and Bedford 2011). These modifications include monomethylarginines (MMA), asymmetric dimethylarginines (ADMA), and symmetric dimethylarginines (SDMA) (Di Lorenzo and Bedford 2011). Arginine methylation are gene activating at the following sites: H3R17, H3R26, H4R3, and H2AR3 (Di Lorenzo and Bedford 2011). Methylation modifications at the following arginines may repress gene expression: H3R2, H3R8, H4R3, and H2R3 (Di Lorenzo and Bedford 2011). Histone methylation may occur at lysine residues on histone H3, histone H4, linker histone H1, and its isotype H1.4 and may mark an expressed or repressed gene (Black, Van Rechem et al. 2012; Labbe, Holowatyj et al. 2013; Shmakova, Batie et al. 2014). These sites may be mono- (me1), di- (me2), or trimethyl- (me3) marks (Labbe, Holowatyj et al. 2013). Three lysine methylation sites on histones allow gene activation, that include: H3K4, H3K36, and H3K79 (Kouzarides 2007). The lysine modification sites that correspond with gene repression are: H3K9, H3K27, and H4K20 (Kouzarides 2007). Enzymes called methyltransferases and histone demethylases are key in regulating these marks.

Histone Lysine Demethylase Families

Histone lysine methylation is regulated by histone methyltransferases and histone demethylases. Histone lysine methyltransferases, a family of enzymes that utilize S-adenosylmethionine as a methyl group donor, such as Disrupter of Telomeric Silencing 1-Like (DOT1L), are responsible for adding methyl marks to lysine (Labbe, Holowatyj et al. 2013; Hancock, Dunne et al. 2015). Histone lysine demethylases are more diverse and can be classified into two enzymatic families. The first family includes the flavin adenine dinucleotide (FAD)-dependent amine oxidases such as LSD1 and LSD2 (Varier and Timmers 2011; Black, Van Rechem et al. 2012). The second family consists of the Jumonji C (JmjC)-domain containing proteins, which utilize a dioxygenase reaction, requiring Fe^{2+}, α-ketoglutarate, and molecular oxygen (Labbe, Holowatyj et al. 2013; Hancock, Dunne et al. 2015).

Identification of Jumonji Proteins

Jumonji proteins are one of the major histone demethylase families, implicated in regulating a variety of normal cell processes and tumorigenic pathways (Kouzarides 2007). Jumonjis were identified and named in a gene trap study as an essential contributor in neural tube formation in mouse development (Takeuchi, Yamazaki et al. 1995). A "cruciform" or jumonji (the Japanese translation) morphology was observed in the brains of mutant jumonji mice (Takeuchi, Yamazaki et al. 1995). The normal neural groove and abnormal grooves on the neural plates formed a cross shape in these mutants (Takeuchi, Yamazaki et al. 1995). Currently, there are 32 jumonji proteins identified by their JmjC-domain (Hancock, Dunne et al. 2015). 24 of these identified jumonjis act as histone demethylases (Klose, Kallin et al. 2006; Hancock, Dunne et al. 2015). The KDM4 subfamily is one subset of JmjC-domain containing proteins.

KDM4 Family of Histone Demethylases

KDM4 Family

The JMJD2 (Jumonji Domain 2) or KDM4 (Lysine-specific demethylase 4) proteins are histone demethylases that target histone residues H3K9, H3K36, and H1.4K26 (Yang, Lin et al. 2011; Berry and Janknecht 2013; Labbe, Holowatyj et al. 2013). The KDM4 family contains 4 genes (KDM4A-KDM4D) and 2 pseudogenes (KDM4E and KDM4F) (Fig. 1.2). The KDM4 family is highly conserved with orthologs found in other vertebrates (Labbe, Holowatyj et al. 2013). KDM4A, KDM4B, and KDM4C are very similar proteins, each containing a JmjN domain, JmjC domain, 2 Plant Homeodomains (PHD), and 2 Tudor domains (Berry and Janknecht 2013; Labbe, Holowatyj et al. 2013). KDM4D and KDM4E are smaller and lack the C-terminal region, which contain the PHD and Tudor domains (Katoh and Katoh 2004; Whetstine, Nottke et al. 2006; Berry and Janknecht 2013). Each KDM4 domain plays an important role in the enzymes structure and function. JmjC domain facilitates catalytic activity for these proteins while the JmjN domain interacts with JmjC and provides structural integrity (Katoh and Katoh 2004;

Whetstine, Nottke et al. 2006; Berry and Janknecht 2013). The C-terminal PHD and Tudor domains are responsible for targeting and histone mark reading (Berry and Janknecht 2013). Research has shown Tudor domains of KDM4A recognize H3K4me3/me2 and H4K20me3/me2 (Labbe, Holowatyj et al. 2013). At this time no studies have established the molecular function for PHD domains in KDM4 family members.

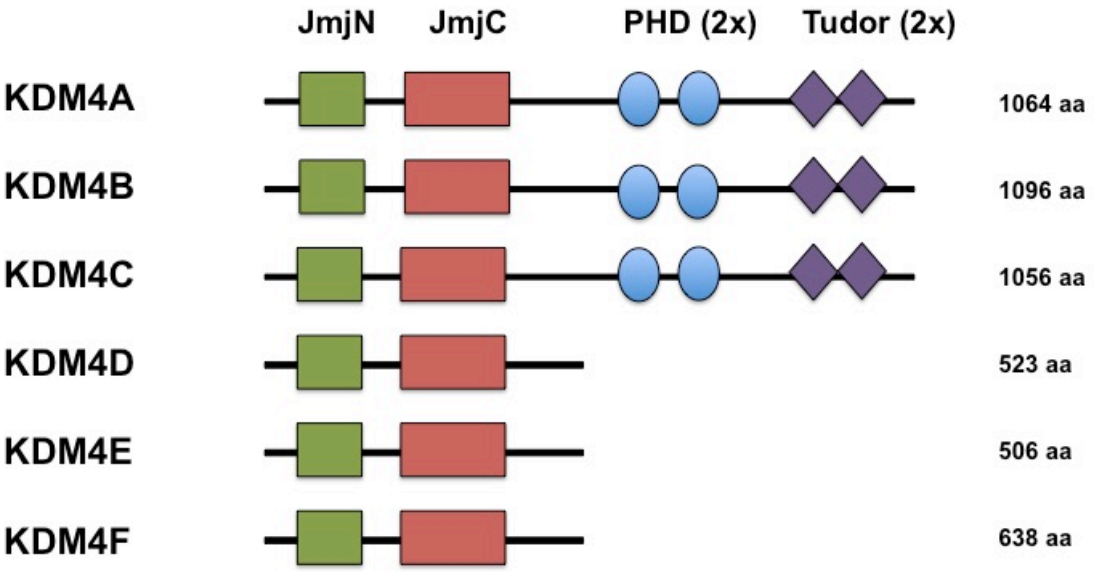
JmjN
JmjC
PHD (2x)
Tudor (2x)
KDM4A
KDM4B
KDM4C
KDM4D
KDM4E
KDM4F
1064 aa
1096 aa
1056 aa
523 aa
506 aa
638 aa

Figure 1.2 KDM4 Family Proteins

The KDM4/JMJD2 family is a subset of the jumonji-containing proteins. There are 4 characterized genes and 2 pseudogenes. KDM4A-KDM4C are very similar, containing a JmjN, JmjC, 2 PHD, and 2 Tudor domains. KDM4D-F are smaller, lacking the C-terminal targeting end containing the PHD and Tudor domains (Katoh and Katoh 2004).

KDM4 family proteins modify a variety of residues (Hillringhaus, Yue et al. 2011). H3K9me3 is normally associated with constitutive heterochromatin, which is transcriptionally repressed (Kouzarides 2007). KDM4A-KDM4D have been shown to remove H3K9me3 and H3K9me2 to activate gene expression (Whetstine, Nottke et al. 2006). H3K36me3 is localized within the gene body of an actively transcribed gene in euchromatin (Black, Van Rechem et al. 2012). KDM4A-KDM4C has also been shown to remove H3K36me3 and H3K36me2 which terminates transcription (Berry and Janknecht 2013). Linker histone H1 is also demethylated by KDM4A-KDM4D, demethylating a tri-methylation mark from H1.4K26me3 to activate gene transcription (Whetstine, Nottke et al. 2006; Trojer, Zhang et al. 2009; Krishnan and Trievel 2013). KDM4D is also capable of removing H1.4K26me2 (Krishnan and Trievel 2013). KDM4A and KDM4B have also been shown to bind and remove H4K20me2 to increase genome instability (Lee, Thompson et al. 2008). In addition to demethylating histone methylation marks, KDM4C has also been shown to demethylate the Polycomb Repressive Complex (Pc2) to promote gene activation (Yang, Lin et al. 2011). Each of these sites of methylation influence different cellular processes in different tissue and disease types.

KDM4 proteins are ubiquitously expressed in the body, at a variety of levels (Labbe, Holowatyj et al. 2013). RNA Sequencing Atlas has demonstrated KDM4 family member expression in many human tissue types (Yang, Imoto et al. 2000). KDM4A, B, and C are expressed in many normal human tissues with high expression in the spleen, ovary and colon (Yang, Imoto et al. 2000). While KDM4D and KDM4E are weakly expressed in many tissue types, they are more highly expressed in the testes (Labbe, Holowatyj et al. 2013). Different regulatory mechanisms control the activity, expression, and transcription of KDM4 family proteins.

Regulators of KDM4 Family Expression

A variety of mechanisms regulate expression, activity, and localization of KDM4 proteins. Transcription factors such as HIF-1α can induce KDM4B and KDM4C expression (Beyer, Kristensen et al. 2008; Pollard, Loenarz et al. 2008; Krieg, Rankin et al. 2010; Tausendschon, Dehne et al. 2011; Luo,

Chang et al. 2012). β-catenin, a key transcription factor in developmental processes, regulates KDM4B (Han, Ren et al. 2016). The tumor suppressor p53 also may regulate KDM4B (Palomera-Sanchez, Bucio-Mendez et al. 2010; Li, Zhao et al. 2011; Zheng, Chen et al. 2014). KDM4B can be regulated by nuclear hormone receptors including estrogen receptor (ER), androgen receptor (AR), and glucocorticoid receptors (GR) (Yang, Jubb et al. 2010; Kawazu, Saso et al. 2011; Shi, Sun et al. 2011; Coffey, Rogerson et al. 2013; West, Pan et al. 2016). Ubiquitination has also been shown to regulate the protein stability of KDM4A (Tan, Lim et al. 2011). KDM4A can be controlled by the SKP1-Cul1-F-box and SCF^{FBXO22} ubiquitin ligase that targets it for proteasomal degradation (Tan, Lim et al. 2011; Van Rechem, Black et al. 2011; Johmura, Sun et al. 2016). KDM4A and KDM4B may also be regulated by ubiquitination in response to DNA damage by RNF8 and RNF168 (Mallette, Mattiroli et al. 2012). Heat Shock Protein 90 (HSP90) has also been shown to interact with and stabilize KDM4B by blocking ubiquitin-dependent degradation (Ipenberg, Guttmann-Raviv et al. 2013). KDM4B and KDM4D may also be recruited by PARP-1 and participate in double stranded break repair in a PARP-1 dependent manner (Young, McDonald et al. 2013; Khoury-Haddad, Guttmann-Raviv et al. 2014; Khoury-Haddad, Nadar-Ponniah et al. 2015). MicroRNAs (miRNAs) are a class of small non-coding RNAs that repress gene expression by binding to 3'UTR of mRNA targets and stopping translation (Hui, Yiling et al. 2015). miR-491-5p, a known tumor suppressor, has been shown to target KDM4B and slow breast cancer tumorigenesis (Hui, Yiling et al. 2015). In addition to these mechanisms, protein-protein interaction can influence KDM4 family expression and activity.

Binding Partners that Influence KDM4 Family Epigenetic Regulation

Different proteins have been shown to bind to KDM4 proteins, influencing their epigenetic and transcriptional activity. Through these interactions, KDM4 demethylases regulate a variety of target genes involved with development, cell processes, and disease states. At this point, KDM4 family members have been shown to bind to each other, transcription cofactors, nuclear hormone receptors, and other transcriptional regulators. All KDM4 proteins have the capacity to form homodimers, though only

KDM4A, KDM4B, and KDM4C form heterodimers (Shin and Janknecht 2007). KDM4 proteins have also been shown to bind to the transcription factors β-catenin, MyoD, and C/EBPβ to facilitate target gene expression in a demethylase-dependent manner by removing H3K9me3 and H3K9me2 repressive marks (Guo, Li et al. 2012; Zhao, Li et al. 2013; Berry, Kim et al. 2014; Choi, Song et al. 2015). KDM4C has also been shown to bind to HIF-1α, facilitating epigenetic activation of HIF-1α downstream target genes (Luo, Chang et al. 2012). NF-κβ, the major transcriptional regulator of inflammatory response, has also been shown to interact with KDM4B (Han, Ren et al. 2016). p53 interacts with KDM4A to direct demethylase activity (Kim, Shin et al. 2012). KDM4B also binds estrogen receptor (ER), androgen receptor (AR), and ecdysone receptor (EcR) to facilitate histone demethylase activity (Yang, Jubb et al. 2010; Kawazu, Saso et al. 2011; Shi, Sun et al. 2011; Coffey, Rogerson et al. 2013; Tsurumi, Dutta et al. 2013). KDM4 proteins associate with Polycomb 2, the G9a methyltransferase, and chromodomain Y-like protein (CYDL1) (Kawazu, Saso et al. 2011; Yang, Lin et al. 2011). KDM4A, KDM4B, and KDM4C are also known to complex with members of SWI/SNF chromatin-remodeling complex and may interact with inhibitory complexes including histone deacetylases, N-CoR, or pRB tumor suppressor (Gray, Iglesias et al. 2005; Zhang, Yoon et al. 2005; Klose, Kallin et al. 2006). Inositol hexakisphosphate kinase 1 (IP6K1) interacts with KDM4C and regulates its demethylase function (Burton, Azevedo et al. 2013). Each of these regulatory complexes provides interesting insight into the versatile nature of KDM4 family binding and function. KDM4 family histone demethylases have established connections to cancer pathogenesis in many tumor models. ***For this body of work, the focus is on the role of KDM4B.***

KDM4B

KDM4B Structure and Enzymology

KDM4B is hypoxia-inducible, KDM4 family member that requires molecular oxygen, Fe^{2+}, and α-ketoglutarate for enzymatic activity (Beyer, Kristensen et al. 2008). KDM4B is structurally similar to KDM4A and KDM4C, and functions through a dioxygenase reaction (Figure 1.2 and 1.3) (Berry and Janknecht 2013; Langley, Brinko et al. 2016). KDM4B localizes to the human chromosome 19p13.3 and

has 12 transcript variants (Berry and Janknecht 2013). The protein KDM4B is 1096 amino acids in size with binding affinity for the histone residues H3K9me3, H3K9me2, H3K36me3, H3K36me2, H4K20me2, and H1.4K26me3 (Hillringhaus, Yue et al. 2011; Berry and Janknecht 2013). The demethylation proceeds in two steps (Fig. 1.3). For example, when KDM4B demethylates H3K9me3, KDM4B directly hydroxylates the methyl group on H3K9me3 (Langley, Brinko et al. 2016). In the second step, which does not need dioxygenase activity, formaldehyde is released from the hydroxylated methyl group to generate H3K9me2 (Langley, Brinko et al. 2016). This reaction is conserved for all sites demethylated by KDM4B.

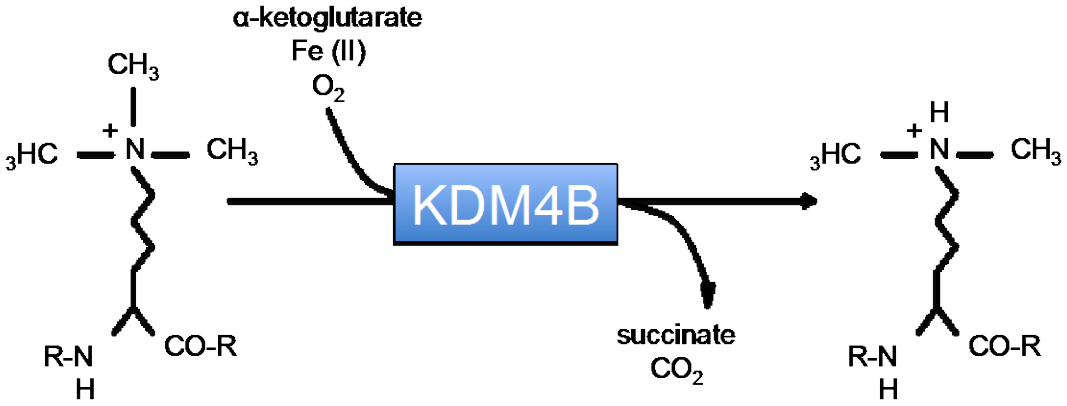
α-ketoglutarate
Fe (II)
O_2
CH_3
$_3HC$
N
CH_3
R-N
H
CO-R
KDM4B
succinate
CO_2
H
$_3HC$
N
CH_3
R-N
H
CO-R

Figure 1.3 KDM4B Enzymology

KDM4B is a Fe^{2+} and α-ketoglutarate-dependent dioxygenase. It demethylates histone lysine residues as indicated above. (Figure adapted from Adam Krieg Lab diagram.)

Catalytic activity at a variety of sites suggests an important role for KDM4B in regulating the balance of histone methylation genome wide. The demethylase activity of KDM4B is largely focused on H3K9me3 and H3K9me2, due to their highest affinity and enzymatic capabilities on these residues (Hillringhaus, Yue et al. 2011). When H3K9me3 and H3K9me2 repressive marks are removed, genes are expressed (Kouzarides 2007). However, KDM4B can still demethylate H3K36me3 and H3K36me2 with dramatically decreased specificity and catalytic ability (Hillringhaus, Yue et al. 2011). H3K36me3 and H3K36me2 can mark transcriptionally active or repressed sites (Kouzarides 2007). KDM4B also shows high affinity and catalytic function on H4K20me2 and H1.4K26me3 (Trojer, Zhang et al. 2009; Mallette, Mattiroli et al. 2012). H1.4K26me3 indicates gene repression and genes are expressed upon demethylation (Trojer, Zhang et al. 2009). Demethylation of H4K20me2 by KDM4B has been linked to genomic instability (Mallette, Mattiroli et al. 2012). The expression and catalytic functions of KDM4B has been linked to diseases like cancer, highlighting the necessity of designing a KDM4B inhibitor.

Inhibitors of KDM4B

High-quality and specific inhibitors are non-existent for individual KDM4 family proteins. KDM4 inhibitors indirectly target other KDM4 or jumonji proteins or disrupt HIF stability. Considering their significant implications in diseases like cancer, it is important to identify a specific inhibitor for individual KDM4 family proteins like KDM4B. At this time, KDM4 inhibitors can be divided into 3 groups: α-ketoglutarate or 2-oxoglutarate (2-OG) cofactor mimic and disruptor, metal cofactor mimics, and histone substrate analogs (Labbe, Holowatyj et al. 2013).

The vast majority of KDM4 inhibitors are α-ketoglutarate or 2-oxoglutarate (2-OG) cofactor competitive inhibitors that bind iron Fe^{2+} in the catalytic site (Rotili and Mai 2011; Labbe, Holowatyj et al. 2013; Maes, Carceller et al. 2015). All JmjC containing proteins require α-ketoglutarate for activity so these inhibitors lack specificity, targeting multiple members of this histone demethylase family (Labbe, Holowatyj et al. 2013). The α-ketoglutarate analogues N-oxalylglycine (NOG) and dimethyloxalylglycine (DMOG), commonly used to induce HIF signaling, also target PHD proteins,

affecting their role in maintaining intracellular levels of jumonji and KDM4 proteins (Rotili and Mai 2011). Other α-ketoglutarate analogues include 2,4-Pyridinedicarboxylic acid (PDCA) (Labbe, Holowatyj et al. 2013). In addition to these inhibitors, ML324 was identified from a high throughput screen to bind and inhibit the catalytic site of KDM4A and KDM4E (Rai, Kawamura et al. 2010). However, this compound has not been explored for its efficacy on KDM4B. At this time, α-ketoglutarate inhibitors are not specific for individual JmjC KDM4 proteins and other dioxygenases.

Metal cofactor mimics and histone substrate analogs are two additional routes of KDM4 inhibition. Disrupting iron cofactors interferes with KDM4 catalytic activity (Sekirnik, Rose et al. 2009; Giri, Passantino et al. 2013). Non-iron metals like nickel have been shown to block catalytic activities of KDM4A and KDM4C (Sekirnik, Rose et al. 2009; Giri, Passantino et al. 2013). Few histone substrate inhibitors have been designed besides the weakly effective tudor domain inhibitors WAG-003 and the methyllysine cofactor mimic MS-275 (Luo, Liu et al. 2011; Wagner, Nath et al. 2012). JIB-04 has been identified from cell-based screens and inhibits KDM4 family proteins (Wang, Chang et al. 2013). JIB-04 is not a competitive inhibitor of α-ketoglutarate (Wang, Chang et al. 2013). Its mode of function and effects on additional jumonji proteins has not been delineated (Wang, Chang et al. 2013). Despite these setbacks in specificity and targeting, it is important to continue developing effective inhibitors for KDM4 family members.

KDM4B and Development

Epigenetic modifiers are important contributors to developmental processes (Dambacher, Hahn et al. 2010). KDM4B has been of particular interest in stem cell biology and development. KDM4B activity has been connected to different aspects of embryonic stem cell (ESC) biology. ESCs are indefinitely self-renewing and differentiating cell populations, with identities maintained or differentiation controlled by activation of specific genes through transcription factors or chromatin regulators (Dambacher, Hahn et al. 2010; Das, Shao et al. 2014; Volarevic, Bojic et al. 2014). KDM4B is expressed in undifferentiated and differentiated ESCs (Katoh and Katoh 2007). KDM4B participates in

embryonic stem cell self-renewal and induced pluripotent stem cell generation in mouse models by associating with Nanog (Das, Shao et al. 2014). KDM4B and KDM4C work synergistically to mediate proper gene expression as mouse ESCs differentiate (Das, Shao et al. 2014). KDM4B dependent reduction of H3K9me3 improved reprogramming of embryonic stem cells into cloned embryos (Antony, Oback et al. 2013). Correct reprogramming of epigenetic modifications is important for cloning and repressive histone lysine methylation marks are very stable and prove problematic (Antony, Oback et al. 2013). This reduction of H3K9me3 levels improved *in vitro* development of cloned embryos (Antony, Oback et al. 2013).

KDM4B regulates mesenchymal stem cell (MSC) fate, identifying a possible control mechanism to exploit in directing MSC lineage (Ye, Fan et al. 2012; Qu, Liu et al. 2014). MSCs are multipotent progenitor cells with multilineage differentiation potentials (Ye, Fan et al. 2012). KDM4B controls MSC differentiation and fate by removing H3K9me3 and activating *DLX* (Ye, Fan et al. 2012; Qu, Liu et al. 2014). Loss of KDM4B reduced osteogenic differentiation and increased adipogenic differentiation (Ye, Fan et al. 2012; Qu, Liu et al. 2014). This provides a promising therapeutic target for diseases such as osteoporosis, which are commonly associated with a loss of MSC commitment (Ye, Fan et al. 2012; Qu, Liu et al. 2014).

KDM4B participates in chondrogenesis and adipogenesis in MSCs (Guo, Li et al. 2012; Lee, Yu et al. 2016). TGF-β dependent KDM4B expression removes the repressive H3K9me3 mark from the *SOX9* promoter, inducing expression of one of the master regulators of chondrogenesis (Lee, Yu et al. 2016). In adipogenesis, KDM4B binds C/EBPβ (CCAAT/enhancer-binding protein) to promote mitotic clonal expansion, an important process preadipocytes enter as they differentiate (Tang, Otto et al. 2003; Guo, Li et al. 2012). KDM4B binds C/EBPβ, demethylates H3K9me3 to regulate expression of cell cycle genes *CDC45I*, *MCM3*, and *CDC25C* and driving mitotic clonal expansion (Guo, Li et al. 2012).

In addition to stem cell maintenance and differentiation, KDM4B is involved in developmental biology. KDM4B is a critical component in development of the central nervous system (CNS) (Fujiwara,

Fujita et al. 2016). Neuron-specific KDM4B knockout mice displayed neurodevelopmental disorders including spinal malformations and hippocampal impairment (Fujiwara, Fujita et al. 2016). The hippocampus exhibited hyperactive behavior, deficits in working memory, and spontaneous epileptic seizures (Fujiwara, Fujita et al. 2016). This KDM4B knockout model provides a novel system for neurodevelopmental disorder *in vivo* investigations (Fujiwara, Fujita et al. 2016).

In addition to CNS development, KDM4B regulates inner ear invagination and ear development (Uribe, Buzzi et al. 2015). KDM4B is expressed during early stages of chick inner ear formation and lost expression results in defective otic placode invagination and morphological changes (Uribe, Buzzi et al. 2015). KDM4B regulates *DLX3*, a marker for inner ear, by demethylating H3K9me3 in its promoter region (Uribe, Buzzi et al. 2015). This study provides one of the first connections between a histone demethylase and ear development.

KDM4B is linked to spermatogenesis and mammary gland development (Yoshioka, McCarrey et al. 2009; Kawazu, Saso et al. 2011). Increased KDM4B and decreased H3K9me3 were identified during prespermatogenesis (Yoshioka, McCarrey et al. 2009). This suggests a role for KDM4B in reorganization of constitutive heterochromatin during a period of necessary epigenetic modifications required for gamete function (Yoshioka, McCarrey et al. 2009). KDM4B binds to estrogen receptor to regulate mammary gland development (Kawazu, Saso et al. 2011). A mammary-epithelium specific conditional KDM4B knockout mouse shows defective mammary gland development, identifying KDM4B as an important epigenetic component (Kawazu, Saso et al. 2011).

In addition to mammalian systems, KDM4B has been implicated in regulating *Drosophila* development (Palomera-Sanchez, Bucio-Mendez et al. 2010; Tsurumi, Dutta et al. 2013). KDM4B is essential for mediating ecdysteroid hormone signaling during drosophila larval development (Tsurumi, Dutta et al. 2013). KDM4A and KDM4B demethylate H3K9me3 specifically at the promoter of genes responsive to ecdysone signaling, such as Broad Complex (*BR-C)*, allowing increased expression (Tsurumi, Dutta et al. 2013). Double knock out of KDM4A and KDM4B results in developmental arrest (Tsurumi, Dutta et al. 2013). Rescuing these double knockouts with expression of KDM4A or KDM4B,

demonstrates that at least one of these proteins are essential for *Drosophila* development and survival (Tsurumi, Dutta et al. 2013). In addition to developmental processes, KDM4B has been shown to play a significant role in cancer progression.

KDM4B and Cancer

Tumorigenesis

The hallmarks of cancer are adaptations cancer cells can acquire during neoplastic transformation (Hanahan and Weinberg 2011). These hallmarks are: sustained proliferative signaling, resisting cell death, inducing angiogenesis, enabling replicative immortality, evading immune destruction, reprogramming energy metabolism, evading growth suppressors, and activating invasion and migration (Hanahan and Weinberg 2011). Their alterations may provide an additive effect to drive tumor formation. These altered hallmarks will also promote genome instability, disrupting any remaining normal homeostatic cell processes and interference with the cell's relationship with their microenvironment (Hanahan and Weinberg 2011). The underlying neoplastic genome changes driving tumorigenesis may occur both at the genetic and epigenetic level.

The role of the tumor microenvironment is an essential component in driving tumor progression. One such environmental effector is hypoxia (Kim, Lin et al. 2009). Considering its well-established connection to tumor aggressiveness, hypoxia is correlated to poor patient outcome (Welford and Giaccia 2011). Tumor hypoxia is a paradox. Not only does low-oxygen drive tumorigenic changes within cells, it also selects for cells equipped to survive oxygen stressed conditions (Hielscher and Gerecht 2015). This indicates hypoxia can play a pivotal role in transformation of normal cells to neoplasms. Hypoxia can occur in tissue more than 100-200 μm away from a blood supply and in various regions within the tumor (Helmlinger, Yuan et al. 1997). Using HIF transcription factors to induce expression, hypoxia promotes cellular adaptations such as increased proliferation, increased angiogenesis, increased glycolysis, cellular immortality, and resistance to apoptosis (Harris 2002). When studying the role of hypoxia in tumor biology, it is important to not overlook its role in inducing epigenetic changes.

Aberrant genetic and epigenetic factors are key steps in driving genome instability in a tumor (Balch, Fang et al. 2009). These are well-established concepts in cancer biology research (Hanahan and Weinberg 2011). Understanding the function of epigenetic changes in tumorigenesis is very attractive for chemotherapeutic design, providing a way to target aberrant gene expression without disrupting the genome sequence. Multiple studies have also shown hypoxic induced changes in chromatin marks (Hancock, Dunne et al. 2015). The mechanisms for hypoxia-dependent chromatin remodeling may occur through different mechanisms. HIF binding at HRE in promoters could signal recruitment of chromatin remodeling proteins, such as SWI/SNF or KDM3A (Perez-Perri, Acevedo et al. 2011). The jumonji protein KDM4B is known to be a direct target of HIF, with increased expression under hypoxia (Beyer, Kristensen et al. 2008). HIF may act as a direct binding partner of remodeling proteins to enhance their activity. For example, HIF can complex with Histone Deacetylase 1 (HDAC1), bind to an HRE within a promoter, and facilitate HDAC1 deacetylation and repression of *VEGF* (Lee, Kim et al. 2010). The methyltransferase G9a has been shown to increase under hypoxia, correlating with increased in H3K9me2 (Chen, Yan et al. 2006). Different types of epigenetic modifiers work through varying mechanisms to drive tumorigenesis.

Lysine-specific methyltransferases and lysine-specific demethylases work together to maintain global histone modifications and are implicated in tumor progression. When their activity and expression levels are disrupted, neoplasms may form (Xu, Yang et al. 2011). Many histone demethylases are deregulated during pathogenesis, either activating expression of oncogenes, repressing expression of tumor suppressors, altering DNA repair, disrupt chromosomal stability or interact with key hormonal receptors that control proliferation (Varier and Timmers 2011). The correlation between increased histone demethylase expression and tumor development has been established for many enzymes, such as LSD1 and KDM4C (Hoffmann, Roatsch et al. 2012). Optimizing inhibitors to specifically target JmjC containing KDMs have become a novel facet of therapy design (Thinnes, England et al. 2014). Recent bodies of work have studied the role of KDM4B and characterized its function in tumorigenesis in both solid and hematological tumor types (Chizuka, Suda et al. 2006). Developing a clearer picture of the

activity of KDM4B in cancer models helps clarify its involvement in tumorigenesis, both dependent and independent of hypoxia.

KDM4B in Breast Cancer

The involvement of KDM4B in breast cancer has a clear contribution to the aggressive nature of the disease in ER+ subtypes (Kawazu, Saso et al. 2011). KDM4B is highly expressed in estrogen receptor (ER)-positive, aggressive subtypes (Pollard, Loenarz et al. 2008; Yang, Jubb et al. 2010; Kawazu, Saso et al. 2011). Glucocorticoid receptor (GR) and ER-α may also induce KDM4B in an estrogen dependent manner in breast cancer (Yang, Jubb et al. 2010; Kawazu, Saso et al. 2011; West, Pan et al. 2016). KDM4B is required for ERα dependent transcription, where loss of KDM4B decreases cell proliferation *in vitro* and tumor progression *in vivo* (Yang, Jubb et al. 2010; Shi, Sun et al. 2011) (Hui, Yiling et al. 2015). KDM4B may also coordinate with additional epigenetic regulators to regulate histone modifications. KDM4B can bind ER-α and MLL2 to coordinate demethylation and methylation of H3K4 and H3K9 (Shi, Sun et al. 2011). KDM4B and ER-α can also bind SWI-SNF-B remodeling complex to mediate the expression of ER responsive genes, *MYB*, *MYC*, and *CCND1* (Kawazu, Saso et al. 2011). miR-491-5p, a tumor suppressor can bind KDM4B and slow ER-α+ breast cancer development (Hui, Yiling et al. 2015). KDM4B may provide an innovative therapeutic target for ER+ breast cancer.

KDM4B in Prostate Cancer

KDM4B expression can associate to the aggressive nature of prostate cancer (Chu, Wang et al. 2014). In prostate cancer cells, KDM4B expression, which correlates with the severity of tumor types, can cooperate with AR to induce the AR response (Coffey, Rogerson et al. 2013). KDM4B also stabilizes AR through inhibiting its ubiquitination and degradation (Coffey, Rogerson et al. 2013). Knockdown of KDM4B results in decreased AR expression (Coffey, Rogerson et al. 2013). The progression of prostate cancer from androgen-dependent to androgen-independent is one characteristic of this disease's lethal progression (Heinlein and Chang 2004). KDM4B promotes prostate cancer

development through an AR-independent mechanism, by activating the transcription of BMYB-target genes like Polo-like kinase 1 (*PLK1*), important for cell-cycle progression and drives tumorigenesis (Li and Dong 2015). KDM4B expression interferes with HDAC inhibitor efficacy by a novel mechanism. When KDM4B was knocked out, HDAC inhibitor trichostatin A (TSA) treatment enhanced induction of apoptosis (Li and Dong 2015). These observations lend KDM4B to be a potentially useful therapeutic target in prostate cancer, for both androgen-dependent and androgen-independent tumor types (Li and Dong 2015). Inhibition of KMD4B in combination with other chemotherapeutic drugs may improve current treatment options for prostate cancer.

KDM4B in Colorectal Cancer

KDM4B is highly expressed and is a known contributor to colorectal cancer (CRC) (Hwang, Heo et al. 2015). In addition to being regulated by HIF-1α in this model, KDM4B can act as an oncogene and induce tumorigenesis through a variety of mechanisms (Beyer, Kristensen et al. 2008). KDM4B, induced by *PRL-3*, a gene linked to CRC metastasis can promote CRC tumorigenesis by promoting proliferation, colony formation and migration of human colorectal cancer cells (Hwang, Heo et al. 2015). KDM4B silencing induced DNA damage triggers senescence, apoptosis, and cell cycle arrest by the suppression of STAT3 signaling (Toyokawa, Cho et al. 2011). In addition, KDM4B suppression can drive CRC apoptosis through mitochondria-mediated and death receptor-mediated pathways (Qiu, Fan et al. 2015). KDM4B, in conjunction with TC4 also binds with β-catenin to regulate expression of the oncoproteins *JUN*, *MYC*, and *Cyclin D1* (Berry, Kim et al. 2014). Considering the significance role of KDM4B in regulating many aspects of CRC, targeting this enzyme may be useful in therapeutic design.

KDM4B in Gastric Cancer

KDM4B is connected to gastric cancer carcinogenesis, lending itself as a possible novel biomarker or target for inhibition. Increased expression of KDM4B has been shown to drive gastric cancer proliferation, promote epithelial-mesenchymal transitions, and induce COX-2 dependent

inflammation (Li, Zhao et al. 2011; Agger, Miyagi et al. 2016; Han, Ren et al. 2016). Similar to colorectal cancer, KDM4B functions in a complex with β-catenin and increase expression of genes involved in the epithelial-mesenchymal transition in a demethylase-dependent manner (Zhao, Li et al. 2013). KDM4B can induce Helicobacter *pylori* infection and resulting gastric inflammation, one of the strongest risk factors for gastric cancer development (Han, Ren et al. 2016). β-catenin stimulates KDM4B expression that induces COX-2 expression in a histone demethylase-dependent manner (Han, Ren et al. 2016). These mechanisms establish KDM4B as a significant participant in gastric cancer.

KDM4B in Osteosarcoma

KDM4B is highly expression and has been connected to osteosarcoma tumorigenesis, a cancer type that effects young adults and is plagued with recurrence (Li and Dong 2015; Abarrategi, Tornin et al. 2016). KDM4B expression been shown to drive tumorigenesis and participate in the DNA damage response (Li and Dong 2015). KDM4B can promote proliferation, migration, and invasion through induction of Fibroblast growth factor 2 (FGF2) (Li and Dong 2015). Hsp90 has also been shown to stabilize KDM4B in osteosarcoma cell models, identifying Hsp90 inhibitors as a possible target for KDM4B driving tumor types (Ipenberg, Guttmann-Raviv et al. 2013). KDM4B also participates in regulating the DNA damage response in osteosarcoma models (Mallette, Mattiroli et al. 2012; Young, McDonald et al. 2013). After irradiation, KDM4B is recruited to DNA damage in a PARP1 dependent manner to remove the repressive H3K9me3 mark (Young, McDonald et al. 2013). KDM4B activity can influence 53BP1 recruitment to DNA damage sites (Mallette, Mattiroli et al. 2012). After recruitment to double strand breaks, KDM4B is marked by RNF8 and RNF168 and degraded in the proteasome (Mallette, Mattiroli et al. 2012). These findings combined suggest KDM4B expression could provide a novel risk factor or biomarker to consider in osteosarcoma diagnosis and treatment.

KDM4B in Liver, Lung, and Bladder Cancers

KDM4B activity is linked to liver, lung, and bladder cancer development (Toyokawa, Cho et al. 2011; Hwang, Heo et al. 2015; Lu, Ho et al. 2015). KDM4B shows increased expression correlating with tumor grade severity in Hepatocellular carcinoma (HCC) (Lu, Ho et al. 2015). KDM4B is highly expressed in lung and bladder tissue compared to normal tissues (Toyokawa, Cho et al. 2011). Knockdown of KDM4B in lung and bladder cancer models showed decreased proliferation and decreased colony formation, through its loss of regulation of *CDK6* (Toyokawa, Cho et al. 2011). These studies provide relevant links between KDM4B and tumorigenesis, lending KDM4B as a feasible molecular target for chemotherapy.

KDM4B in Neuroblastoma and Uveal Melanoma

KDM4B has been shown to play a role in regulating the N-Myc pathway in neuroblastoma, lending itself to be a useful therapeutic target in this cancer type (Yang, AlTahan et al. 2015). KDM4B and N-Myc are highly expressed in neuroblastoma tumors and correlate with poor outcome (Yang, AlTahan et al. 2015). Co-IP analysis showed binding between KDM4B and N-Myc (Yang, AlTahan et al. 2015). When KDM4B is knocked down, there is decreased proliferation, differentiation and tumor growth in neuroblastoma models (Yang, AlTahan et al. 2015).

KDM4B expression has also been explored in uveal melanoma to investigate possible links between enzymatic deregulation and tumor progression (Herlihy, Dogrusoz et al. 2015). In addition to aberrations of other histone modifiers, KDM4B was found to be down regulated in uveal melanoma with monosomy 3 (Herlihy, Dogrusoz et al. 2015). Monosomy 3 is one of the predictive markers of poor prognosis in this cancer type (Sisley, Cottam et al. 1992). These findings suggest KDM4B plays a role in these types of cancers.

KDM4B in Hematological Tumors

The role of KDM4B activity in hematological cancers has been explored in acute myeloid leukemia (AML) and multiple myeloma (MM) (Wen, Chen et al. 2012; Agger, Miyagi et al. 2016). AML

with translocations of the mixed-lineage leukemia 1 (MLL1) gene are aggressive hematopoietic malignancies, developing resistance to chemotherapies (Agger, Miyagi et al. 2016). Using KDM4A, KDM4B, and KDM4C triple knockout mice, KDM4 demethylation of H3K9me3 was shown to be required for MLL-AF9 translocated AML pathogenesis *in vitro* and *in vivo* (Agger, Miyagi et al. 2016). A possible redundant role was identified for KDM4 family proteins in AML and non-transformed bone marrow (Agger, Miyagi et al. 2016). When only KDM4C is knocked out in AML mouse models, leukemic cells survive (Agger, Miyagi et al. 2016). *IL3RA* ectopic expression alleviated the need for KDM4 proteins for survival and was shown to be a critical downstream target for KDM4 proteins in AML (Agger, Miyagi et al. 2016). These findings lend KDM4 family members, like KDM4B to be promising drug targets for consideration in AML.

Multiple Myeloma is a plasma cell neoplasm characterized by the accumulation of terminally differentiated monoclonal plasma cells in the bone marrow and is one of the most diagnosed hematological cancer types (Wen, Chen et al. 2012). Evidence suggests epigenetics are involved in the gene expression changes driving MM progression (Wen, Chen et al. 2012). Triptolide induces apoptosis in AML and was explored for its effects on histone methylation and antitumor effect on MM (Wen, Chen et al. 2012). Triptolide treatment induced apoptosis, and decreased KDM4B and H3K9me2 expression in MM (Wen, Chen et al. 2012). These findings are consistent with previous studies that show KDM4B may have a protective role in apoptosis, mediating the DNA damage response (Wen, Chen et al. 2012). These observations suggest high KDM4B expression may drive MM progression but needs further exploration.

Role of KDM4B in Gynecological Cancers

KDM4B has been poorly explored in gynecological cancers. KDM4B has been shown to promote endometrial cancer progression by regulating androgen receptor, c-myc, and $p27^{kip1}$ (Qiu, Fan et al. 2015). Gynecological cancers are plagued with late diagnoses, where standard therapies will not prove as effective (Cho and Shih Ie 2009). Recurrence and metastases are also problematic in these tumor types

due to chemotherapeutic resistance (Armstrong 2002). ***A clear knowledge gap exists regarding the identification of the role of KDM4B and histone modifiers in other types of gynecological cancers, such as ovarian cancer.*** Improving the understanding of KDM4B expression and function would help explain the enzymatic activities of KDM4B in ovarian cancer tumorigenesis and provide new biomarkers and targets for chemotherapeutic design. The studies in this body of work would only improve interventions and resources available to fight this devastating malignancy.

Ovarian Cancer

Etiology of Epithelial Ovarian Cancer

The origin of EOC is subject of debate. Three anatomical sites are the potential sites of origin for serous carcinoma development: the ovarian surface epithelium (OSE), the fallopian secretory fimbrial cells, and the mesothelium lining the peritoneal cavity (Lengyel 2010). Currently, the fallopian tube fimbrae and OSE are highly debated as the precursors for tumor initiation (Auersperg 2013). In the past, the idea that cells from the single layer of OSE give rise to neoplasms was widely accepted. OSE are relatively isolated and quiescent cells but have considerable access to cytokines, growth factors, and hormones within the ovarian stroma and circulating in the peritoneal fluid (Auersperg 2013). Ovulation has been pinpointed as the major contributor for OSE transformation (Lengyel 2010). Incessant ovulation theory suggests that frequent cycles of ovulation and surface repair drive OSE cells towards malignancy (Lengyel 2010). The OSE etiology theory is countered by evidence suggesting ovarian cancer could potential arise from the fallopian fimbrae.

In addition to OSE neoplasms forming, it is possible that secretory cells in the fallopian fimbrae could contain the precursors for serous carcinoma (Auersperg 2013). The fimbrae comprise the most distal part of the oviduct and they sweep over the ovarian surface at ovulation to capture oocytes and transport them through the oviducts (Auersperg 2013). Serous tubal intraepithelial carcinoma (STIC) are common malignancies with *BRCA1* mutations found in the fallopian tubes (Auersperg 2013). STICs with *BRCA1* or *BRCA2* mutations can be found within 20% to 60% of high-grade serous carcinoma in the

general ovarian cancer patient population (Crum, Herfs et al. 2013). It has also been shown that fallopian tubes of women predisposed to developing ovarian cancer frequently show dysplasia, accompanied by changed in cell-cycle and apoptosis, indicating an increased risk of ovarian cancer (Piek, van Diest et al. 2001). This suggests that in high-risk ovarian cancer patients, bilateral salpingio-oopherectomy and hysterectomy would cut the risk of recurrent ovarian cancers originating from the fallopian tube (Piek, van Diest et al. 2001; Leeper, Garcia et al. 2002).

Ovarian Cancer Epidemiology

Epithelial ovarian cancer (EOC) causes more deaths in the United States than any other type of female reproductive tract cancer (Siegel, Miller et al. 2015). The American Cancer Society identifies a woman's risk of getting ovarian cancer is roughly 1 in 75 while a woman's risk of dying from ovarian cancer is 1 in 100 (Siegel, Miller et al. 2015). The worldwide incidence of this cancer is 225,500 diagnoses per year; in the United States in 2015 there were 21,290 new cases (Siegel, Miller et al. 2015). Approximately 60% of ovarian cancers are diagnosed at advanced stages and 40% of women can expect to survive 5 years (Siegel, Miller et al. 2015). While fewer than 20% of ovarian cancers are localized to the ovaries at diagnosis, the five-year survival rate for women with tumors confined to the ovaries exceeds 90% for all ethnicities (Siegel, Miller et al. 2015). The high mortality of this cancer type is largely explained by the fact that the majority of patients present at an advanced stage, with widely metastasized tumors in the peritoneal cavity (Armstrong 2002). Global mortality of ovarian cancer remains high and minimal improvement in patient survival has been observed over the past decade (Liu and Matulonis 2014; Siegel, Miller et al. 2015).

Ovarian Cancer Presentation and Diagnosis

Ovarian cancer is a heterogeneous disease, each patient presenting a different subtype and degree of metastasis (Cho and Shih Ie 2009). Patients usually are diagnosed in later stages or more advanced disease states, due to symptoms being mistaken by clinicians for other ailments (Cho and Shih Ie 2009).

The measurement of circulating levels of ovarian tumor antigen CA-125, Cancer Antigen 125, is commonly used to monitor disease presence and recurrence in combination with transvaginal ultrasonography (Vaughan, Coward et al. 2011). Primary tumors are localized to the ovaries while metastases form in the pelvic region and peritoneal cavity (Vaughan, Coward et al. 2011). The main site of metastasis is the omentum, with 80% of all serous ovarian carcinoma cases showing this preferred localization (Nieman, Kenny et al. 2011). Ovarian cancer progression is unique, disseminating through the peritoneal fluid (Cho and Shih Ie 2009). However, hematogenous dissemination has been shown to be important in ovarian cancer progression but is not the main mode of metastasis (Nieman, Kenny et al. 2011). Ovarian cancer biomarkers such as CA-125 are debated due to their poor consistency and efficiency for detecting early stages of this disease (Armstrong 2002). Even though the ovaries are one of the largest production sites of estrogen, it is unclear what role estrogen plays in ovarian cancer progression (Chan, Wei et al. 2008). Hormonal contraceptives are linked to a decreased risk for ovarian cancer (Burkman, Schlesselman et al. 2004).

Ovarian Cancer Staging, Types, and Treatment

Identifying the stage of ovarian cancer disease progression helps direct therapeutic strategies developed by clinicians. Ovarian cancer stages are determined by the guidelines set in the International Federation of Gynecology and Obstetrics (FIGO) classifications (Mutch and Prat 2014). Stage I is limited to one or both ovaries (Mutch and Prat 2014). Stage II involves tumor placement at one or two ovaries and fallopian tubes with pelvic extension (Mutch and Prat 2014). Stage III tumors are located at one or both ovaries with metastases spread to the peritoneum outside the pelvis (Mutch and Prat 2014). Stage IV includes tumor burden at the ovaries, fallopian tubes, and distant metastases (Mutch and Prat 2014). While other cancer types may rely on gene expression to identify stages, ovarian cancer is typically classified based on radiographic and surgical presentations (Armstrong 2002).

Several distinct tumor types or grades with unique features are classified and identified in ovarian cancer diagnoses. Ovarian cancer is not a homogenous disease; each case presents different tumors and

displays different biological behavior (Armstrong 2002). CA-125/MUC16 in blood serum can be used as a biomarker for ovarian cancer, but types are primarily diagnosed by histopathology (Jacobs and Menon 2004). Approximately 90% of ovarian cancer arises from the epithelium while much less frequent germ cell tumors and sex cord-stromal tumors may form (Mutch and Prat 2014). Epithelial ovarian cancers are divided into two types, Type 1 (low-grade) and Type 2 (high-grade), based on degree of tumor progression and molecular profiles (Cho and Shih Ie 2009). The 5 main histotypes of epithelial ovarian cancers are: low-grade serous carcinoma (5%), high-grade serous carcinoma (70%), endometriod carcinoma (10%), clear cell carcinoma (10%), and mucinous carcinoma (3%) (Prat 2012; Mutch and Prat 2014). Their respective morphological appearances are diagnosed through light microscopy (Cho and Shih Ie 2009). Regardless of 60% of epithelial ovarian cancer tumors expressing ER, ER does not provide a reliable prognostic indicator for EOC (Cunat, Hoffmann et al. 2004; Chan, Wei et al. 2008). Tamoxifen, an ER antagonist, provides inconsistent efficacy in EOC patient treatments (Schwartz, Chambers et al. 1989; Perez-Gracia and Carrasco 2002).

Serous carcinomas, arising from epithelial cells on the ovary or the fallopian fimbrae, are the most common types of epithelial ovarian cancer (Vang, Shih Ie et al. 2009; Prat 2012; Mutch and Prat 2014). High-grade serous are the most common ovarian carcinomas and most patient's present at an advanced, more metastasized stage at the time of diagnoses (Prat 2012). In high-grade serous ovarian cancer, wild-type p53 function is lost in 96% of cases (Cole, Dwight et al. 2016). High-grade serous usually display p53, WT1, p16 and Ki-67 in immunohistochemical (IHC) analysis (Bowtell 2010; Prat 2012). Low-grade serous are much less frequent than their high-grade serous counterparts (Prat 2012). Their molecular profiles are similar with lower expression of *Ki-67* and mutations in *BRAF*, *KRAS*, and *ERBB2* (Prat 2012).

Mucinous carcinomas account for 10% of all primary ovarian tumors, however 80% are benign (Cho and Shih Ie 2009; Prat 2012). The origin of these tumors is debated. The cells in mucinous carcinomas may resemble the gastric pylorus, intestine, or cervix (Prat 2012). Benign mucinous tumors have a low risk of recurrence and are primarily confined to the ovary (Prat 2012). Malignant mucinous

tumors are often heterogeneous, displaying benign, borderline, and malignant characteristics (Hart 2005; Prat 2012). The gene expression profile of mucinous carcinomas differs from serous, endometeriod, and clear cell (Vang, Shih Ie et al. 2009). *KRAS* mutations and cytokeratin 7 (*CK7*) are genetic attributes of mucinous tumors (Prat 2012).

The final two histotypes are endometriod and clear cell carcinoma (Vang, Shih Ie et al. 2009). Endometriod and clear cell tumors closely resemble uterine cancers (Vaughan, Coward et al. 2011; Prat 2012). Endometriosis may be a possible precursor for endometriod tumorigenesis (Vaughan, Coward et al. 2011). Endometriod tumors may have mutations in β-catenin and *PTEN* (Prat 2012). These tumor types are immunoreactive for vimentin, cytokeratin 7, and estrogen receptor (Prat 2012). Simultaneous endometriod carcinomas from the ovary and the uterus can occur (Prat 2012). Clear cell carcinoma is associated with poor prognosis at later stages and has an association with endometriosis (Prat 2012). This histotype has a distinct pathology among ovarian cancer types and are usually positive for HNF1-β (Prat 2012).

Standard treatments for ovarian cancer include tumor debulking combined with cisplatin or carboplatin plus taxol drugs like Paclitaxel (Weberpals, Koti et al. 2011). Women at high risk of ovarian cancer often undergo risk-reducing bilateral salpingo-oophorectomy, removal of the ovaries and fallopian tubes (Berek, Chalas et al. 2010). Other commonly used drugs include bevacizumab and olaparib (Armstrong 2002). Bevacizumab, A VEGF inhibitor helps decrease tumor burden in ovarian cancer patients (Della Pepa and Banerjee 2014). Olaparib, a PARP inhibitor, is another drug for ovarian cancer used in a small number of ovarian cancer patients (Ai, Lu et al. 2016). Niraparib, another PARP inhibitor, was recently shown to extend survival for several months in clinical studies (Sandhu, Schelman et al. 2013; AlHilli, Becker et al. 2016). Despite good initial responses to platinum drugs, resistance often develops (Armstrong 2002). For patients suffering from ascites fluid buildup, therapies include: diuretics, radioactive isotopes, paracentesis, and shunt placement (Smolle, Taucher et al. 2014). These approaches have stressful impacts and may cause toxic side effects (Smolle, Taucher et al. 2014). Repeat paracentesis can also cause severe stress to the patient's body. Each of these factors can drive

chemoresistance in EOC, limiting the efficacy of the most robust therapy options. Understanding the molecular and genetic mechanisms that drive the development of chemoresistance in addition to tumor progression will help improve current therapies for ovarian cancer treatment. Another factor complicating chemoresistance are genetic and epigenetic changes driven by tumor hypoxia.

HIF, KDM4B, and Epithelial Ovarian Cancer Progression

Hypoxia, Tissue Homeostasis, and the Hypoxic Response

Responding to changes in environmental oxygen is critical to maintaining cellular homeostasis and survival. Oxygen availability is key to energy metabolism. Exposure to low oxygen or hypoxic conditions may harm tissue homeostasis. A constant supply of O_2 is required to carry out oxidative phosphorylation in the mitochondria to generate ATP (Harris 2002). The series of physiological changes that connect environmental oxygen to cellular metabolism is termed the oxygen transport cascade (Dzal, Jenkin et al. 2015). The oxygen transport cascade is composed of four steps: ventilation, diffusion of oxygen from the air to the blood, circulation, and diffusion of oxygen from the blood into the cells (Fisher and Burggren 2007; Dzal, Jenkin et al. 2015). Physiologically normoxic conditions varies between human tissue types (Simon and Keith 2008). While ambient air is 21% O_2, normoxic or typical ranges in tissues vary between 1% O_2-15% O_2 (Simon and Keith 2008). The greatest partial pressure of oxygen is found in the alveoli of the lungs (115 mm Hg) while the lowest partial pressures can be found in the thymus or kidney (7 mm Hg) (Simon and Keith 2008; Hanahan and Weinberg 2011; Welford and Giaccia 2011).

In addition to maintaining cell functions in normoxic conditions, organisms have developed physiological adaptations to survive hypoxia or low oxygen tension (Harris 2002; Dzal, Jenkin et al. 2015). The definition of hypoxia is an oxygen concentration of $\leq$ 2% (Hancock, Dunne et al. 2015). All nucleated cells sense and respond to hypoxia (Semenza 2011). Cells can initiate a variety of biological adaptations in response to low oxygen conditions. The first major hypoxic response includes the shift from aerobic to anaerobic metabolism (Dang and Semenza 1999). Angiogenesis, new blood vessel

formation and remodeling, is another of the most well studied physiological responses (Dang and Semenza 1999; Span and Bussink 2015). Hypoxia also increases erythropoietin (EPO) production, a hormone essential in red blood cell production (Dang and Semenza 1999). The hypoxia inducible factors or HIF, transcriptionally regulate the signaling pathways that mediate the cellular response to low-oxygen environmental stresses (Dang and Semenza 1999; Span and Bussink 2015).

Hypoxia-inducible Factors Induce Transcription in Response to Low Oxygen

The hypoxia-inducible factors (HIF) regulate the primary transcriptional response to hypoxic stress in normal and transformed cells (Semenza 2011; Keith, Johnson et al. 2012). HIFs are basic helix-loop-helix-PER-ARNT-SIM (bHLH-PAS) proteins that form heterodimeric complexes between the oxygen-labile HIF-1α subunit and the oxygen-stable HIF-1β subunit or ARNT (Semenza 2011). HIF-1α and HIF-1β have similarly arranged functional domains. The N-termini of the proteins contain the DNA-binding basic region, followed by the HLH and PAS (PER-ARNT-SIM) domains (Pawlus and Hu 2013). The C-terminal ends of HIF-1α contain the N-terminal activation domain (N-TAD) that overlaps with the oxygen-dependent degradation (ODD) domain, followed by an inhibitory domain (IH), and the C-terminal activation domain (C-TAD) (Semenza 2011; Pawlus and Hu 2013). The bHLH and PAS domains mediate dimerization between HIF-1α and HIF-1β while the basic regions from HIF-1α and HIF-1β direct DNA binding (Semenza 2011; Pawlus and Hu 2013). This complex binds hypoxia-responsive elements (HREs) that contain the conserved sequence RCGTG (Semenza 2011). Additional transcriptional coactivators may bind to the C-TAD, such as CBP/p-300 and SRC-1 to initiate transcription (Liu and Simon 2004). However, the oxygen tension dependent expression of HIF-1α regulates the activity of the HIF transcriptional complex (Semenza 2011; Pawlus and Hu 2013).

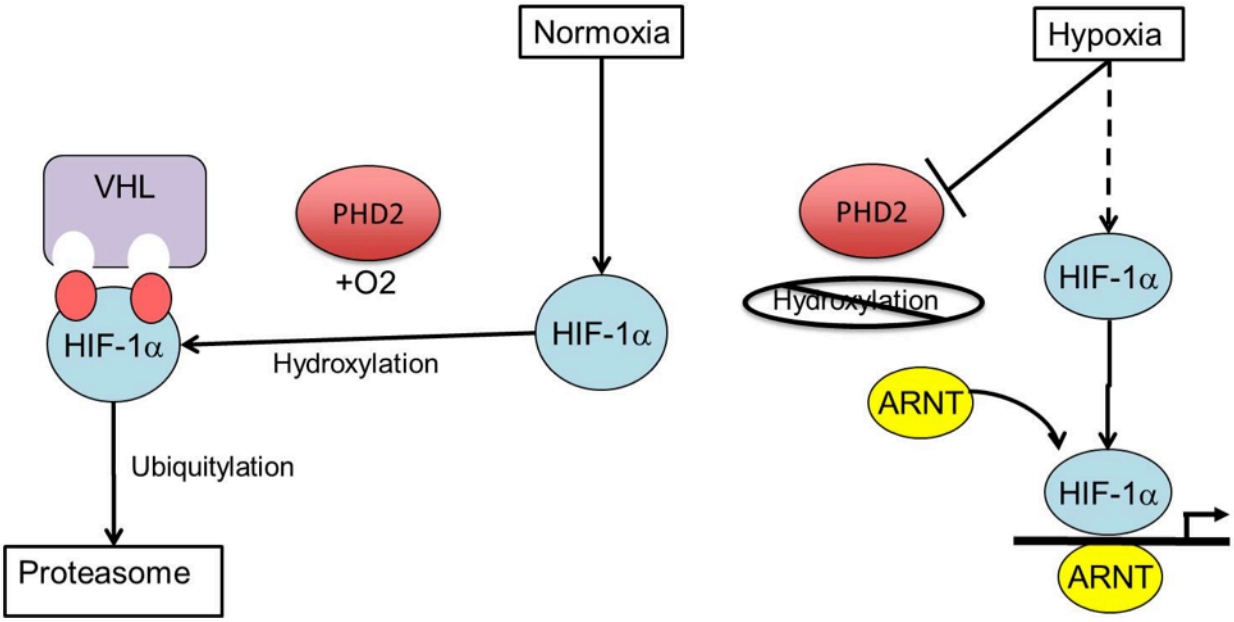
Normoxia
VHL
PHD2
+O2
HIF-1α
HIF-1α
Hydroxylation
Ubiquitylation
Proteasome
Hypoxia
PHD2
Hydroxylation
HIF-1α
ARNT
HIF-1α
ARNT

Figure 1.4 HIF-1α is Regulated by Prolyl hydroxylase domain-containing protein 2 (PHD2).

Under normoxic conditions, HIF-1α expression is labile and degraded at the proteasome. It is designated for degradation by PHD2 and VHL. PHD2 hydroxylates HIF-1α at Proline 402 and 564 by PHD2 followed by VHL ubiquitination. Under hypoxic conditions, this regulatory mechanism is suppressed. PHD2 function is inhibited, freeing HIF-1α to bind HIF-1β (ARNT) and translocate to the nucleus to activate hypoxic gene transcription. (Figure adapted from Adam Krieg Lab Diagram.)

Oxygen-Dependent HIF-1α Degradation

While ARNT is oxygen-stable and constitutively expressed, the HIF-1α subunit is oxygen-labile (Fig. 1.4). Under tissue-specific normoxic conditions, HIF-1α is largely undetectable and is rapidly degraded (Liu and Simon 2004; Semenza 2011). When oxygen levels are lower (<6%), HIF-1α is stabilized and translocate to the nucleus to dimerism with ARNT (Semenza 2011). Oxygen-dependent degradation of HIF-1α is regulated by the hydroxylation of two key Proline residues: PRO^{402} and PRO^{564} (Liu and Simon 2004; Semenza 2011). Prolyl hydroxylase domain-containing protein 2 (PHD2) is the enzyme responsible for this reaction (Liu and Simon 2004). These proline hydroxylations guide the interaction of HIF-1α with the von Hippel-Lindau (pVHL) tumor suppressor (Semenza 2011). pVHL is an E3 ubiquitin-ligase complex that targets HIF-1α, ubiquitinates it, targeting it for degradation in the proteasome (Semenza 2011). This oxygen-labile regulation of HIF-1α provides the main control for HIF complex dimerization and activity.

The Role of HIF-1α in Epithelial Ovarian Cancer Progression

Hypoxic tumor microenvironments contribute to progression in many tumor models such as breast cancer, prostate cancer, brain cancer, and ovarian cancer (Harris 2002). Nuclear expression of HIF-1α has been shown to be a marker of poor prognosis in ovarian carcinoma and an indicator of advanced stages (Osada, Horiuchi et al. 2007). HIF-1α expression localized to necrotic regions of the tumor with mutated p53 (Birner, Schindl et al. 2001). HIF-1α targets such as Carbonic Anhydrase IX (CAIX) and Glucose Transporter 1 (GLUT1) also show increased expression in patient tumor tissue (Cantuaria, Fagotti et al. 2001; Woelber, Mueller et al. 2010). HIF-1α has not only been demonstrated to regulate angiogenic factors such as VEGF and PDGFB in ovarian cancer, it also drives ovarian cancer metastasis by promoting invasion through the downregulation of E-cadherin (*CDH1*) or increasing *LOX* expression (Cheng, Klausen et al. 2013; Ji, Wang et al. 2013). Ovarian cancer spheroids develop hypoxia induced metabolic adaptations and become more chemoresistant (Liao, Qian et al. 2014). Combined, these observations demonstrate HIF-1α plays a pivotal role in ovarian cancer oncogenesis.

Hypoxia increases resistance to chemotherapeutics (Agarwal and Kaye 2003; Della Pepa and Banerjee 2014; McEvoy, O'Toole et al. 2015). HIF1 is an attractive target for combatting the tumor hypoxic response but has been challenging for drug design (Xia, Choi et al. 2012). Most drugs are designed to alter direct targets of the HIF pathway, such as VEGF inhibitors (Horiuchi, Imai et al. 2002). In the case of patients with resistance to platinum-based treatments, Bevacizumab, a VEGF inhibitor, has been used (Della Pepa and Banerjee 2014). Considering the connection between EOC tumorigenesis and hypoxia, it is important to explore and dissect the roles of HIF genetic and epigenetic targets such as KDM4B.

Knowledge Gap – Identification of Roles of Epigenetic Regulators in Ovarian Cancer Progression

Due to the complexity of EOC, understanding the genetic and epigenetic regulatory factors is important. Not only does this help design new therapeutic targets for ovarian cancer patients, it helps dissect the mechanisms that are driving their tumor progression. A variety of altered epigenetic states are associated with ovarian tumorigenesis (Seeber and van Diest 2012). Aberrant DNA methylation and histone modifications have both been demonstrated in ovarian cancer (Balch, Fang et al. 2009). DNA methylation is one of the most studied epigenetic modifications in ovarian cancer, with DNA methylation profiles being suggested as potential biomarkers for epithelial ovarian cancer types (Gloss and Samimi 2014). Deregulated DNA methyl-transferase (DNMT) activity has been associated with repressing tumor suppressors such as *BRCA1* and *p16* by hypermethylation of the CpG islands in promoter regions (Balch, Fang et al. 2009). At this point, DNMT inhibitors like azacitidine and decitabine have demonstrated limited efficacy in phase I/II trials for ovarian cancer (Weberpals, Koti et al. 2011). However, this does not negate the use of DNMT inhibitors in combinatorial therapies.

Histone deacetylation is another transcriptional silencing mechanism studied in ovarian cancer. HDAC inhibitors can relieve epigenetic gene repression by inhibiting the deacetylation of histones and non-histone proteins (Balch, Fang et al. 2009). Poor results have been shown in clinical trials for HDAC

inhibitors such as vorinostat, but may still be useful in combination with other therapies (Balch, Fang et al. 2009).

Limited research has investigated the roles of histone demethylases in ovarian cancer progression. At this time, only one jumonji protein, JARID1B has been investigated in ovarian cancer (Chen, Ge et al. 2015; Wang, Mao et al. 2015). JARID1B expression correlated with poor prognosis and chemoresistance in patient samples, but no molecular function was described in this model (Wang, Mao et al. 2015). **At this time, there is little to no knowledge existing that characterizes jumonji protein function, protein enzyme dynamics, downstream target genes, and connections to tumorigenic pathways such as invasion and migration in epithelial ovarian cancer.**

Project Goal - Dissecting the Role of KDM4B in Epithelial Ovarian Cancer

Overall Purpose and Significance

The purpose of my dissertation is to dissect and demonstrate the *in vitro* and *in vivo* roles of KDM4B in epithelial ovarian cancer progression. At this time, there is no background explaining the enzymatic activity of KDM4B or its functional activity in ovarian cancer tumorigenesis. Ovarian cancer is a disease plagued with poor outcomes, late diagnoses and recurrence. Identifying KDM4B regulated genes may provide novel therapeutic targets to consider in combination with other ovarian cancer therapies. Understanding the role of KDM4B may provide additional biomarkers to consider when staging epithelial ovarian cancer. *Most importantly, this body of work will characterize another mechanistic link between the hypoxic tumor microenvironment and ovarian cancer progression.* Increasing the knowledge base on the global effects of tumor hypoxia will help clarify the entire picture of the ovarian tumor's hypoxic response.

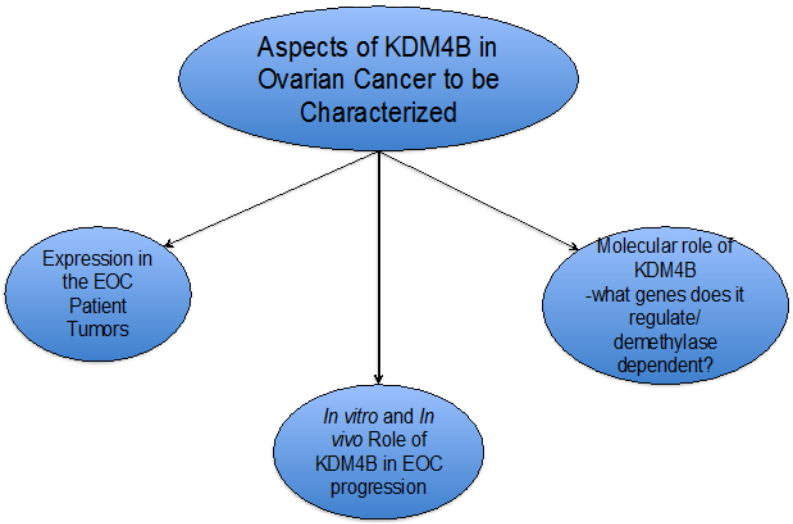
Aspects of KDM4B in Ovarian Cancer to be Characterized
Expression in the EOC Patient Tumors
In vitro and In vivo Role of KDM4B in EOC progression
Molecular role of KDM4B -what genes does it regulate/ demethylase dependent?

Figure 1.5 Unknown Areas of KDM4B to be Addressed in this Project

At this time, little is known about KDM4B expression in EOC progression. This project will characterize 3 main aspects: Expression levels in EOC Patient Tumors, *in vitro* and *in vivo* role of KDM4B in EOC Progression, and identify target genes and their mode of regulation by KDM4B in EOC tumorigenesis.

Research Objective and Specific Aims

At this time, little is known about KDM4B expression in EOC progression. This project will characterize 3 main aspects: Expression levels in EOC Patient Tumors, *in vitro* and *in vivo* role of KDM4B in EOC Progression, and identify target genes and their mode of regulation by KDM4B in EOC tumorigenesis (Fig. 1.5).

There are two specific aims in this research project, which are:

1. To identify the relevance of KDM4B *in vitro* and *in vivo* using serous carcinoma models.
2. To identify mechanisms regulated by KDM4B that drive metastasis and EOC peritoneal dissemination.

Experimental findings relating to Specific Aim 1 are presented in and those associated with Specific Aim 2 are presented in Chapter 3.

CHAPTER 2:

THE HISTONE DEMETHYLASE KDM4B REGULATES PERITONEAL SEEDING OF OVARIAN CANCER*

(UNPUBLISHED MANUSCRIPT)

NOTE:

*This chapter is an unpublished manuscript with first authorship shared between myself and a former graduate student in the Krieg lab, Lei Qiu. This project was conceptualized, funded, and directed by my mentor Adam Krieg. The general premise and backbone of this paper originated in his COBRE award from 2010. His former student, Lei Qiu, and myself worked on completing his original aims and expanding the investigations with our own intellectual input, creativity, and skills. Without our teamwork, dedication, and commitment to finalizing this initial large project, submission and publication of this manuscript would not have been possible. I also recognize the individual efforts of each of the other authors on this paper for providing their time, work, and expertise. This manuscript provided the bulk of my learning and skill building for my graduate work and I am forever grateful. *

ABSTRACT

Epithelial ovarian cancer (EOC) has poor prognosis and rapid recurrence due to widespread dissemination of peritoneal metastases at diagnosis. Multiple pathways contribute to the aggressiveness of ovarian cancer, including hypoxic signaling mechanisms. In this study, we have determined that the hypoxia-inducible histone demethylase KDM4B is expressed in approximately 60% of EOC tumors assayed, including primary and matched metastatic tumors. Expression of KDM4B in tumors is positively correlated with expression of the tumor hypoxia marker CA-IX, and is robustly induced in EOC cell lines exposed to hypoxia. KDM4B regulates expression of metastatic genes and pathways, and demethylates promoter regions of target genes like *LOXL2*, *LCN2*, and *PDGFB*. Suppressing KDM4B inhibits ovarian cancer cell invasion, migration and spheroid formation *in vitro*. KDM4B also regulates seeding and growth of peritoneal tumors in vivo, where its expression corresponds to hypoxic regions. This is the first demonstration that a Jumonji-domain histone demethylase regulates cellular processes required for peritoneal dissemination of cancer cells, one of the predominant factors affecting prognosis of EOC. The pathways regulated by KDM4B may present novel opportunities to develop combinatorial therapies to improve existing therapies for EOC patients.

INTRODUCTION

Epithelial ovarian cancer (EOC) is the most deadly of gynecologic cancers, and is the fifth leading cause of cancer mortality in women (1). EOC is a heterogeneous disease, generally stratified by the aggressiveness of growth, with slower growing Type I tumors having better prognosis than more rapidly growing Type II tumors (Vang, Shih Ie et al. 2009). The majority of Type II EOC patients are diagnosed at an advanced International Federation of Gynecology and Obstetrics stage (FIGO stage III or IV), with widespread dissemination of metastatic tumors throughout the peritoneal cavity (Naora and Montell 2005; Vang, Shih Ie et al. 2009; Lengyel 2010). Of the 4 general pathological subtypes that comprise EOC (serous, endometrioid, mucinous, and clear cell), the majority of Type II EOC are high-grade serous adenocarcinoma (HGSA), representing 70% of the total EOC cases (Vang, Shih Ie et al. 2009; Lengyel 2010). Front-line therapy for HGSA consists of surgical debulking followed by treatment with platinating agents and taxol derivatives (Lengyel 2010). The initial response to therapy is generally effective; however recurrent chemo-resistant tumors reseed the peritoneal cavity within 2 to 5 years, causing mortality. Rapid re-establishment of tumor growth suggests that the stresses imposed by the metastatic process, surgery, and chemotherapy drive adaptations that facilitate epithelial ovarian cancer progression.

The hypoxic tumor microenvironment is a potent contributor to malignancy in multiple cancer types, including EOC (Birner, Schindl et al. 2001; Chi, Wang et al. 2006; Semenza 2012). The hypoxia-inducible factors (HIFs) are primary regulators of the hypoxic response, inducing transcription of genes that promote homeostasis and tumor progression via metabolic adaptation, self-renewal, angiogenesis, and metastasis (Semenza 2012). HIF-1α also induces expression of several Jumonji domain histone demethylases (JmjC-KDMs), including KDM4B (Lysine-specific histone demethylase 4B, also called JMJD2B), establishing a compelling link between the hypoxic tumor microenvironment and epigenetic remodeling to support tumorigenesis (Beyer, Kristensen et al. 2008; Pollard, Loenarz et al. 2008; Xia, Lemieux et al. 2009; Krieg, Rankin et al. 2010). KDM4B is thought to regulate gene expression by demethylating tri- and di-methylated histone H3 at Lysine 9 (H3K9me3/me2) and lysine 36

(H3K36me3/me2) (Whetstine, Nottke et al. 2006). Despite the importance of KDM4B to general tumor growth, its contribution to EOC progression has not been investigated. Since HIF-1α and hypoxic signaling contribute to EOC (Chi, Wang et al. 2006), KDM4B may also influence EOC progression. Using immunohistochemical analysis of patient samples and *in vitro* and *in vivo* functional analyses of ovarian cancer cell lines, we have determined that KDM4B is abundantly expressed in EOC tumors, and contributes to multiple pathways required for peritoneal seeding. Thus KDM4B represents a novel link between the hypoxic tumor microenvironment and EOC, mobilizing mechanisms that facilitate the establishment of peritoneal tumors.

MATERIALS and METHODS

Cell Lines and Culture Conditions. All OVCAR cell lines were maintained in RPMI-1640 (Invitrogen) supplemented with 10% heat-inactivated fetal bovine serum (HI-FBS) and 1% pen-strep (Invitrogen). SKOV3ip.1 cells were from Dr. Erinn Rankin (Stanford University) with permission from Dr. Gordon Mills (M.D. Anderson Cancer Center). OVCAR3, OVCAR4, OVCAR5, OVCAR8, and IGROV1 cells were from the NCI-Frederick Cancer DCTD Tumor/Cell line Repository. OVCAR10, UPN275, and HIO80 cells were from Dr. Andrew Godwin. Upon receipt, cells were expanded in culture to establish early passage stocks. After transducing with lentivirus, cells were used for experiments within 1-2 months to minimize cell drift or contamination, and were periodically screened for mycoplasma. For transient knockdown of KDM4B, SKOV3ip.1 cells were transfected with a pool of small interfering RNAs (siRNAs) targeting KDM4B or an irrelevant control (siK4B, Dharmacon siGenome Smartpool, Thermo Scientific) as previously described (Krieg, Rankin et al. 2010). For xenografts, cells were transduced with lentivirus to express firefly luciferase and selected in neomycin (pLenti PGK V5-LUC Neo (w623-2), from Eric Campeau (Addgene plasmid # 21471 (Campeau, Ruhl et al. 2009)). For stable knockdown, cells were transduced with pLKO.1-shRNA constructs targeting KDM4B (Open Biosystems; TRCN0000018014 (shK-1) and TRCN0000018016 (shK-2)) and selected in puromycin. For hypoxic treatment, cells were incubated for 16-24 hours in Ruskinn InVivo300 glove-box hypoxic incubators (Baker) set to desired oxygen tensions.

Tumor Microarray Samples. Ovarian tumor microarrays (TMAs) were constructed by the University of Kansas Cancer Center (KUCC) Biospecimen Repository Core Facility using archival formalin fixed, paraffin embedded samples of primary ovarian carcinoma with matched metastatic tissue samples. Samples were identified from the pathology departmental archives of the University of Kansas Medical Center from 1998-2009. TMAs were composed of tumor samples from 48 patients with ovarian cancer: 14 patients with primary, recurrent, and metastatic samples (including one patient with distant metastasis to the brain), 27 patients with primary and metastatic samples, and 7 patients with primary and recurrent

samples and included serous (30), mixed (14; 12 of which included a serous component), carcinosarcoma (1), clear cell (1), papillary carcinoma, not otherwise specified (NOS) (1) and adenocarcinoma, NOS (1) samples. For every sample, hematoxylin and eosin stained slides were reviewed by a board certified pathologist who selected tumor rich areas. Using the semi-automated TMArrayer (Pathology Devices, Inc., Westminster, MD) TMA paraffin blocks were assembled with triplicate 1.0 mm cores using the marked slide as a guide.

Immunohistochemical Analysis (IHC). IHC was performed using standard peroxidase/DAB methods and hematoxylin counterstain (See Figure 2.1 for specific antibodies and conditions). Representative images were captured using a Nikon 80i microscope with a Photometrics CoolSNAP ES camera and NIS-Elements AR software. Human TMA slides were scanned using an Aperio slide-scanning microscope (Leica) at the University of Kansas Medical Center, Department of Pathology; and the University of California San Francisco, Department of Radiation Oncology (Courtesy of Dr. Denise Chan). Individual spot images were extracted using Aperio TMALab. Slides were blinded and independently evaluated by at least 2 pathologists (authors GT, TK, OWT). If more than 10% of tumor epithelium in a tumor had nuclear staining of KDM4B, the section was classified as having high expression (Goode, Chenevix-Trench et al. 2011). For CA-IX staining, tumors were scored on a qualitative scale (0 = no staining, 1 = weak staining, 2 = moderate staining, 3 = strong staining). Scores for triplicate spots from each tumor sample were averaged for statistical analysis. SPSS (IBM) was used to determine significance of CA-IX and KDM4B staining with Bivariate correlation (Spearman's ρ).

Assay	Antigen	Supplier	Product NO.	Description	Dilution
Western	KDM4B	Cell Signaling	8639	Rabbit mAb	1:1,000
	HIF1α	BD	610959	Mouse mAb	1:1,000
	β-Actin	Sigma	A1978	Mouse mAb	1:2,000
	H3K9me3	Abcam	ab8898	Rabbit pAb	1 μg/ml
	H3K9me2	Abcam	ab1220	Mouse mAb	1 μg/ml
	H3K9me	Abcam	ab9045	Rabbit pAb	1:500
	H3K36me3	Abcam	ab9050	Rabbit pAb	0.5 μg/ml
	H3K36me2	Abcam	ab9049	Rabbit pAb	0.5 μg/ml
	H3K36me	Abcam	ab9048	Rabbit pAb	1:1,000
	histone H3	Abcam	ab1791	Rabbit pAb	1:4,000
	α-Tubulin	Thermo	MS-581-PABX	Mouse mAb	1:2,000
ChIP	KDM4B	Cell Signaling	8639	Rabbit mAb	1:100
	histone H3	Abcam	ab1791	Rabbit pAb	2 μg per 1 million cells
	H3K9me3	Abcam	ab8898	Rabbit pAb	2-4 μg per 25 μg chromatin
	IgG control	Cell Signaling	3900S	Rabbit mAb	560 ng/ml as control for KDM4B; 2μg per ChIP as control for histones
IHC	KDM4B	Cell Signaling	8639	Rabbit mAb	1:100
	IgG control	Cell Signaling	3900S	Rabbit mAb	1:100
	CA-IX	Thermo	MA5-15737	Mouse mAb	1:8000
	PAX8	Biocare	ACI438A	Mouse mAb	1:100
	Ki67	Thermo	RM-9106-S0	Rabbit mAb	1:800
	Pimonidazole	Hypoxyprobe, Inc.	70132-50-2	Mouse mAb	1:5000

Figure 2.1. List of Antibodies Used in the Study.

QRT-PCR. Quantitative real-time PCR (qRT-PCR) was conducted as previously described using an ABI VIIA sequence detection system using 18S rRNA as an internal control (Krieg, Rankin et al. 2010). Primers (Figure 2.2) were designed using the Roche Universal Probe Library Design Tool (http://lifescience.roche.com/shop/products/universal-probelibrary-system-assay-design). Melt curve analysis confirmed formation of single amplicons of the expected size.

Assay	Gene	Forward (5'-3')	Reverse (5'-3')	
QRT-PCR	hsKDM4B	ggactgacggcaacctctac	cgtcctcaaactccacctg	
QRT-PCR	hsKDM4A	gccgctagaagtttcagtgag	gcgtcccttggacttcttatt	
QRT-PCR	hsKDM4C	aggcgccaagtgatgaag	gagaggtttcgcccaagact	
QRT-PCR	hsKDM4D	ggacaagcctgtaccactgag	ctgcacccagaagccttg	
QRT-PCR	hsPDGFB	ctggcatgcaagtgtgagac	cgaatggtcacccgagttt	
QRT-PCR	hsIGFBP1	aatggattttatcacagcagacag	ggtagacgcaccagcagagt	
QRT-PCR	hsLCN2	ctccacctcagacctgatcc	acataccacttcccctggaat	
QRT-PCR	hsLOXL2	tgacctgctgaacctcaatg	tggcacactcgtaattcttctg	
QRT-PCR	hsLOX	ggatacggcactggctactt	gacgcctggatgtagtaggg	
QRT-PCR	18S rRNA	gcccgaagcgtttactttga	tccattattcctagctgcggtatc	
QRT-PCR	hsGAPDH	agccacatcgctcagacac	gcccaatacgaccaaatcc	
Assay	Gene	Forward (5'-3')	Reverse (5'-3')	Genomic coordinates
ChIP	PDGFB-1	gagccctccgccttaacc	cagccaggcgcaggaa	chr22:39,638,710-39,638,763
ChIP	PDGFB-2	cctggcactcgggagctt	tccaggttgaggctagatgga	chr22:39,641,397-39,641,470
ChIP	LCN2	aagtgtttccgcaggagttg	gggatctagggtgggttgat	chr9:130,911,623-130,911,702
ChIP	LOX	actgagcgcaggaacttctc	cactggttccaagctggcta	chr5:121,413,216-121,413,314
ChIP	LOXL2-1	agcgcctgcgtaaaagttgt	gctacagctgatcccaatcttga	chr8:23,260,663-23,260,733
ChIP	LOXL2-2	tgccttgtccacctcctatcc	aacactttcattcggcagcttt	chr8:23,261,969-23,262,053
ChIP	DESERT-C16D8	gagcaagcagaccctaatgc	ctgtccactcaggagccttc	chr16:62,316,298-62,316,449

Figure 2.2. List of Primers Used for qRT-PCR and ChIP analysis.

Microarray Analysis. RNA (100 ng) was profiled using GeneChip® Human Exon 1.0 ST exonic transcript arrays (Affymetrix). Normalization and differential gene expression analysis was performed in the Partek Genomic suite (v 6.5, Partek Inc.). All experiments were performed in triplicate. The exon-arrays were RMA-background corrected, quantile-normalized and gene-level summarized using the Median Polish algorithm (Irizarry, Hobbs et al. 2003). The resulting log (base 2) transformed signal intensities were used in a 2-way ANOVA model to calculate differential expression. P-values were corrected for multiple-hypothesis testing by the Benjamini and Hochberg method (Klipper-Aurbach, Wasserman et al. 1995). Genes displaying fold change of <-1.4 or lower following siK4B knockdown ($P<0.05$) compared to the siCon transfected cells were considered to be regulated by KDM4B. GeneVenn (http://www.bioinformatics.org/gvenn/) identified overlapping expression between different oxygen tensions and knockdown constructs. Specific pathways influenced by KDM4B were identified using Ingenuity Pathway Analysis (Ingenuity Systems). Microarray data was deposited under accession number GSE66894 in the NCBI Gene Expression Omnibus (Edgar, Domrachev et al. 2002).

Immunoblotting. Immunoblots were performed using standard procedures as previously described (Krieg, Rankin et al. 2010). See Figure 2.15 for antibody dilution information.

Growth Curves. Cells (50 000) were seeded in triplicate to 6 cm dishes, cultured in HeraCell 150 incubators (ThermoFisher Scientific, Inc.) set to desired oxygen tension, counted, and reseeded every three days, as described by Welford, et al (Welford, Bedogni et al. 2006).

Migration and Matrigel Invasion Assay. Invasion and migration assays were performed as described by Swenson-Fields et al. (Swenson-Fields, Vivian et al. 2013), with minor modifications. Cells (50 000) suspended in RPMI + 2% FBS were seeded to Boyden chambers (BD Falcon, 8 micron pore size) suspended in RPMI + 10% FBS. For invasion assays, chambers were coated with 100 uL 1 mg/mL Matrigel (BD Biosciences). After 24 hours incubation (see Cell Culture Section), cells were released by

trypsinization and DNA content quantified using CyQUANT Cell Proliferation Assay Kit (Life Technologies) according to manufacturer's protocol. Invasion and migration were normalized to seeding and monolayer proliferation controls. Representative membranes were fixed and stained with Siemens Diff Quik Stain Set (Neobits, Inc.) and imaged using a Leitz LABORLUX12 microscope equipped with a Leica EC3 camera.

Spheroid Formation Assay. 600 cells were seeded per well of 96-well ultra-low attachment plates (Corning Incorporated). After four days, spheroids were imaged by brightfield microscopy using a Leica DMI 4000 inverted microscope equipped with a Leica CCD camera (Courtesy of Dr. Michael J. Soares, KUMC). Volume ($V=4/3*\pi r^3$) was calculated after measuring the diameter and radius of each spheroid using NIH Image J (Vinci, Gowan et al. 2012). Differences in average spheroid volume were analyzed by two-tail paired Student's t-test. Sixteen spheroids were analyzed per cell line and oxygen condition in each independent experiment.

Intraperitoneal Tumor Xenografts. Cells (1,000,000 SKOV3ip.1-luc-neo or 5,000,000 OVCAR8-luc-neo) were injected i.p. into NCR-nu/nu athymic mice (Taconic; 4-6 weeks old females, 10 mice per group, randomly assigned for injection). Study numbers allow detection of an effect size of 1.6 relative to control with a power of 85% ($P<0.05$ using Student's T-test), assuming a tumor take rate of 80%. Tumor growth was monitored weekly (non-blinded) using the IVIS Spectrum *in vivo* imaging system (Perkin Elmer) in the KUMC Center for Molecular Imaging, until shGFP control mice achieved humane endpoints. Mice prematurely removed from the study were excluded from analysis. Mice were injected with 200-250 μl D-Luciferin (Gold Biotechnology, Inc.) 15 minutes prior to imaging. Pimonidazole (Hypoxyprobe, HPI) was injected i.p. 30 minutes before euthanasia to label hypoxic cells. Portions of the largest tumors (primarily omental masses) were fixed in 4% paraformaldehyde and processed for IHC. Frozen tumor samples were homogenized for RNA purification and analysis. Statistical significance was determined as described in the Statistical analysis section.

Chromatin Immunoprecipitation Assay (ChIP). ChIP was performed as described previously (Krieg, Rankin et al. 2010), with minor modifications. 8-50 µg of sonicated DNA was incubated with 1-5 µg antibody (Figure 2.1). Enrichment to promoters and regulatory regions was measured using QPCR calibrated to a dilution series of pooled input DNA and normalized to the respective input controls. For histone H3K9me3 analysis, input normalized signal was adjusted by subtracting IgG signal, with further normalization to gene desert control (C16D8). Fold changes in enrichment were calculated relative to shGFP control cells at 21% O2. Primers to promoters and control regions were designed using Primer Express software (Life Technologies) and validated for amplification efficiency and generation of a single amplicon (Figure 2.2).

Statistics. Data represent the mean ± SEM or median ± upper and lower quartiles for at least three independent experiments. Human tumor data and mouse xenografts were analyzed with non-parametric methods such as Kruskal-Wallace, Mann-Whitney U-test and Spearman's correlation to account for non-normal distributions of data. Two-tailed Student's T tests or ANOVA were used as appropriate for *in vitro* experiments. P values of 0.05 or less were considered statistically significant.

Study approvals. Animal studies were approved by the KUMC Institutional Animal Care and Use Committee. De-identified human patient samples and any corresponding clinical data were provided by the KU Cancer Center's Biospecimen Repository Core Facility (BRCF) with informed consent from patients. Collection and use of de-identified human patient samples for this study was approved by the KUMC Human Subjects Committee.

Conflicts Of Interest

The authors have no competing financial interests relating to this manuscript.

Acknowledgements

Research was supported by an Institutional Development Award (IDeA) P20GM104936 (AJK and SG), an American Cancer Society Institutional Research Grant ACS IRG-09-062-04 (AJK), KUMC Dept. of OB/GYN start-up funds (AJK). The authors thank the staff of the University of Kansas Cancer Center's Biospecimen Repository Core Facility staff for specimen collection (Colleen Reilly and Zaid Naima) and for excellent histological assistance in the creation of the TMAs (Dr. Rashna Madan and Tara Meyer). The authors acknowledge the KU Cancer Center's Cancer Center Support Grant (P30 CA168524). Special appreciation is given to Dr. Denise A. Chan (UCSF), whose untimely passing in 2014 prevents inclusion as a co-author.

RESULTS

KDM4B is Abundantly Expressed in Hypoxic High Grade Ovarian Serous Adenocarcinoma Tumors and OVCAR Cell Lines. Hypoxic regulation of KDM4B is a common mechanism in many different cancer cell types (Beyer, Kristensen et al. 2008; Wellmann, Bettkober et al. 2008; Xia, Lemieux et al. 2009; Krieg, Rankin et al. 2010), suggesting that KDM4B would also be robustly expressed in EOC. Expression of KDM4B was measured in ovarian cancer tissue microarrays (TMAs) (See Methods and Figures 2.3 and 2.4).

Samples		Score (% of tissue)			% nuclei positive for KDM4B			
		High	Low	Total	Mean	Median	STDEV	Range
Normal Ovary		0	9 (100)	9	0.4	0.3	0.4	0-1
High Grade Serous	Primary	19 (63.3)	11 (36.7)	30	22.4	20.8	18.6	0.7-61.1
	Metastases	20 (69)	9 (31)	29	19	17.6	13.6	0-54.2
	Totals	39 (66)	20 (33)	59	20.7	18.7	16.3	0-61.1
Mixed	Primary	9 (64.3)	5 (35.7)	14	17.5	14.4	15.9	0.4-44.5
	Metastases	3 (37.5)	5 (62.5)	8	10.4	5.1	10.9	1.3-30.2
	Totals	12 (54.5)	10 (46.5)	22	14.9	11.4	14.4	0.5-44.5
Other	Primary	4 (100)	0	4	18.6	18.5	6.9	10.4-27.1
	Metastases	2 (50)	2 (50)	4	19.9	18.5	19.3	1.8-40.7
	Totals	6 (75)	2 (25)	8	19.3	18.5	13.4	1.8-40.7

Figure 2.3. Summary of KDM4B staining in KUCC OVCAR TMAs. Nuclear staining of KDM4B was scored as described in Materials and Methods (represented as n (%)). Tumors with > 10% nuclei staining positive for KDM4B were considered "high," in a modification of a method described in (Goode, et al. 2011). “Mixed” contain various combinations of clear cell, endometrioid, and mucinous characteristics, all with a serous component. “Other” contains individual tumors with diagnoses of endometrioid, clear cell, or carcinosarcoma.

Patient	**Grade**	histosubtype	tumor type	KDM4B (Avg. % nuclear staining)	CA9 (Avg Intensity Score)
1	III	serous	primary	35.47	3
2	III	serous	primary	2.9	2
3	III	serous	primary	21.93	3
4	III	serous	primary	30.1	1.67
6	III	serous	primary	1.5	2.33
7	III	serous	primary	20.7	2
8	II	serous	primary	29.13	2.33
9		serous	primary	56.4	2.67
12	III	serous	primary	23	2
13		serous	primary	34.43	2.67
16	III	serous	primary	33.57	2
17	III	serous	primary	6.6	3
20	III	serous	primary	4.13	2
21	III	serous	primary	37.9	2.67
22	III	serous	primary	27.9	2
23		serous	primary	14.33	2.67
24	III	serous	primary	54.35	3
25	III	serous	primary	61.07	2
26	III	serous	primary	4.5	2
31	III	serous	primary	40.07	3
38	III	serous	primary	2.73	2
39	III	serous	primary	56.85	3
40	III	serous	primary	0.73	2
41	III	serous	primary	7.37	2
42	III	serous	primary	1.53	2
43	III	serous	primary	15.93	3
45	III	serous	primary	15.97	3
46	III	serous	primary	2.77	2.33
47	III	serous	primary	6.07	2
49	II	serous	primary	20.83	3
1	III	serous	metastasis	24.73	2.67
2	III	serous	metastasis	1.33	2
3	III	serous	metastasis	38.87	3
4	III	serous	metastasis	8.53	2
6	III	serous	metastasis	5.6	2
7	III	serous	metastasis	15.7	2.33
8	II	serous	metastasis	14.97	2
9		serous	metastasis	54.2	3
12	III	serous	metastasis	21.8	2
13		serous	metastasis	24.67	3

16	III	serous	metastasis	25.43	2
17	III	serous	metastasis	28.2	2
20	III	serous	metastasis	6.37	1.33
21	III	serous	metastasis	18.7	NA
22	III	serous	metastasis	39.13	2
23		serous	metastasis	16.3	2
24	III	serous	metastasis	42.97	2
25	III	serous	metastasis	19.87	2
26	III	serous	metastasis	7	2.5
38	III	serous	metastasis	10.97	2
39	III	serous	metastasis	33.1	3
40	III	serous	metastasis	14.83	2
41	III	serous	metastasis	17.57	2.67
42	III	serous	metastasis	0	NA
43	III	serous	metastasis	0.87	2.33
45	III	serous	metastasis	19.13	3
46	III	serous	metastasis	3.1	2
47	III	serous	metastasis	7.6	2
49	II	serous	metastasis	28.3	3
10	II	mixed	primary	1.2	1.33
18	III	mixed	primary	42.2	2
19	III	mixed	primary	15.43	2.33
27	III	mixed	primary	44.5	2
28	III	mixed	primary	24.53	2
29	III	mixed	primary	7.97	3
30	III	mixed	primary	13.33	2.67
32	II	mixed	primary	43.1	2
33	III	mixed	primary	11.6	2
34	III	mixed	primary	1.23	2
35	III	mixed	primary	1.23	1
36	III	mixed	primary	0.47	2
44	III	mixed	primary	21.43	2
48	III	mixed	primary	16.1	1
10	II	mixed	metastasis	30.23	2
18	III	mixed	metastasis	4.5	2
19	III	mixed	metastasis	24.17	3
34	III	mixed	metastasis	4.13	2
35	III	mixed	metastasis	1.3	1
36	III	mixed	metastasis	2.13	2
44	III	mixed	metastasis	11.23	2
48	III	mixed	metastasis	5.7	2
5	III	other	primary	27.13	3
11	III	other	primary	19.27	2.67

14	III	other	primary	10.37	2
15	III	other	primary	17.7	2
5	III	other	metastasis	31.83	3
11	III	other	metastasis	1.83	2.33
14	III	other	metastasis	5.23	1.67
15	III	other	metastasis	40.73	2.33
37	III	not EOC	primary	10.57	3
37	III	not EOC	metastasis	4.53	2

Figure 2.4. Immunohistochemical Scoring Data for KUCC OVCAR TMAs. Tumors are listed by de-identified patient sample # with corresponding tumor grade (most are FIGO grade III), pathology histological subtype (histosubtype; serous, mixed, other, and not EOC), tumor type (primary, metastasis), and average scores for KDM4B nuclear staining (% nuclear staining) and CA9 intensity scores (0-3, in increments of 0.3). Scoring was applied as described in Methods. Data are ranked by histosubtype, then tumor type, then patient sample #. Sections with spots damaged during IHC are labeled “NA”

Nuclear KDM4B staining was greater in tumor epithelium of HGSA tumors compared to normal ovarian sections (Fig. 2.5A, quantified in 2.5C). Heterogeneous distribution of KDM4B nuclear staining was observed throughout primary and metastatic tumor sections (Fig. 2.5A). Over 60% of primary and metastatic tumors displayed "high" expression of KDM4B (Fig. 2.5B, quantified in 2.5D, See Methods). Nuclear expression of KDM4B in metastatic tumors positively correlated with KDM4B expression in the corresponding primary tumors (Fig. 2.5E, Spearman $r=0.7192$, $P<0.0001$). Independent measurements using sections from nine normal ovaries showed weak KDM4B staining in normal ovarian surface epithelium (OSE, Fig. 2.5F), one potential source tissue for EOC (Lengyel 2010).

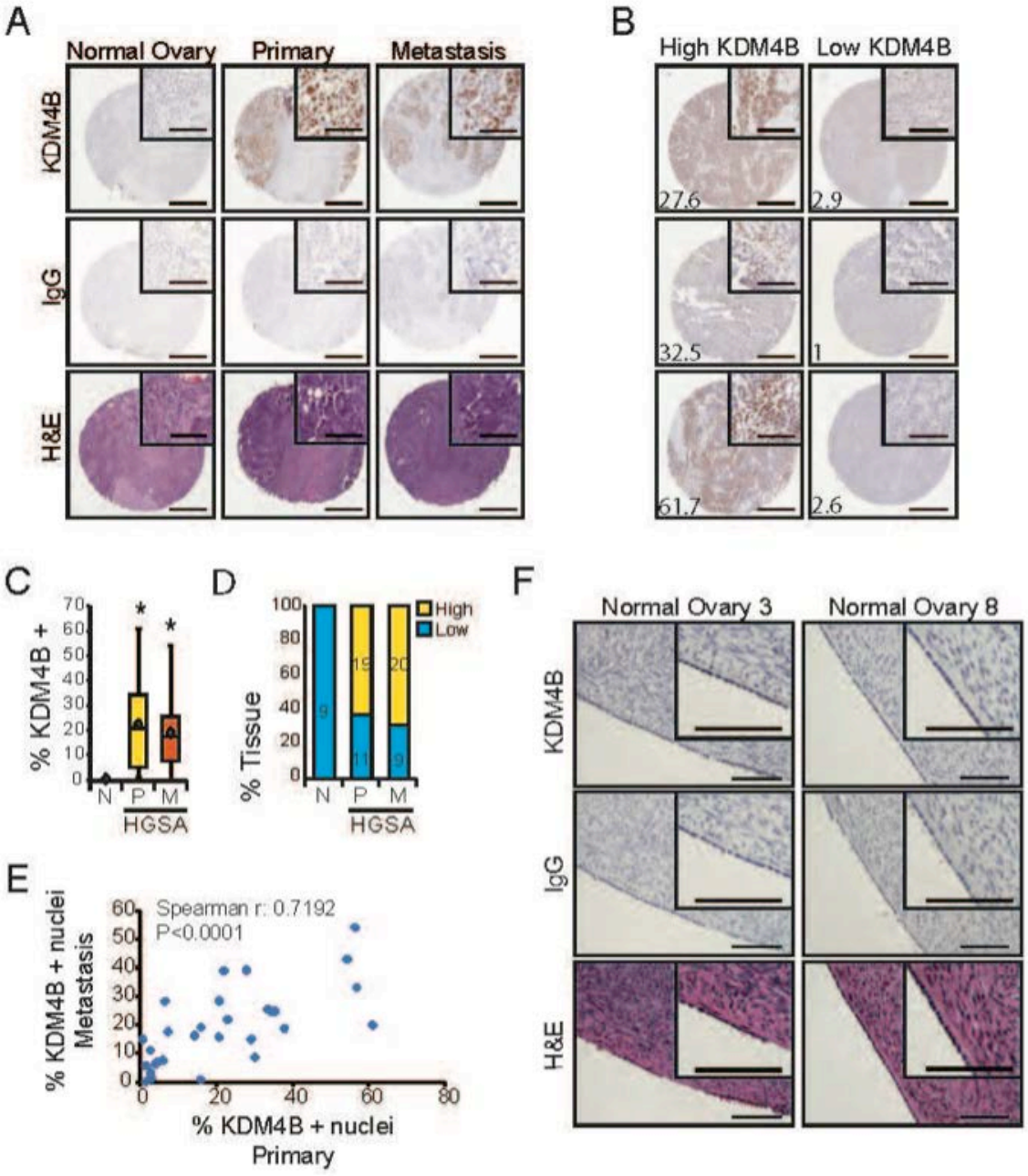
A
Normal Ovary
Primary
Metastasis
KDM4B
IgG
H&E
B
High KDM4B
Low KDM4B
27.6
2.9
32.5
1
61.7
2.6
C
% KDM4B +
N
P
M
HGSA
D
% Tissue
High
Low
19
20
11
9
E
% KDM4B + nuclei
Metastasis
Spearman r: 0.7192
P<0.0001
% KDM4B + nuclei
Primary
F
Normal Ovary 3
Normal Ovary 8
KDM4B
IgG
H&E

Figure 2.5. KDM4B is robustly expressed in ovarian cancer tissue and ovarian cancer cell lines compared to normal ovarian surface epithelial cells. A. Representative immunohistochemical detection of KDM4B (top row; brown, DAB; blue, hematoxylin) in Tumor Microarray sections from normal ovary and high-grade ovarian serous adenocarcinoma biopsies with matched primary and metastatic tumor sections. IgG (middle) and H&E (hematoxylin and eosin, bottom) serve as controls for non-specific DAB staining and tissue structure controls, respectively. **B**. Representative IHC images of tumor sections with high (left) and low (54) KDM4B. For each image, the percentage of cancer cell nuclei staining positive for KDM4B is denoted in the lower left corner. For **A** and **B**, scale bar for entire section, 100 μm; scale bar for inset, 50 μm. **C**. Box-whisker plot of KDM4B nuclear staining in normal ovary (N, n=9), primary HGSA tumors (P, n=30) and metastases (M, n=29). Diamond, mean; Significance of staining differences was determined using Kruskal-Wallace, with Mann-Whitney U-test (*, $P<0.001$). **D**. Percentage of total patient samples in each category (normal, primary and metastasis) staining for high or low KDM4B (high > 10% nuclei staining positive for KDM4B, low <10%). **E**. Correlation between KDM4B staining in Metastases (n=29) compared to matched primary tumors (n=29). Significance determined by Spearman's correlation. **F**. KDM4B expression in representative normal ovarian surface epithelium. Scale bar, 100 μm.

The expression of the tumor hypoxia marker Carbonic anhydrase 9 (CA-IX) was also scored in the TMAs (Fig. 2.6A and 2.6B, Fig. 2.4). Average intensity of CA-IX staining for triplicate tumor sections in the HGSA tumors (range 0-3) was positively correlated to the percentage of KDM4B-positive tumor nuclei (Fig. 2.6B). When the primary and metastatic tumors were analyzed separately, this correlation extended to each group, although significance was achieved only in the metastases (P=0.03). Additionally, KDM4B was robustly expressed in multiple cell lines representing a broad range of EOC genotypes, particularly in response to hypoxia (0.5% oxygen, Fig. 2.6C). There was weak hypoxic induction of KDM4B in the immortalized OSE cell line HIO80 (Fig. 2.6C). KDM4B is expressed in hypoxic epithelial ovarian cancer cells, and may contribute to progression of HGSA.

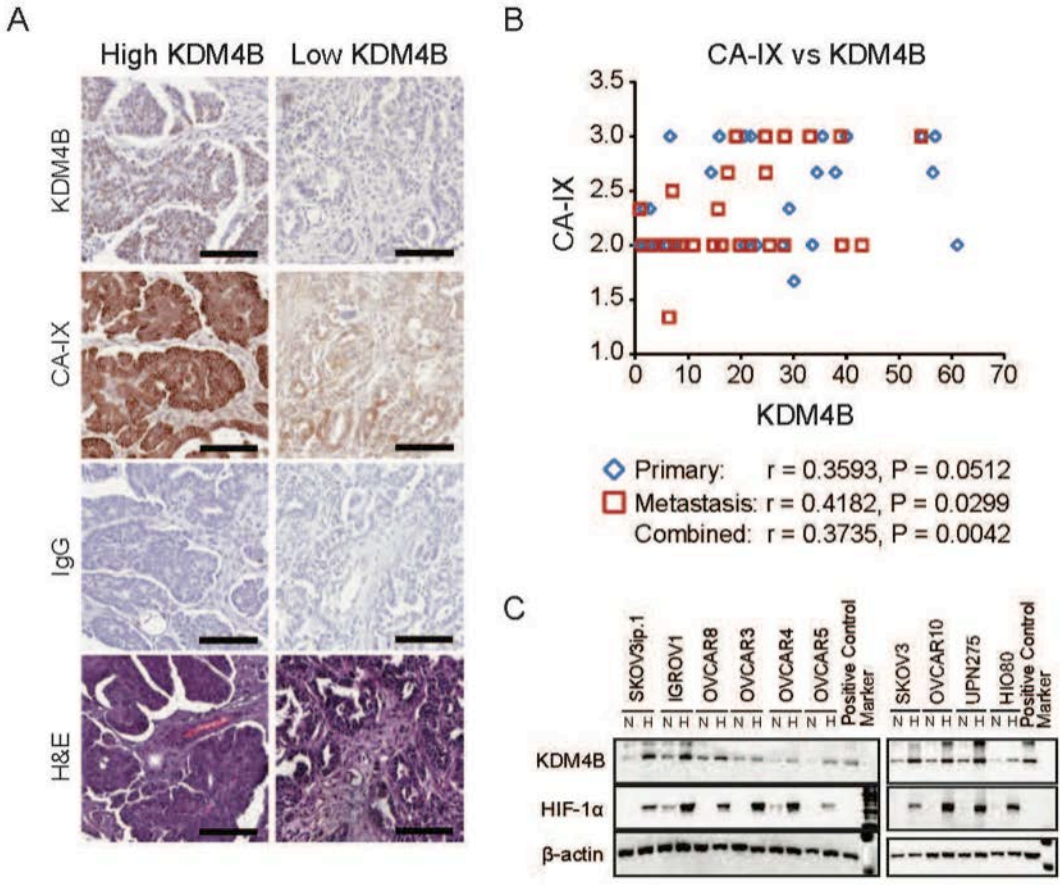
A
High KDM4B
Low KDM4B
KDM4B
CA-IX
IgG
H&E
B
CA-IX vs KDM4B
CA-IX
KDM4B
Primary: r = 0.3593, P = 0.0512
Metastasis: r = 0.4182, P = 0.0299
Combined: r = 0.3735, P = 0.0042
C
SKOV3ip.1
IGROV1
OVCAR8
OVCAR3
OVCAR4
OVCAR5
Positive Control Marker
SKOV3
OVCAR10
UPN275
HIO80
Positive Control Marker
KDM4B
HIF-1α
β-actin

Figure 2.6. KDM4B is expressed in hypoxic ovarian cancer tumors and EOC cell lines. A. Representative images of TMA sections demonstrating association between elevated KDM4B staining with elevated CA-IX staining. IgG and H&E serve as negative and tissue structure controls, respectively. Scale bar = 50 μm. **B**. Scatter plot of hypoxia (CA-IX staining) vs. KDM4B staining in TMA sections. Blue diamonds, primary tumors (n=30); red squares, metastatic tumors (n=29). Statistical significance determined using Spearman's correlation. P value < 0.05, is considered significant. **C**. Immunoblot detection of KDM4B and HIF-1α in a panel of ovarian cancer cell lines in normoxia (N, 21% oxygen) and in hypoxia (H, 0.5% oxygen). HIO-80 cells serve as non-transformed OSE control. HIF-1α indicates cellular hypoxia, Beta-actin serves as loading control.

KDM4B Differentially Regulates Gene Expression in Atmospheric and Hypoxic Growth Conditions. In order to identify genes regulated by KDM4B in EOC, SKOV3ip.1 cells were transiently transfected with siRNA to KDM4B (siK4B) or an irrelevant control (siCon), achieving robust knockdown in both normoxia (21% oxygen) and hypoxia (0.5% oxygen) (Fig. 2.7A-2.7B). SKOV3ip.1 cells form peritoneal xenograft tumors in a manner consistent with human EOC, facilitating translation of gene expression data to functional analysis (Yoneda, Kuniyasu et al. 1998; Rankin, Fuh et al. 2010). Consistent with prior reports (Beyer, Kristensen et al. 2008), loss of KDM4B did not increase bulk H3K9 trimethylation (H3K9me3) or dimethylation (H3K9me2) in SKOV3ip.1 or OVCAR8 cell lines (Fig. 2.7A, Fig. 2.8A, respectively). Similar results were observed for bulk H3K36 trimethylation and dimethylation (Fig. 2.7A, Fig. 2.8A). These results suggest that KDM4B regulates gene expression through specific mechanisms rather than global shifts in chromatin modification (Beyer, Kristensen et al. 2008). Genes dependent on KDM4B in either 21% or 0.5% oxygen were identified by expression microarray analysis (See Methods). KDM4B positively regulated expression of 1864 gene probes in normoxia, and 932 gene probes in hypoxia, with an overlap of 185 genes regulated in both conditions (Fig. 2.7C). The predominant pathways regulated by KDM4B in each oxygen condition were distinctly different (Fig. 2.9). In normoxia, KDM4B predominantly regulated genes involved in cancer, cell cycle (including DNA replication, recombination, and repair), and cell death pathways. In hypoxia, KDM4B regulated genes associated with inflammatory response, cellular development, and cellular movement, implying a possible role in metastasis. Complete microarray data was deposited under accession number GSE66894 in the NCBI Gene Expression Omnibus, which can be accessed to see all genes differentially regulated in normoxia and hypoxia with or without KDM4B (Edgar, Domrachev et al. 2002). Several genes were associated with metastatic pathways: Platelet derived growth factor beta (*PDGFB*, a potent angiogenic, lymphangiogenic, and transformative factor (Schito, Rey et al. 2012)); lipocalin 2 (*LCN2* or neutrophil gelatinase, a protease associated with cell invasion and inflammatory response); and lysyl oxidase-like 2 (*LOXL2*, a collagen hydroxylase associated with metastasis (Erler, Bennewith et al. 2006; Barker, Chang et al. 2011; Barker and Erler 2011)) were dependent on KDM4B in both oxygen tensions

(Fig. 2.7D). Regulation of *PDGFB*, *LCN2*, *LOXL2*, and *LOX* (lysyl oxidase, another collagen hydroxylase associated with metastasis (Erler, Bennewith et al. 2006)) was further validated in SKOV3ip.1 cells stably transduced with two shRNA constructs specifically targeting *KDM4B* (shK-1 and shK-2, Fig. 2.7E, See Fig. 2.8 for specificity compared to other KDM4 family members). *LCN2* was decreased by approximately 50% following KDM4B knockdown in normoxia and hypoxia, while hypoxic induction of *PDGFB*, *LOX*, and *LOXL2* decreased by 25-30%. Knockdown of KDM4B in OVCAR8 cells decreased expression of *PDGFB* and *IGFBP1* approximately 50% in both normoxia and hypoxia (Fig. 2.8F). Increased expression of *LOX* in EOC patient tumor samples associates with poor progression-free survival (Gyorffy, Lanczky et al. 2012), linking a putative KDM4B target gene to disease progression (Fig. 2.7F). Combined, these data suggest KDM4B regulates distinct functions in different oxygen tensions, providing multiple avenues to affect EOC tumor growth.

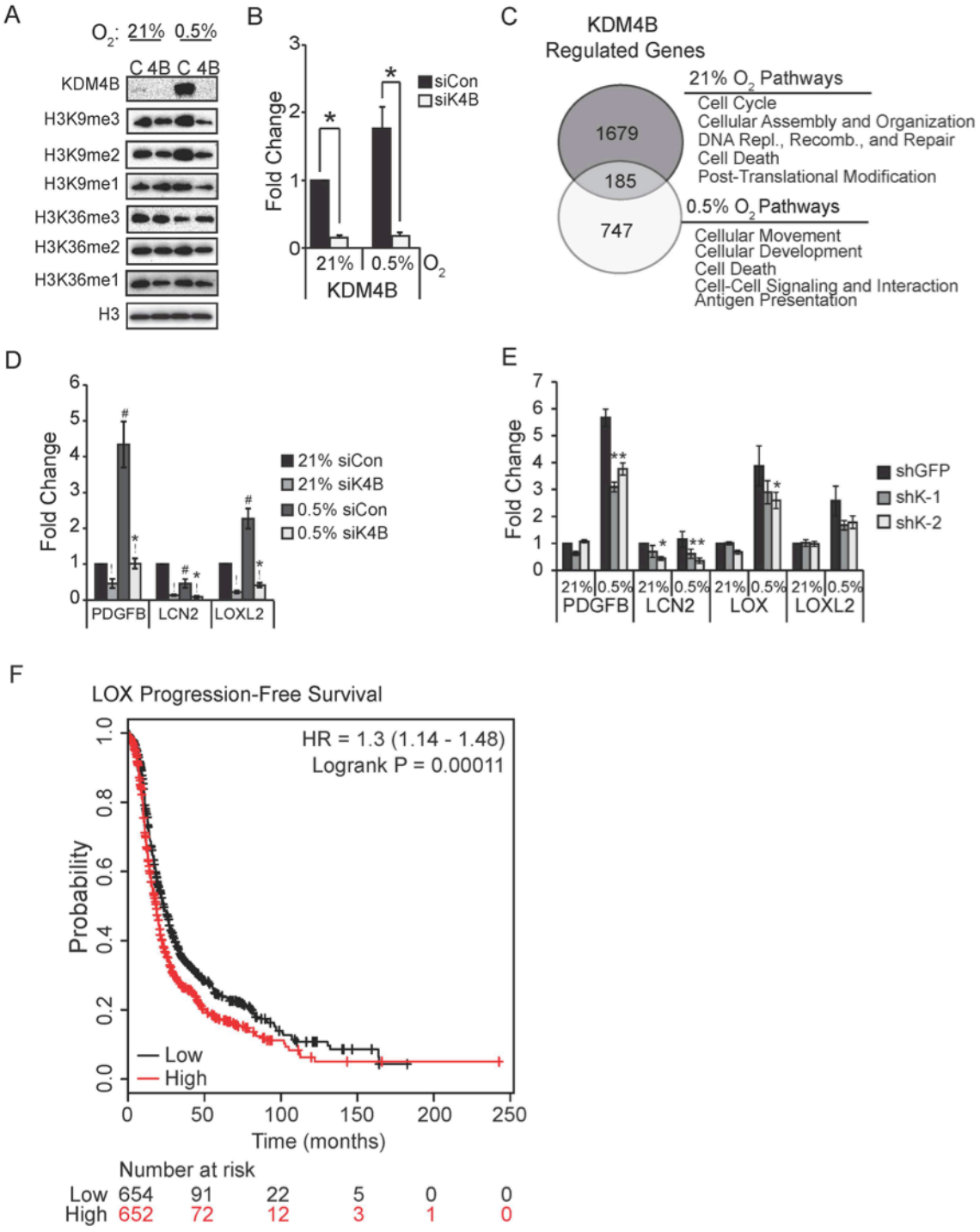
A
O2: 21% 0.5%
C 4B C 4B
KDM4B
H3K9me3
H3K9me2
H3K9me1
H3K36me3
H3K36me2
H3K36me1
H3
B
Fold Change
siCon
siK4B
21%
0.5%
O2
KDM4B
C
KDM4B
Regulated Genes
1679
185
747
21% O2 Pathways
Cell Cycle
Cellular Assembly and Organization
DNA Repl., Recomb., and Repair
Cell Death
Post-Translational Modification
0.5% O2 Pathways
Cellular Movement
Cellular Development
Cell Death
Cell-Cell Signaling and Interaction
Antigen Presentation
D
Fold Change
21% siCon
21% siK4B
0.5% siCon
0.5% siK4B
PDGFB
LCN2
LOXL2
E
Fold Change
shGFP
shK-1
shK-2
21%
0.5%
PDGFB
LCN2
LOX
LOXL2
F
LOX Progression-Free Survival
HR = 1.3 (1.14 - 1.48)
Logrank P = 0.00011
Probability
Low
High
Time (months)
Number at risk
Low 654 91 22 5 0 0
High 652 72 12 3 1 0

Figure 2.7. KDM4B regulates different pathways in normoxia and hypoxia. A. Immunoblotting of KDM4B expression, H3K9me3, H3K9me2, H3K9me1, H3K36me3, H3K36me2, and H3K36me1 in SKOV3ip.1 cells transfected with siRNA to *KDM4B* (4B) or control siRNA (C) in Panel A. Histone H3 serves as control for protein loading. **B**, Quantitative RT-PCR of *KDM4B* expression in SKOV3ip.1 cells transfected with siRNA to *KDM4B* (siK4B) or control siRNA (siCon) and exposed to 21% or 0.5% oxygen for 16 hours. **C**, Venn diagram showing the overlap between genes down-regulated greater than 1.4 fold by siK4B in normoxia (top circle) and hypoxia (bottom circle). **D**, Quantitative RT-PCR validation of selected metastasis-associated genes regulated by KDM4B. Data in B and D represent mean fold change ± S.E.M. normalized to 18S rRNA, calculated relative to siCon in 21% O2 (black bars). Results were averaged from three independent experiments, measured in triplicate. Significance of differences was calculated using two-tailed paired Student's T-test (!, $P<0.05$ for siK4B compared to siCon,; #, $P<0.05$ for hypoxia compared to normoxia) or two-way ANOVA (*, $P<0.05$ for interactions between oxygen conditions and KDM4B expression). **E**. qRT-PCR measurement of *PDGFB*, *LCN2*, and *LOX* in SKOV3ip.1 cells expressing shRNA to *KDM4B* (shK-1, dark grey and shK-2, light grey) cultured in the indicated oxygen tensions. Data in Panels E represents mean fold change ± S.E.M, normalized to 18S rRNA and shGFP control at 21% oxygen (n=5 measured in triplicate). *, $P<0.05$, determined by two-tailed paired Student's t-test, relative to shGFP control at the respective oxygen tension. **F**. Kaplan Meier progression-free survival plot of *LOX* expression in all stages of serous epithelial ovarian cancer from data set curated by Gyorffy et al. 2012 ($P<0.05$).

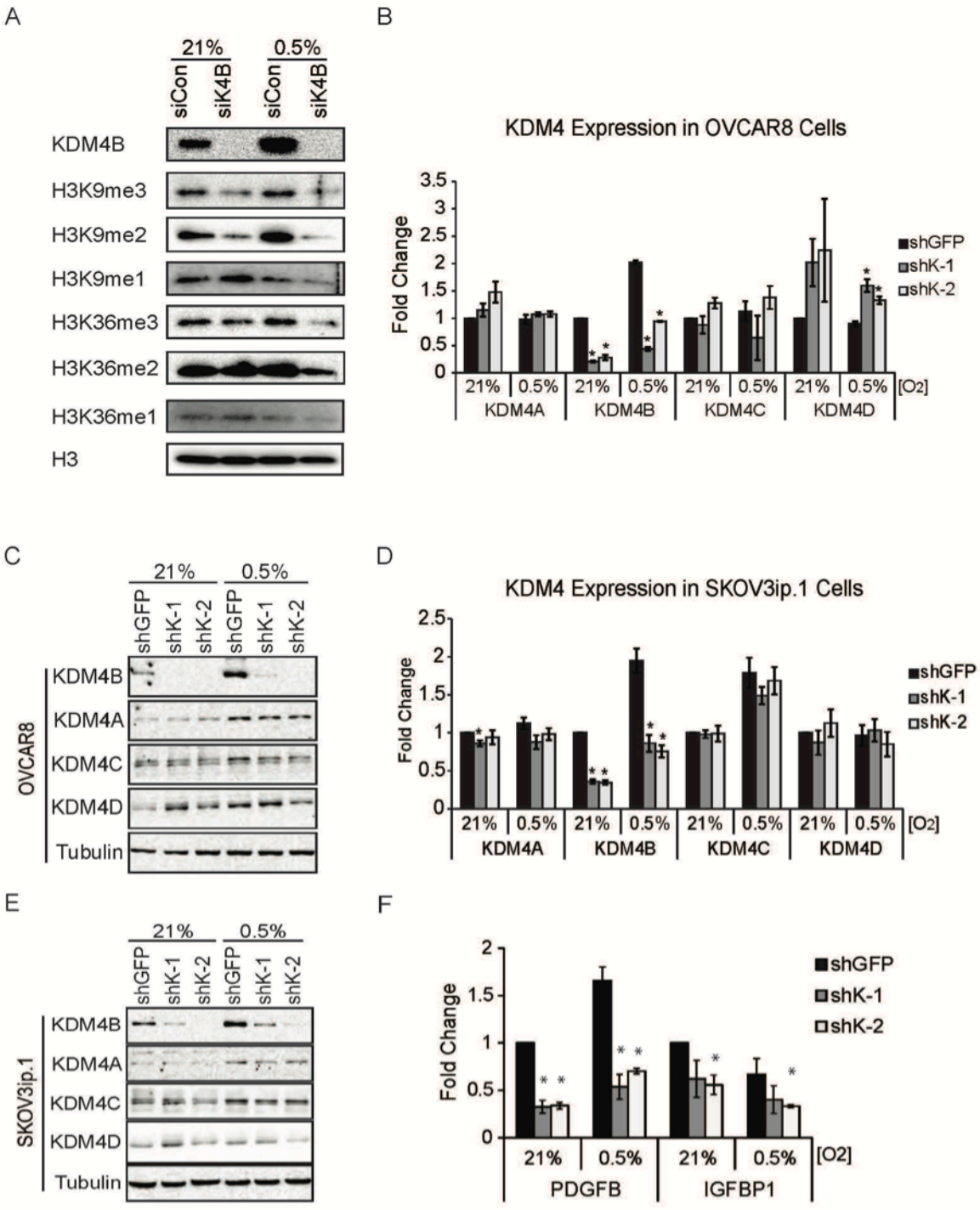
A
21%
0.5%
siCon
siK4B
siCon
siK4B
KDM4B
H3K9me3
H3K9me2
H3K9me1
H3K36me3
H3K36me2
H3K36me1
H3
B
KDM4 Expression in OVCAR8 Cells
Fold Change
shGFP
shK-1
shK-2
21%
0.5%
[O2]
KDM4A
KDM4B
KDM4C
KDM4D
C
21%
0.5%
shGFP
shK-1
shK-2
OVCAR8
KDM4B
KDM4A
KDM4C
KDM4D
Tubulin
D
KDM4 Expression in SKOV3ip.1 Cells
Fold Change
shGFP
shK-1
shK-2
[O2]
KDM4A
KDM4B
KDM4C
KDM4D
E
21%
0.5%
shGFP
shK-1
shK-2
SKOV3ip.1
KDM4B
KDM4A
KDM4C
KDM4D
Tubulin
F
Fold Change
shGFP
shK-1
shK-2
[O2]
PDGFB
IGFBP1

Figure 2.8. KDM4B Regulates Expression of PDGFB and IGFBP1 in OVCAR8 expressing shRNA to KDM4B. **A**. Immunoblotting of KDM4B, H3K9me3, H3K9me2, H3K9me1, H3K36me3, H3K36me2, and H3K36me1 expression in OVCAR8 cells. Histone H3 serve as control for protein loading. **B**. Quantitative RT-PCR measurement of KDM4 subfamily members in SKOV3ip.1 cells. **C**. Immunoblot of KDM4 subfamily members in SKOV3ip.1 cells. α-Tubulin serves as a loading control. **D**. Quantitative RT-PCR measurement of KDM4 subfamily members in OVCAR8 cells. Data represent mean ± S.E.M., normalized to 18S rRNA and shGFP control at 21% O2. Results were averaged from three independent experiments, measured in triplicate. *, $P<0.05$, determined by two-tails paired Student's t-test. **E**. Immunoblot of KDM4 subfamily members in OVCAR8 cells. Tubulin serves as a loading control. **F**. Quantitative RT-PCR measurement of *PDGFB* and *IGFBP1* in OVCAR8 cells expressing shRNA to KDM4B (shK-1, dark grey and shK-2, light grey) in 21%, and 0.5% oxygen. QPCR data in panels B, D, and F represent the mean ± S.E.M., normalized to 18S rRNA and shGFP control at 21% O2. Results were averaged from three independent experiments, measured in triplicate. *, $P<0.05$, determined by two-tailed paired Student's t-test.

Top Bio Functions in 21% Oxygen			**Top Bio Functions in 0.5% Oxygen**		
Diseases and Disorders			Diseases and Disorders		
Name	P-value	# Molecules	Name	P-value	# Molecules
Cancer	6.37E-20 - 7.63E-04	496	Inflammatory Response	1.64E-12 - 5.57E-03	97
Gastrointestinal Disease	4.81E-16 - 8.16E-04	422	Inflammatory Disease	5.53E-05 - 4.52E-03	90
Hematological Disease	5.56E-13 - 7.63E-04	141	Renal and Urological Disease	5.53E-05 - 3.50E-03	29
Genetic Disorder	2.03E-11 - 7.94E-04	249	Respiratory Disease	1.46E-04 - 2.11E-03	22
Infectious Disease	9.82E-11 - 6.64E-04	187	Hematological Disease	1.48E-04 - 3.26E-03	8
Molecular and Cellular Functions			Molecular and Cellular Functions		
Name	P-value	# Molecules	Name	P-value	# Molecules
Cell Cycle	7.00E-15 - 8.16E-04	239	Cellular Movement	2.51E-10 - 5.57E-03	77
Cellular Assembly and Organization	6.70E-14 - 7.94E-04	197	Cellular Development	8.92E-10 - 4.14E-03	99
DNA Replication, Recombination, and Repair	6.70E-14 - 8.16E-04	182	Cell Death	4.59E-07 - 5.57E-03	100
Cell Death	8.00E-14 - 8.19E-04	353	Cell-To-Cell Signaling and Interaction	8.13E-07 - 5.57E-03	78
Post-Translational Modification	1.29E-08 - 7.92E-04	153	Antigen Presentation	1.00E-06 - 4.46E-03	50

Figure 2.9. Summary of Ingenuity Pathway Analysis of KDM4B-Regulated Genes in 21% and 0.5% Oxygen.

KDM4B Binds and Demethylates Regulatory Regions of Target Genes to Promote Expression. KDM4B primarily regulates gene expression by demethylating H3K9me3, enhancing transcription by removing a modification associated with repression (Mosammaparast and Shi 2010). Stable loss of KDM4B did not result in any changes in bulk histone H3K9me3 in either SKOV3ip.1 or OVCAR8 cells under any oxygen tensions examined (Fig. 2.10A). In order to determine if KDM4B directly regulated putative target gene expression, SKOV3ip.1cells were exposed to 21% and 0.5% oxygen for 16 hours, and chromatin immunoprecipitation (ChIP) was performed using antibodies against KDM4B and H3K9me3. In SKOV3ip.1-shGFP cells, KDM4B was localized to regions near the transcription start sites of *PDGFB*, *LCN2*, *LOX*, and *LOXL2* (Fig. 2.10B and 2.10C), with a 3-6 fold increase in association in 0.5% oxygen. Following knockdown, association of KDM4B to regulated promoters decreased to levels similar to an isotype specific IgG control. Knockdown of KDM4B increased enrichment of H3K9me3 at the promoters of *PDGFB*, *LCN2*, *LOX*, and *LOXL2* in 21% oxygen (Fig. 2.10D). In 0.5% oxygen, knockdown of KDM4B elevated H3K9me3 compared to the control. However, the overall magnitude of association at PDGFB, LCN2, and LOX decreased in hypoxia, making this difference less significant. The enrichment of H3K9me3 on a control "gene desert" region was not significantly affected by loss of KDM4B or by hypoxia (Fig. 2.10E). Combined, these results demonstrate that KDM4B associates with regulatory regions of target genes, and demethylates histones residing near transcription start sites to regulate gene expression.

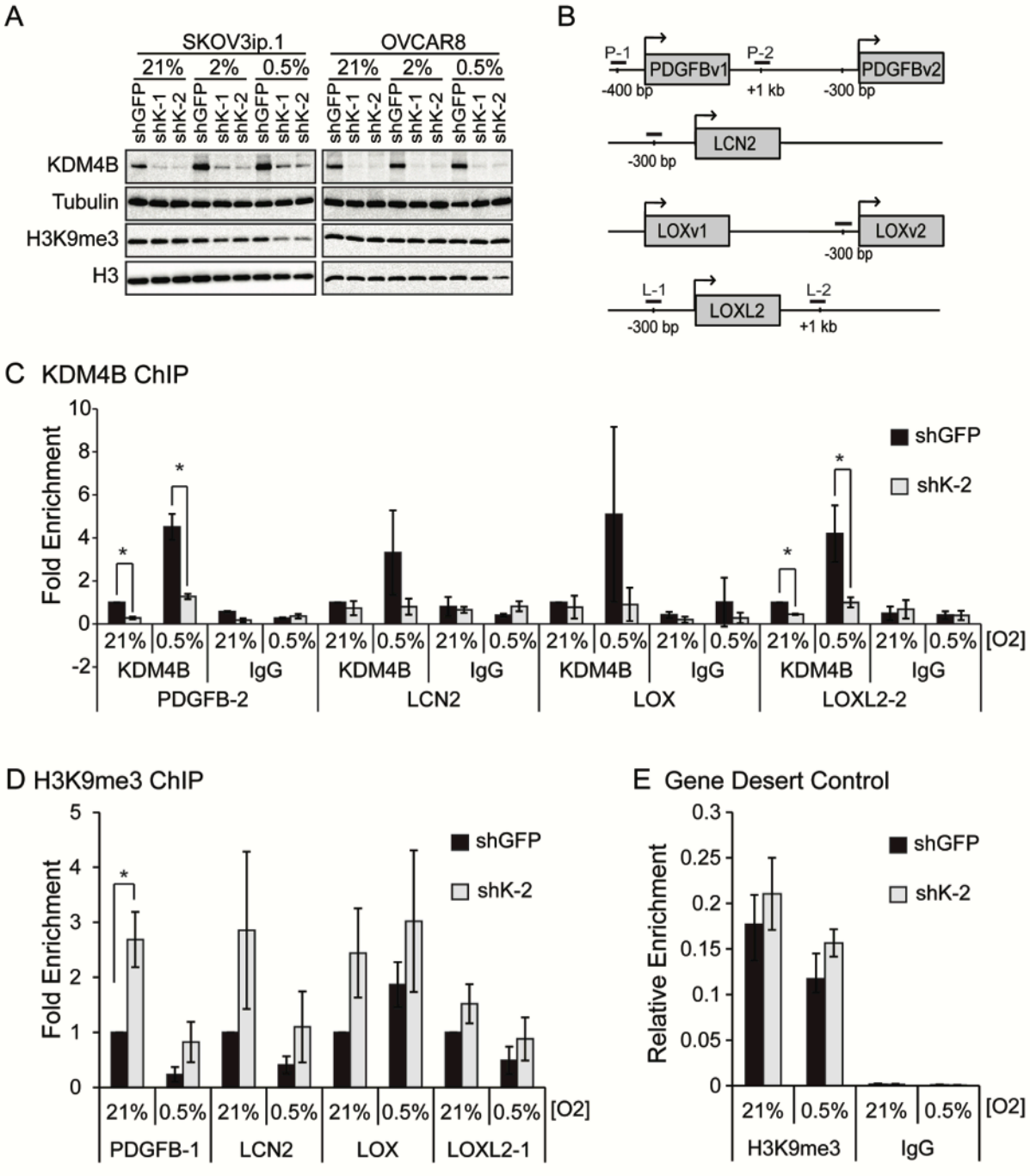
A
SKOV3ip.1
OVCAR8
21%
2%
0.5%
shGFP
shK-1
shK-2
KDM4B
Tubulin
H3K9me3
H3
B
P-1
PDGFBv1
P-2
PDGFBv2
-400 bp
+1 kb
-300 bp
LCN2
LOXv1
LOXv2
L-1
LOXL2
L-2
C KDM4B ChIP
Fold Enrichment
shGFP
shK-2
[O2]
KDM4B
IgG
PDGFB-2
LCN2
LOX
LOXL2-2
D H3K9me3 ChIP
PDGFB-1
LOXL2-1
E Gene Desert Control
Relative Enrichment
H3K9me3

Figure 2.10. KDM4B binds regions proximal to target gene promoters and demethylates histone H3K9me3 to regulate expression. **A**. Immunoblot measurement of KDM4B and H3K9me3 in SKOV3ip.1 and OVCAR8 cells expressing shRNA targeting *KDM4B* (shK-1 and shK-2) or GFP (control) in 21%, 2%, and 0.5% O2. Tubulin and histone H3 serve as loading controls. **B**. Map of ChIP-qPCR primers sets used to measure KDM4B association and histone H3K9 methylation at or near target gene promoters. **C**. ChIP assay for KDM4B near promoters of *PDGFB*, *LCN2*, *LOX*, and *LOXL2* genes in SKOV3ip.1 cells expressing shRNA to *KDM4B* (shK-2, light grey bars) compared to shGFP control (black bars). Cells were treated with normoxia (21%) or hypoxia (0.5%) for 16 hours. Data represent mean fold enrichment ± S.E.M of three independent experiments (n=3) measured in triplicate, normalized input and then to GFP control at 21% O2. **D**. ChIP qPCR analysis of H3K9me3 on indicated promoter regions of the *PDGFB*, *LCN2*, *LOX*, and *LOXL2* genes following shRNA to *KDM4B* (shK-2, light grey bars) compared to shGFP control (black bars). Data represent the mean of four independent experiments ± S.E.M (n=4) measured in triplicate, and normalized to shGFP control following subtraction of IgG signal and normalization to a gene desert control region as described in Material and Methods. **E**. H3K9me3 ChIP to a gene desert control region. Data represent the mean of four independent experiments ± S.E.M (n=4) measured in triplicate normalized to input. Significance relative to shGFP control was determined using paired Student's t-test (*, $P < 0.05$).

KDM4B Regulates Cell Invasion, Migration, and Spheroid Formation *In Vitro*. In order to determine if KDM4B mediates metastatic phenotypes, SKOV3ip.1 and OVCAR8 cells were seeded to Boyden chamber migration and invasion assays (Fig. 2.11A-2.11F). Following KDM4B knockdown, both cell lines demonstrated a significantly reduced invasion through Matrigel with up to 60% decrease in invasion (Fig. 2.11A, 2.11C, 2.11D, 2.11E). Migration through uncoated inserts was decreased by approximately 25-30% in SKOV3ip.1 cells (Fig. 2.11B). In OVCAR8 cells, migration through uncoated chambers was severely attenuated (>80%, Fig. 2.11E), indicating that while KDM4B was universally important for regulating invasive behavior in both cell lines, its effects on invasion and migration may be mediated through distinct, but overlapping mechanisms. Stable knockdown of KDM4B had little effect on cellular doubling time in SKOV3ip.1 and OVCAR8 cells (Figs. 2.12A and 2.12B), nor were there significant differences between proliferation controls used for Boyden chamber assays (Fig. 2.12C and 2.12D).

Another characteristic of EOC is the tendency to form clusters of cells suspended in ascites that seed the peritoneal compartment (Lengyel 2010). Using *in vitro* spheroid formation assays (Vinci, Gowan et al. 2012), loss of KDM4B significantly reduced the volume of spheroids by 50% in SKOV3ip.1 cells, with similar results in OVCAR8 cells (Fig. 2.11G and 2.11I). Decreased spheroid volume was significant under 21% O_2 and 2% O_2 treatments for SKOV3ip.1 and OVCAR8 spheroids (Fig. 2.11G and 2.11I). Additionally, the control spheroids were more rounded and smoother in appearance, indicating more robust cell-to-cell contact (Fig. 2.11H and 2.11J). Combined, these results indicate that KDM4B may influence ovarian cancer progression by promoting formation of ascites spheroids in the peritoneal cavity and subsequent invasion of these clusters to peritoneal tissues.

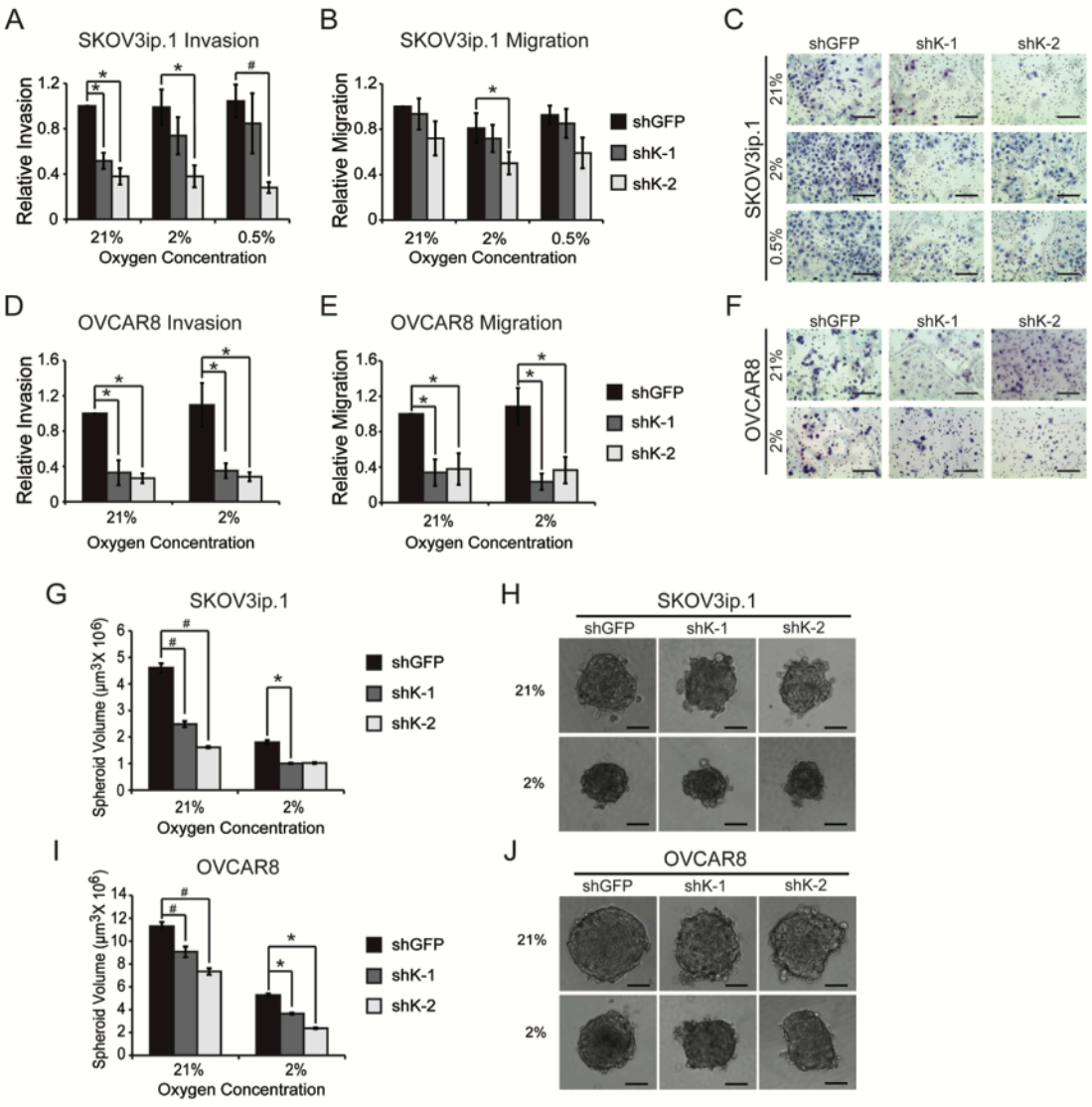
A
SKOV3ip.1 Invasion
Relative Invasion
1.2
0.8
0.4
0
21%
2%
0.5%
Oxygen Concentration
B
SKOV3ip.1 Migration
Relative Migration
shGFP
shK-1
shK-2
C
shGFP
shK-1
shK-2
SKOV3ip.1
21%
2%
0.5%
D
OVCAR8 Invasion
1.6
E
OVCAR8 Migration
F
OVCAR8
G
SKOV3ip.1
Spheroid Volume (μm3X 10^6)
H
I
OVCAR8
J

Figure 2.11. KDM4B supports ovarian cancer cell invasion, migration, and 3D spheroid formation. **A**. SKOV3ip.1 Matrigel Invasion Assay. 5×10^4 SKOV3ip.1 cells expressing the indicated shRNA were seeded to Boyden Chambers coated with Matrigel and cultured for 24 hours in the indicated oxygen tensions. Cells were trypsinized and quantified as described in Methods. **B**. Migration Assay. 5×10^4 SKOV3ip.1 cells were seeded to empty Boyden chambers, cultured and quantified as in Panel A. Data in Panel A and B represent mean ± S.E.M for five independent experiments (n=3). **C**. Representative image of SKOV3ip.1 invasion assay. Filters treated in parallel to those in Panel A were fixed and stained, as described in Methods. 100X magnification, scale bar = 200 μm. **D**. OVCAR8 invasion assay performed as in panel A. **E**. Migration assay for OVCAR 8 cells, treated as in Panel B. Data in Panel D and E represent the mean ± S.E.M for four independent experiments, n=3. **F**. Representative images of OVCAR8 Matrigel invasion assay. 100X magnification, scale bar = 200 μm. **G**. SKOV3ip.1 spheroid formation assay. SKOV3ip.1 cells transduced with the indicated shRNA were cultured in ULA dishes in 21% and 2% O2 as described in Methods. After four days, spheroid volume was calculated. Data represent mean volume ± S.E.M. n=16. **H**. Representative images (median volume) of SKOV3ip.1 spheroids. 100X magnification, scale bar = 100 μm. **I**. OVCAR8 spheroid formation assay, conducted as described for G. **J**. Representative images (median volume) of OVCAR8 spheroids. 100X magnification, scale bar = 100 μm. For Panels A, B, D, E, G and I, significance was calculated relative to shGFP control at each oxygen condition, using Mann Whitney U-tests (*, $P<0.05$; #, $P<0.005$**).**

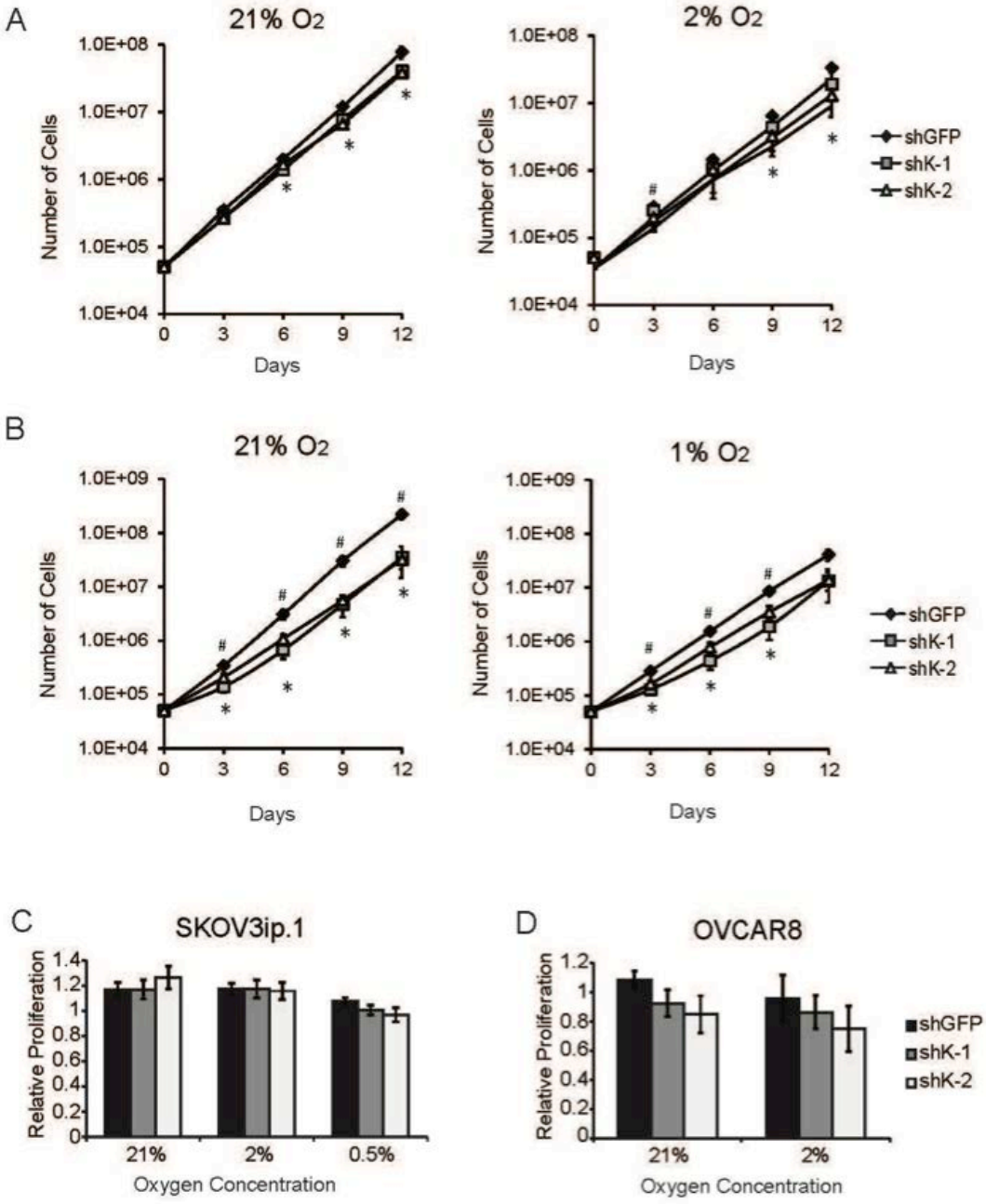
A
21% O2
2% O2
Number of Cells
Days
shGFP
shK-1
shK-2
B
21% O2
1% O2
C
SKOV3ip.1
Relative Proliferation
21%
2%
0.5%
Oxygen Concentration
D
OVCAR8

Figure 2.12. Suppression of KDM4B Does Not Regulate Proliferation In SKOV3ip.1 and OVACR8 cells. A. SKOV3ip.1 cells transduced with shRNA to *KDMB* (shK-1 and shK-2) were seeded for growth curve experiments as described in Methods, and cultured in 21% O_2 and 2% O_2. Data represent four independent experiments conducted in triplicate. **B**. OVCAR8 cells transduced with shRNA to *KDMB* (shK-1 and shK-2) were seeded for growth curve experiments as described in Supplemental Methods, and cultured in 21% O2 and 1% O2. Data represent three independent experiments, conducted in triplicate. Data in panels A and B represent mean ± S.E.M. #, $P<0.05$, comparing shK-1 to shGFP; *, $P<0.05$, comparing shK-2 to shGFP; determined by two-tailed paired Student's t-test. **C-D**, Proliferation controls for Boyden Chamber Migration and Matrigel Invasion Assay. 25 000 cells were seeded as monolayers in parallel with cells seeded for Boyden chamber assays. After 24 hours, cells were trypsinized, frozen, and analyzed as described in Methods. Data represent mean ± S.E.M. Results were averaged from five (SKOV3ip.1, C) or four (OVCAR8, D) independent experiments conducted in triplicate. * = $P<0.05$, determined by two-tailed paired Student's t-test.

KDM4B Regulates Seeding and Growth of Peritoneal Tumors. The *in vivo* role of KDM4B in EOC tumor progression was determined using intraperitoneal (i.p.) tumor xenografts. Loss of KDM4B significantly inhibited peritoneal seeding and tumor growth for both SKOV3ip.1 and OVCAR8 cells, as measured by bioluminescence (Fig. 2.13). This effect was significant for both constructs in SKOV3ip.1 cells (Fig. 2.13A-2.13C), whereas shK-2 showed the most significant effect in OVCAR8 cells, with a trend of reduced growth for shK-1 (Fig. 2.13D-2.13F). Total endpoint tumor weight was decreased by at least 50% in SKOV3ip.1 cells and OVCAR8 cells (Fig. 2.13G-2.13H). OVCAR8 cells expressing shRNA to KDM4B developed less ascites fluid compared to controls, consistent with the effect on tumor seeding and growth. (Fig. 2.13I). Terminal necropsy confirmed a general decrease in the size of metastatic nodules in the omentum, viscera, and peritoneal wall (Fig. 2.13J). Immunohistochemical detection of KMD4B in xenograft tumors confirmed the stability of knockdown throughout the study (Fig. 2.14A-2.14D). KDM4B was expressed in hypoxic regions of tumor epithelium as determined by pimonidazole and PAX8 staining (Fig. 2.14E-2.14H, and 2.14I-2.14L, respectively). There was no apparent difference in cell proliferation (Ki-67 staining, Fig. 2.14M-2.14P), consistent with *in vitro* experiments (Fig. 2.12). QPCR measurement of *KDM4A, KDM4B, KDM4C,* and *KDM4D* RNA in xenograft tumors (Fig. 2.14Y and 2.14Z, respectively) confirmed stable knockdown of *KDM4B*, while also identifying slight increases in expression of *KDM4A* and *KDM4D*. Combined, these studies demonstrate a role for hypoxic expression of KDM4B in the establishment and growth of peritoneal tumors.

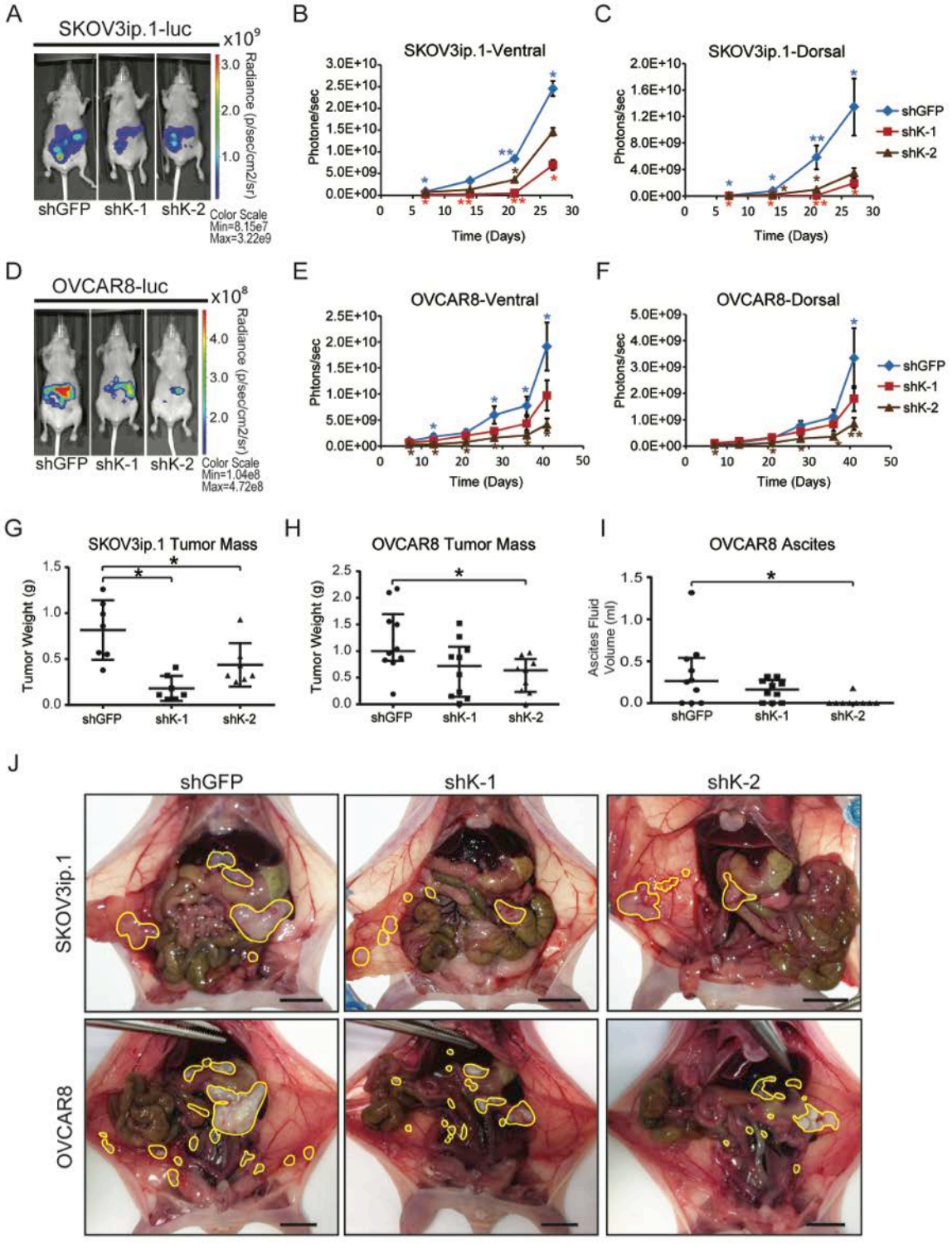
A
SKOV3ip.1-luc
x10^9
Radiance (p/sec/cm2/sr)
3.0
2.0
1.0
shGFP
shK-1
shK-2
Color Scale
Min=8.15e7
Max=3.22e9
B
SKOV3ip.1-Ventral
Photone/sec
Time (Days)
C
SKOV3ip.1-Dorsal
Photons/sec
Time (Days)
shGFP
shK-1
shK-2
D
OVCAR8-luc
x10^8
Radiance (p/sec/cm2/sr)
Color Scale
Min=1.04e8
Max=4.72e8
E
OVCAR8-Ventral
Phtons/sec
Time (Days)
F
OVCAR8-Dorsal
Photons/sec
Time (Days)
G
SKOV3ip.1 Tumor Mass
Tumor Weight (g)
H
OVCAR8 Tumor Mass
Tumor Weight (g)
I
OVCAR8 Ascites
Ascites Fluid Volume (ml)
J
shGFP
shK-1
shK-2
SKOV3ip.1
OVCAR8

Figure 2.13. KDM4B regulates peritoneal seeding and growth of ovarian cancer cells. A. Representative ventral bioluminescent images of nude mice injected with SKOV3ip.1-luc-neo cells transduced with indicated shRNA constructs. Image represents the median tumor load for each group, 28 days after injection. **B**. Longitudinal ventral bioluminescence measurement for all mice injected with SKOV3ip.1-luc-neo transduced with indicated shRNA. Data represents mean total radiance (photons/sec) for each group ± SEM, (n = 9 or 10 mice per group). Blue diamonds = shGFP, red squares = shK-1, brown triangles = shK-2. **C**. Dorsal bioluminescence for SKOV3ip.1 study, analyzed as in B. **D**. Representative images of mice injected with OVCAR8-luc-neo cells transduced with the indicated shRNA constructs. Image was captured at Week 6 of study. **E**. Ventral bioluminescence measurement for all mice injected with OVCAR8-luc-neo transduced with indicated shRNA constructs, analyzed as in B. **F**. Dorsal bioluminescence for OVCAR8 study, analyzed as in B. Statistics for B, C, E and F were calculated with Kruskal Wallis and Mann Whitney U-tests (*, $P<0.05$; **, $P<0.005$). Blue asterisks, difference among all three groups; red asterisks, difference between shK-1 and shGFP; brown asterisks, difference between shK-2 and shGFP. **G**. Box-whisker dot plot of total tumor weight for SKOV3ip.1 xenografts. (n = 7 per group). **H**. Dot plot of tumor weight for OVCAR8 xenografts (n=9 or 10). **I**. Dot plot of ascites fluid volume collected from OVCAR8 experiment. (n = 9 or 10 mice per group). For panels G-I, statistical significance was determined using Mann-Whitney U-test relative shGFP control (*, $P<0.05$). **J**. Representative end-point necropsy demonstrating differential tumor size and distribution in mice injected with SKOV3ip.1 or OVCAR8 cells. Scale bar = 1 cm. Visible tumors are circled in yellow. Note the large cluster of fused omental tumors in the shGFP controls, compared to the knockdown mice.

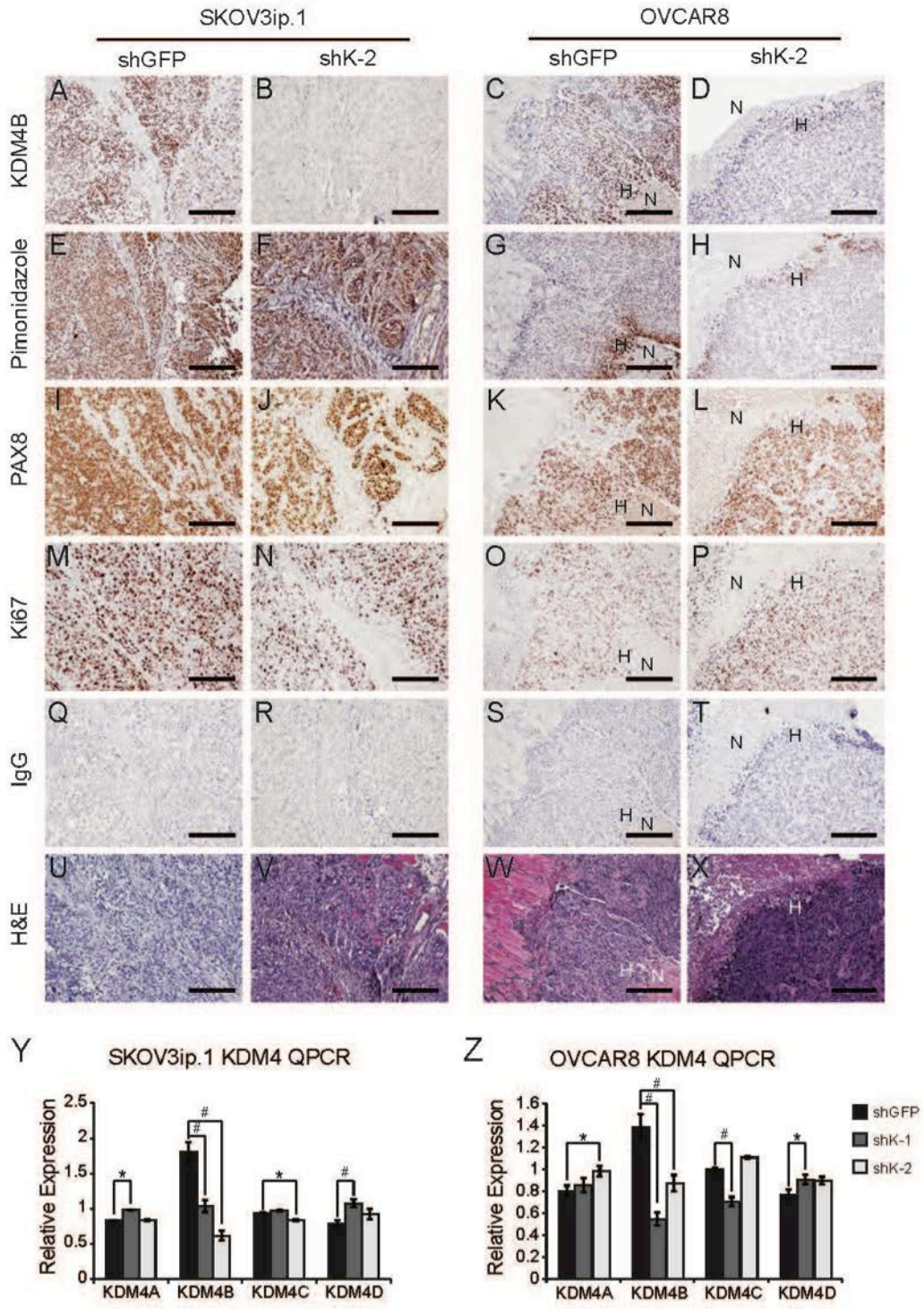
SKOV3ip.1
OVCAR8
shGFP
shK-2
shGFP
shK-2
KDM4B
Pimonidazole
PAX8
Ki67
IgG
H&E
A
B
C
D
E
F
G
H
I
J
K
L
M
N
O
P
Q
R
S
T
U
V
W
X
N
H
Y
SKOV3ip.1 KDM4 QPCR
Relative Expression
KDM4A
KDM4B
KDM4C
KDM4D
Z
OVCAR8 KDM4 QPCR
Relative Expression
KDM4A
KDM4B
KDM4C
KDM4D
shGFP
shK-1
shK-2

Figure 2.14. KDM4B is expressed in hypoxic regions of tumor xenografts. A-D. KDM4B. **E-H.** Pimonidazole. **I-L.** PAX8. **M-P.** Ki67. **Q-T.** IgG. **U-X.** H&E. Scale bar, 100 μm. N, necrosis; H, hypoxia. Panels **A**, **E**, **I**, **M**, **Q**, and **U** correspond to SKOV3ip.1 shGFP control tumor sections. Panels **B**, **F**, **J**, **N**, **R**, and **V** correspond to SKOV3ip.1 shK-2 KDM4B knockdown tumor sections. Panels **C**, **G**, **K**, **O**, **S**, and **W** correspond to OVCAR8 shGFP control tumors. Panels **D**, **H**, **L**, **P**, **T**, and **X** correspond to OVCAR8 shK-2 tumor sections. All IHC sections were counterstained with hematoxylin to visualize cell nuclei. Images were captured at 100X magnification. Scale bar = 200 μm. **Y**, QRT-PCR measurement of KDM4 subfamily members in SKOV3ip.1 xenograft tumors, as described in Methods. (shGFP, n=7; shK-1, n=7; shK-2, n=7). **Z,** QRT-PCR measurement of KDM4 subfamily members in OVCAR8 xenograft tumors. (shGFP, n=10; shK-1, n=9; shK-2, n=8). Data represents average fold change relative to shGFP control, after normalization to homo sapiens *GAPDH*. Significance was calculated by Mann Whitney U-test relative to shGFP control (*, $P < 0.05$). Note co-localization of KDM4B with pimonidazole staining near the necrotic core of the OVCAR8 shGFP biopsy (panels C and G).

Discussion

Developing more effective methods to attenuate peritoneal dissemination and tumor recurrence in ovarian cancer patients depends on improved understanding of the processes contributing to attachment-free growth of cancer cells in malignant ascites, invasion of cancer cells into the mesothelium, and establishment of new tumors. Our data suggests that KDM4B contributes significantly to pathways that influence peritoneal seeding of tumors. As a hypoxia-inducible regulator of peritoneal seeding, KDM4B represents a novel mechanism used by EOC cells to promote progression of ovarian cancer (Fig. 2.15).

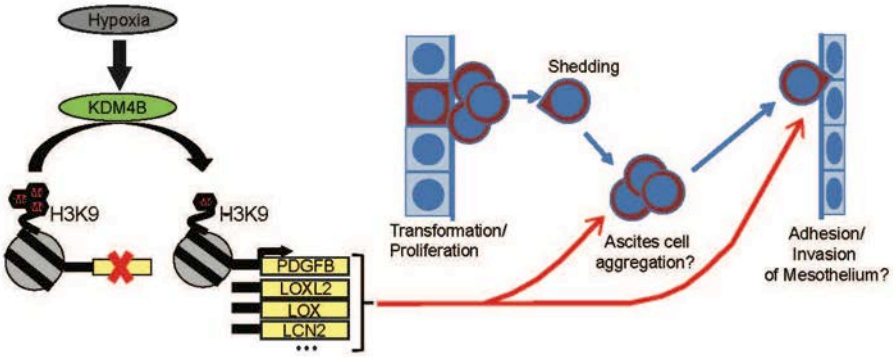
Hypoxia
KDM4B
H3K9
H3K9
PDGFB
LOXL2
LOX
LCN2
Shedding
Transformation/
Proliferation
Ascites cell
aggregation?
Adhesion/
Invasion
of Mesothelium?

Figure 2.15. KDM4B Regulates Peritoneal Seeding of Ovarian Cancer. Hypothesized mechanism of KDM4B signaling to promote ovarian cancer progression. Briefly, hypoxia induces the expression of KDM4B, catalyzing demethylation of histone H3K9me3 at target promoters and regulating expression of genes that facilitate the seeding of metastases in the viscera and peritoneal wall.

KDM4B regulates expression of multiple genes that may contribute to ovarian cancer growth and metastasis (Fig. 2.7). In the case of most proliferative genes identified in the initial screen, regulation by KDM4B was attenuated with stable knockdown (data not shown), most likely due to compensation from other KDM4 family members. KDM4D is a likely candidate, since we observed increased expression of protein and RNA following knockdown of KDM4B *in vitro* and *in vivo*. Compensatory *KDM4B* expression has been observed in the testes of KDM4*D* knockout mice, suggesting that our observations represent an inverse effect (Iwamori, Zhao et al. 2011). Of greater interest is the regulation of genes that may promote tumor metastasis. *PDGFB, LCN2, LOX,* and *LOXL2* depend on KDM4B for expression, corresponding to changes in histone methylation on their respective promoters. Demethylation of promoters in normoxia and hypoxia may facilitate expression of target genes by altering the dynamics of HIF binding, as in the case of KDM4C at the *LDHA* promoter (Luo, Chang et al. 2012). Members of the KDM4 family of histone demethylases, including KDM4B, are inhibited by hypoxic conditions (Beyer, Kristensen et al. 2008; Sanchez-Fernandez, Tarhonskaya et al. 2013). Other KDMs, such as KDM3A, may compensate to demethylate promoters in hypoxia (Beyer, Kristensen et al. 2008; Krieg, Rankin et al. 2010). Recent reports also indicate that KDM4A is stabilized in a HIF-independent manner to facilitate gene amplification, providing an alternate mechanism for hypoxic functions of the KDM4 family (Black, Atabakhsh et al. 2015). Finally, KDM4B forms a complex with MLL2 that associates with ERα to regulate gene expression in breast cancer (Shi, Sun et al. 2011). Future studies examining the interactions between KDM4B, HIF, other KDMs, and lysine methyltransferases (KMTs) will clarify the transcriptional mechanisms that regulate expression of KDM4B target promoters in hypoxia.

Stable knockdown of KDM4B disrupted invasion and migration *in vitro*, consistent with diminished peritoneal tumor load in mouse xenografts. The most striking difference was in the size of fused omental tumors, suggesting that KDM4B may preferentially regulate metastasis to omental tissues. Further, the contribution of KDM4B to the formation and growth of tumor spheroids *in vitro* likely relates to *in vivo* function of KDM4B by facilitating peritoneal seeding (Lengyel 2010). These phenotypes appear to be distinct from the actions of KDM4A in EOC and other cancers, where it promotes copy

number gain and drug resistance (Black, Manning et al. 2013; Black, Atabakhsh et al. 2015). Considering the large number of genes dependent on KDM4B in SKOV3ip.1 cells, it is unclear at this time which specific genes or pathways are primarily responsible for these broad phenotypic effects, although *LCN2*, *LOX*, *LOXL2*, and *PDGFB* make particularly compelling candidates with proven abilities to influence either ovarian cancer growth or general metastasis (Apte, Bucana et al. 2004; Santin, Zhan et al. 2004; Erler, Bennewith et al. 2006; Barker and Erler 2011). Additionally, analysis of data sets curated by Gyorffy et al (Gyorffy, Lanczky et al. 2012) demonstrated that higher expression of *LOX* in tumor samples correlates with reduced progression-free survival in EOC (Fig. 2.7E). In an additional independent proof of concept, blocking PDGFB signaling in SKOV3ip.1 cells with DNA aptamers suppressed growth of peritoneal tumor xenografts (Lu, Shahzad et al. 2010). These results support the potential role of KDM4B target genes, identified in this study, in the pathogenesis of EOC. Combinatorial targeting of the genes regulated by KDM4B may lead to improved methods to suppress peritoneal engraftment of EOC tumor cells, ultimately improving the prognosis of patients with elevated levels of KDM4B.

A key question rising from our study regards the utility of directly targeting KDM4B to improve EOC patient outcome. Although a systematic comparison has not been conducted, KDM4B appears to regulate pathways distinct to each cancer type. In hormone-dependent breast and prostate cancers, KDM4B is induced by steroid hormones, and regulates ER and AR target genes (Yang, Jubb et al. 2010; Coffey, Rogerson et al. 2013). In colon and gastric cancers, KDM4B regulates beta-catenin dependent gene expression and WNT signaling to promote attachment-free growth and metastatic behavior (Berry and Janknecht 2013; Zhao, Li et al. 2013). In EOC, although KDM4B regulates distinct sets of genes in different oxygen tensions, invasive and migratory behaviors appear to be the most robust phenotypes. There is the implication that disrupting KDM4B function with an inhibitor of its demethylase activity could attenuate tumor growth. However, there are significant barriers to creating specific inhibitors to individual histone demethylases (reviewed in (Hojfeldt, Agger et al. 2013; Maes, Carceller et al. 2015)). Despite significant effort in the design of specific inhibitors (Rai, Kawamura et al. 2010; Thalhammer,

Mecinovic et al. 2011), the greatest success has been restricted to inhibition of the KDM6 family (Kruidenier, Chung et al. 2012). A systematic analysis of KDM-inhibitor interactions reported significant cross-reactivity for all inhibitors tested, highlighting the difficulty of developing a specific inhibitor (Joberty, Boesche et al. 2016). Given the importance of KDM4A and KDM4B in regulating various aspects of DNA repair and cell proliferation (Mallette, Mattiroli et al. 2012; Young, McDonald et al. 2013), directly targeting the enzymatic activity of KDM4B may lead to off-target effects in normal tissues. Finally, to advance KDM4B as a direct therapeutic target in EOC, it will be important to demonstrate the extent to which demethylase activity modulates the hypoxic response, invasive phenotype, and *in vivo* growth properties of ovarian cancer cells. Such studies would be best-accomplished using KDM4B catalytic and targeting mutants via *in situ* CRISPR/Case9 gene editing. The importance of hypoxic signaling in EOC is highlighted by the relative success of bevacizumab (Avastin) in the treatment of HGSA (Bast 2011). Although only 25% of HGSA patients responded to bevacizumab, this effect is more robust than all other alternate chemotherapies tested to date (Bast 2011; Li, Zhou et al. 2015). Bevacizumab has limitations stemming from either deleterious side effects, or compensatory hypoxic expression (Conley and Wicha 2012; Li, Zhou et al. 2015). As a facilitator of multiple tumorigenic pathways in normoxia and hypoxia, KDM4B may provide unique opportunities to tailor combinatorial therapies for patients with hypoxic tumor signatures.

Collectively, this study demonstrates that the hypoxia-inducible histone demethylase KDM4B is robustly expressed in the majority of EOC tumors assayed and supports cellular phenotypes associated with seeding of peritoneal tumors, the primary cause of EOC patient morbidity and mortality. To the best of our knowledge, this is the first functional demonstration that a Jumonji-domain histone demethylase contributes to EOC progression. Future studies investigating the specific transcriptional and functional mechanisms regulated by KDM4B and other histone demethylases may reveal novel therapeutic candidates to suppress re-establishment of peritoneal tumors in EOC patients.

CHAPTER 3:

INVESTIGATING MECHANISMS REGULATED BY KDM4B IMPLICATED IN EOC METASTASIS AND PERITONEAL DISSEMINATION *IN VITRO*

ABSTRACT

The hypoxia-inducible histone demethylase, KDM4B is upregulated during the progression of ovarian cancer, connecting the hypoxic tumor microenvironment to epigenetic activation of cancer promoting genes and tumor progression. Knockdown of KDM4B with shRNA reduces tumor growth and peritoneal dissemination in xenograft models (Chapter 2). Loss of KDM4B also corresponds to decreased invasion, migration, and attachment free growth *in vitro*. These results suggest that KDM4B activity is involved with regulating a more invasive or metastatic tumor phenotype in EOC. Based on these observations, specific mechanisms and aspects of metastasis were investigated. RNA Sequencing analysis identified possible target genes involved with invasion and migration, including *MUC1* and *ARID5B*. Based on previous studies, these findings suggest a link between KDM4B and ARID5B through PDGF pathway activation. In order to identify secreted factors involved with remodeling the tumor microenvironment, conditioned media from SKOV3ip.1 and OVCAR8 cells expressing shRNA to *KDM4B* or an irrelevant control (GFP) were used for proteome analysis on an RD angiogenesis array. Using these arrays with affinity for 55 proteins, 11 secreted factors from SKOV3ip.1 and 16 from OVCAR8 cell lines were identified. These results suggest that these targets may be regulated in a KDM4B dependent manner. In addition to identification of secreted proteins, OVCAR8 spheroids expressing shRNA to *KDM4B* or a GFP control were used to investigate spheroid invasion on Type I Collagen. Preliminary results suggest KDM4B expression correlates with increased spheroid invasion. KDM4B expression was identified in patient ascites from EOC patients, demonstrating the clinical relevance of exploring KDM4B in these processes. Future work will include HUVEC assays and 3D spheroid invasion assays to continue dissecting the contribution of KDM4B to these processes in ovarian cancer models.

INTRODUCTION

KDM4B provides a novel epigenetic link between the hypoxic tumor microenvironment and EOC progression. This enzyme plays a role in EOC invasion, migration, and attachment-free growth *in vitro*, key steps in the pathogenesis of this disease (Chapter 2). Considering KDM4B expression is connected to these aspects of the metastatic cascade, it is possible it participates in other processes involved in tumor growth and peritoneal dissemination. These could include angiogenesis, influencing inflammatory cell processes in the tumor microenvironment, and regulating specific proteins dictating the movement of the tumor cell in the patient (Hanahan and Weinberg 2011). Secreted factors could also be responsible for driving these alterations in the tumor microenvironment.

Secreted factors are integral components regulating inflammation and angiogenesis, promoting different steps in these processes. Not only does inflammation influence initial pathogenesis of EOC, it may drive tumorigenesis and metastasis (Auersperg 2013). Depending on the tumor type, inflammation could promote tumor regression or progression (Ness and Cottreau 1999). Endometriosis, a contributing risk factor to EOC progression, involves localized inflammation in regions endometrial tissue implants outside the uterus (Ness and Cottreau 1999). The inflammatory response includes interleukins like IL-8, growth factors like TGF-ß, and other secreted angiogenic factors like VEGF that direct vascular remodeling (Ness and Cottreau 1999). This process acts as a key component in the inflammatory response.

Angiogenesis, the development of new vasculature from existing vasculature, is another key in driving growth and metastases away from sites of primary tumor burden (Horiuchi, Imai et al. 2002). The KDM4B target, PDGFB (Platelet-derived Growth Factor) is an essential component in this process (Chapter 2) (Lu, Shahzad et al. 2010). KDM4B regulates PDGFB in a demethylase dependent manner (Chapter 2). VEGF (Vascular Endothelial Growth Factor) is another notable participant in vascular remodeling (Horiuchi, Imai et al. 2002). PDGF ligands recruit pericytes to wrap and stabilize endothelial cells, playing a key role in their function as blood vessels (Lu, Thaker et al. 2008). PDGF is composed of 4 polypeptide chains that form either the homodimers PDGF-AA, BB, CC, and DD or the heterodimer

PDGF-AB (Kelly, Haldeman et al. 1991; Betsholtz, Karlsson et al. 2001). Receptor activation dictates the function of the bound ligand (Lu, Shahzad et al. 2010). The ligands PDGFAA, PDGFBB, PDGFAB, and PDGFCC bind to the receptor PDGFRα (Lu, Shahzad et al. 2010). PDGFBB and PDGFDD bind to PDGFRβ (Lu, Shahzad et al. 2010). Even though PDGFB knockout mice show abnormal vasculature, the role of this ligand and pathway have not been well established in ovarian tumor vasculature (Lu, Thaker et al. 2008). PDGFAA and PDGFBB have been shown to be upregulated in ovarian cancer tumors and patient serum, correlating with advanced FIGO stages (Madsen, Steffensen et al. 2012). In addition to participating in vascular remodeling, PDGFB has established links to non-transformed and transformed cell motility (Aoki, Nabeshima et al. 2007). This provides another interesting PDGFB-dependent mechanism regulated by KDM4B.

KDM4B is shown to be essential in driving invasion and migration *in vitro* and *in vivo* (Chapter 2). In addition to these aspects, KDM4B expression plays a role in spheroid formation and maintenance (Chapter 2). The ability to invade as single cells or spheroids is a key driving force in EOC metastasis. The accumulation of ascites fluid in the peritoneal cavity is present in one third of ovarian cancer patients (Puiffe, Le Page et al. 2007). The tumor cells in ascites fluid are either single cell or cell aggregates (Smolle, Taucher et al. 2014). Ascites cell clusters adhere and invade at distant sites in the peritoneal cavity (Smolle, Taucher et al. 2014). Despite their importance in EOC progression, no studies have characterized the KDM4B-dependent mechanisms regulating the invasive natures of spheroids. The influence of KDM4B in regulating invasion and migration *in vitro* was previously analyzed using single cells, not spheroid aggregates (Chapter 2). Characterizing the role of KDM4B in spheroid invasion provides a novel perspective on this enzyme in an innovative 3D *in vitro* model. Identifying expression of KDM4B in patient ascites neoplastic cells may establish clinical relevance for the findings from these additional *in vitro* studies.

In this sets of studies, the connection between KDM4B expression and secreted factors and spheroid invasion was explored. RNA Sequencing identified a possible link between KDM4B, PDGF pathway, and ARID5B expression. ARID5B-dependent migration is regulated by PDGF signaling in

mouse embryonic fibroblasts (MEFs), providing a possible link between KDM4B and a demonstrated target gene PDGFB (Chapter 2) (Schmahl, Raymond et al. 2007). KDM4B expression correlated with differential secretion of factors involved in many aspects of metastasis, including angiogenesis and inflammatory responses (Chapter 3). Data indicated increased spheroid invasion *in vitro* with expression of KDM4B and identified putative target genes regulated by KDM4B (Chapter 3). These analyses provide novel explanations for the role of KDM4B in EOC tumorigenesis and interesting new areas for further KDM4B investigations. Establishing potential mechanistic connections between KDM4B and the PDGF pathway may highlight insight into KDM4B-dependent activation of angiogenesis and invasion in EOC.

MATERIALS AND METHODS

Cell Lines and Culture Conditions. All OVCAR cell lines were maintained in RPMI-1640 (Invitrogen) supplemented with 10% heat-inactivated fetal bovine serum (HI-FBS) and 1% pen-strep (Invitrogen). SKOV3ip.1 cells were from Dr. Erinn Rankin (Stanford University) with permission from Dr. Gordon Mills (M.D. Anderson Cancer Center). OVCAR3, OVCAR4, OVCAR5, OVCAR8, and IGROV1 cells were from the NCI-Frederick Cancer DCTD Tumor/Cell line Repository. HIO80 cells were from Dr. Andrew Godwin. Upon receipt, cells were expanded in culture to establish early passage stocks. After transducing with lentivirus, cells were used for experiments within 1-2 months to minimize cell drift or contamination, and were periodically screened for mycoplasma. For stable knockdown, cells were transduced with pLKO.1-shRNA constructs targeting *KDM4B* (Open Biosystems; TRCN0000018014 (shK-1) and TRCN0000018016 (shK-2)) and selected in puromycin. For hypoxic treatment, cells were incubated for 16-24 hours in Ruskinn InVivo300 glove-box hypoxic incubators (Baker) set to desired oxygen tensions.

Patient Ascites Cell Culture. The KU Cancer Center's Biospecimen Repository Core Facility (BRCF) provided de-identified human patient samples and any corresponding clinical data with informed consent from patients. Ascites fluid was obtained during cytoreductive surgery. Samples were spun down post-surgery and maintained in the repository. Ascites cell pellets were cultured and maintained in RPMI medium plus 30% FBS in 10-cm ultra low attachment dishes. Protein for western blotting analysis was harvested using SDS lysis buffer and previously published techniques (Krieg, Rankin et al. 2010).

QRT-PCR. RNA from cells was isolated after two PBS (1X) washes, followed by Trizol (Ambion 15596026) or Purelink mini kit (Ambion 12183020). Quantitative real-time PCR (qRT-PCR) was conducted as previously described using an ABI VIIA sequence detection system using 18S rRNA as an internal control (Krieg, Rankin et al. 2010). Primers (Figure 3.1) were designed using the Roche Universal Probe Library Design Tool (http://lifescience.roche.com/shop/products/universal-probelibrary-

system-assay-design) and verified *in silico* on UCSC genome browser. Melt curve analysis confirmed formation of single amplicons of the expected size.

Assay	Gene	Forward (5'-3')	Reverse (5'-3')
QRT-PCR	hsKDM4B	ggactgacggcaacctctac	cgtcctcaaactccacctg
QRT-PCR	hsKDM4D	ggacaagcctgtaccactgag	ctgcacccagaagccttg
QRT-PCR	hsMUC1v9	cctgcctgaatctgttctgc	catgaccagaacccgtaaca
QRT-PCR	hsIL-8	agacagcagagcacacaagc	atggttccttccggtggt
QRT-PCR	hsPDGFB	ctggcatgcaagtgtgagac	cgaatggtcacccgagttt
QRT-PCR	hsIGFBP1	aatggattttatcacagcagacag	ggtagacgcaccagcagagt
QRT-PCR	hsG0S2	ggaggagaacgctgaggtc	tttccatctcggctctgg
QRT-PCR	hsRNF144B	cctgacatggtgtgcctaaa	cacaggtaccaaacaggcaat
QRT-PCR	hsMYO1D	agaaaagtctcgagtgattgtgc	ttctgaacctccttggagtagc
QRT-PCR	hsARID5B	tggactcaacttcaaagacgttc	acgttcgtttcttcctcgtc
QRT-PCR	hsCMPK1	tcaaggatggaacaagacca	caagacatcgttcaatacaaatctc
QRT-PCR	hsSNN	ctggcctcctgctcagacta	tttttagaagaggcttgggtga
QRT-PCR	hsBPNT1	atgctgtgctgcgagtagg	gaggctttgccttcaatcag
QRT-PCR	hsPPAP2B	gctcatctgcctcgacct	tggtgcttgtctcgatgatg
QRT-PCR	hsCOPS2v1	gtgcgatgatgaggaggact	cacatttggctcggagttacta
QRT-PCR	hsPDGFRβ	catctgcaaaaccaccattg	gagacgttgatggatgacacc
QRT-PCR	hsCDH1	tggaggaattcttgctttgc	cgctctcctccgaagaaac
QRT-PCR	hsCDH3	agggaggctgaagtgacctt	gggcagcccatgaatactt
QRT-PCR	hsICAM6	cactgtgggcgtggaatac	tcaacgtgaagtttcctcctg
QRT-PCR	hsNCAM2	gagcctcctcctctccttct	ctccaacactaagctctactttgct
QRT-PCR	hsITGA6	tttgaagatgggccttatgaa	ccctgagtccaaagaaaaacc
QRT-PCR	hsITGA7	ccctgatagccactacctcct	caatgttggtcacaaaaagca
QRT-PCR	hsMMP15	acggtcgttttgtctttttca	gtcagcggctgtgggtag
QRT-PCR	hsITGA2	tcgtgcacagttttgaagatg	tggaacacttcctgttgttacc
QRT-PCR	hsITGA4	gatgaaaatgagcctgaaacg	gccatactattgccagtgttga
QRT-PCR	hsMMP1	gctaacctttgatgctataactacga	tttgtgcgcatgtagaatctg
QRT-PCR	18S rRNA	gcccgaagcgtttactttga	tccattattcctagctgcggtatc

Figure 3.1. List of primers used in these studies for qRT-PCR analysis.

RNA Sequencing. Total RNA was isolated as previously described. Prior to creating Ilumina Tru-Seq mRNA libraries, RNA integrity was verified via Agilent Bioanalyzer 2100 analysis in the KUMC Genome Sequencing Facility. Stranded mRNA libraries were completed following kit protocol. Library DNA quality and size was verified using Agilent Bioanalyzer 2100. Ilumina Tru-Seq 100 cycle Paired-End (PE) sequencing was completed on an Ilumina Hi-Seq 2500 sequencer. Read alignment and quantification was performed with Qiagen CLC Bio software. Additional statistical edgeR analysis was completed using Qiagen CLC Bio software.

Immunoblotting. Immunoblots were performed using standard procedures as previously described (Krieg, Rankin et al. 2010). See Figure 3.2 for antibody dilution information.

Assay	Antigen	Supplier	Product NO.	Description	Dilution
Western	KDM4B	Cell Signaling	8639	Rabbit mAb	1:1,000
	HIF1α	BD	610959	Mouse mAb	1:1,000
	ARID5B	Bethyl	A302-235A-M	Rabbit pAb	1:1,000
	EPCAM	Thermo	MA5-13917	Mouse mAb	1:500
	β-Actin	Sigma	A1978	Mouse mAb	1:2,000
	α-Tubulin	Thermo	MS-581-PABX	Mouse mAb	1:2,000

Figure 3.2. List of antibodies used in these studies for protein expression immunoblotting.

Spheroid Formation Assay. 600 cells were seeded per well of 96-well ultra-low attachment plates (Corning Incorporated). After four days, spheroids were imaged by bright field microscopy using a Leica DMI 4000 inverted microscope equipped with a Leica CCD camera (Courtesy of Dr. Michael J. Soares, KUMC). Volume ($V=4/3*\pi r^3$) was calculated after measuring the diameter and radius of each spheroid using NIH Image J (Vinci, Gowan et al. 2012). Sixteen spheroids were analyzed per cell line and oxygen condition in each independent experiment. Differences in average spheroid volume were analyzed by two-tail paired Student's t-test. These results are found in Chapter 2 of this work.

Spheroid Invasion Assay. Spheroids formed as indicated in the spheroid formation assay were removed from their 96-well ultra low attachment plate via pipetting and placed upon polymerized Type I Collagen (BD Catalogue Number 354249) in a 48-well culture plates. Individual spheroid and ECM invasion assays were exposed to either 16 hours normoxic (21% O_2) or hypoxic (2% O_2) treatment for the remainder of the study. 1 ml of normal RPMI cell culture maintenance media was added to the top of these and replaced every 3 days to prevent evaporation of media from the well. Spheroid invasion was imaged as indicated on an Olympus IX71 inverted microscope. Measurements were done using NIJ ImageJ program and calculated as shown in the diagram in Figure 3.7. Differences in average invasion area were analyzed by two-tail paired Student's t-test. Results represent one independent experiment with eight technical replicates per cell line and oxygen tension condition.

Angiogenesis Array. OVCAR8 and SKOV3ip.1 cells containing stable knockdown of KDM4B were plated in RPMI + 2% FBS at 1.5 x 10^5 in a 6-well plate for 24 hour. These plates were either placed at 21% or 1% O_2 for 16 hours at 37 either in tri-gas incubators (Fisher) at 21% or Ruskinn InVivo300 hypoxia chambers (Baker) set to 1% O2 and 5% CO2. Conditioned media was collected from both OVCAR8 and SKOV3ip.1 cell lines and cell debris was pelleted and removed. The angiogenesis array (R&D Biosystems, ARY007) procedure was completed as directions indicate using 750 µl of conditioned media.

TCGA Data Statistics. cBIO Genome Portal was used to generate a Kaplan-Meier Disease Free Survival Curve for high-grade serous patients with expression of ARID5B (Z score <1) (Cerami, Gao et al. 2012; Gao, Aksoy et al. 2013).

Statistics. Data represent the mean ± SEM or median ± upper and lower quartiles for at least three independent experiments. Two-tailed Student's T tests or ANOVA were used as appropriate for *in vitro* experiments. P values of 0.05 or less were considered statistically significant.

Study approvals. The KU Cancer Center's Biospecimen Repository Core Facility (BRCF) provided de-identified human patient samples and any corresponding clinical data with informed consent from patients.

Acknowledgements

Research was supported by an Institutional Development Award (IDeA) P20GM104936 (AJK and SG), an American Cancer Society Institutional Research Grant ACS IRG-09-062-04 (AJK), KUMC Dept. of OB/GYN start-up funds (AJK). Special thanks to the staff of the University of Kansas Cancer Center's Biospecimen Repository Core Facility staff for specimen collection (Stephen Hyter). Acknowledgement is made to funding from the KU Cancer Center's Cancer Center Support Grant (P30 CA168524).

RESULTS

Loss of KDM4B Expression Corresponds with Decreased MUC1 and ARID5B Expression. In order to identify genes regulated by KDM4B in EOC, SKOV3ip.1 and OVCAR8 cells were transiently transduced with shRNA targeting *KDM4B* (shK-1 and shK-2) or GFP (control) in 21% and 0.5% O_2. (Fig. 3.3). Genes dependent on KDM4B in either 21% or 0.5% oxygen were identified by CLC Bio edgeR statistical analysis (See Methods). RNA Sequencing identified 73 genes down-regulated in SKOV3ip.1 cells and 495 genes in OVCAR8 cells with loss of KDM4B and hypoxia treatment (Fig 3.3B-Fig 3.3C). A subset of 14 genes, including KDM4B, was commonly down regulated in both SKOV3ip.1 and OVCAR8 (Fig 3.3C). The commonly regulated 14 gene names, descriptions, and basic functions are explained in Fig 3.3C. qPCR validation of these 14 target genes in replicate experiments is also shown in Fig 3.4. These commonly regulated targets are implicated in various cellular processes, including cell cycle control and transcriptional regulation (Heckmann, Zhang et al. 2013; Zhang, Ni et al. 2016). However, *MUC1* provides a connection between KDM4B and tumorigenic invasion.

RNA Sequencing has identified a possible connection between *KDM4B* and Mucin 1 (*MUC1*) expression (Fig 3.3C). *MUC1* encodes an O-glycosylated membrane-bound protein, with links to increased invasion (Wang, Ma et al. 2007). MUC1 has also displayed high expression in both primary epithelial ovarian cancers and matched metastatic ovarian cancer tissue and patient ascites (Wang, Ma et al. 2007; Miyamoto, Ruhaak et al. 2016). Inhibition of MUC1 decreased cellular adhesion and survival on fibronectin in representative EOC models (Yin, Fang et al. 2016). Regulation of MUC1 by KDM4B may facilitate invasion, migration, and attachment-free growth.

Based on these expression results, a link was identified between *KDM4B* and *ARID5B.* ARID5B, provides a potential connection to EOC development and progression. ARID5B functions as a histone demethylase in combination with PHF2 to remove di-methyl marks from H3K9 (Baba, Ohtake et al. 2011). Increased *ARID5B* expression corresponds with decreased survival in high-grade serous patients, demonstrating a strong clinical connection for this presumed KDM4B target gene (Cancer Genome Atlas Research 2011). Identification of these novel connections between *KDM4B, MUC1*, and *ARID5B*

provides another clinically relevant mechanism for exploration in epithelial ovarian cancer progression, in addition *G0S2* and *MYO1D* (Fig 3.3-3.4).

A.

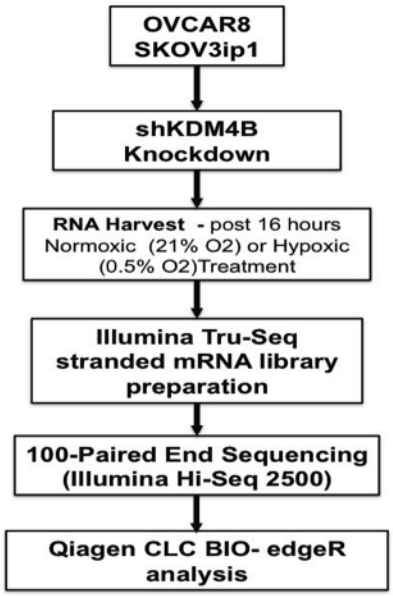

B.

C.

Gene	Description	Function
G0S2	G0/G1switch 2	cell cycle
MUC1	Mucin 1	adhesion
RNF144B	ring finger protein 144B	E3 ubiquitin ligase
MYO1D	Myosin 1D	motor proteins
ARID5B	AT rich interactive domain 5B	transcription coactivation
CMPK1	cytidine monophosphate (UMP-CMP) kinase 1	nucleic acid biosynthesis
FAM214B	family with sequence similarity 214, member B	
KDM4B	***lysine (K)-specific demethylase 4B***	***histone demethylase***
SNRPN	small nuclear ribonucleoprotein N	splicing factor
NUDCD2	NudC domain containing 2	LIS1/dynein pathway
SNN	Stannin	toxic effects of organotins
BPNT1	3'(2'), 5'-bisphosphate nucleotidase 1	nucleotide metabolism
PPAP2B	phosphatidic acid phosphatase type 2B	lipid synthesis
COPS2	COP9 signalosome subunit 2	transcriptional corepression

FDR P<0.05

Figure 3.3. RNA Sequencing identifies 14 genes commonly down regulated under hypoxia and with shKDM4B knockdown in OVCAR8 and SKOV3ip.1 cell lines. A. Steps in RNA isolation and library preparation processes are explained in this flowchart. Libraries were prepared for both SKOV3ip.1 and OVCAR8 cell lines expressing shRNA targeting *KDM4B* (shK-2) or GFP (control) in 21% and 0.5% O_2 (n=3). RNA Sequencing was completed and preliminary gene identification performed using edgeR analysis with CLC BIO; FDR $P<0.05$. **B**. Venn diagram showing 73 genes are down regulated after hypoxic treatment and KDM4B knockdown in SKOV3ip.1 and 495 genes respectively in OVCAR8. 14 genes, including KDM4B are commonly down regulated in both SKOV3ip.1 and OVCAR8. Identities and functions for these 14 genes are listed in **C**.

A.

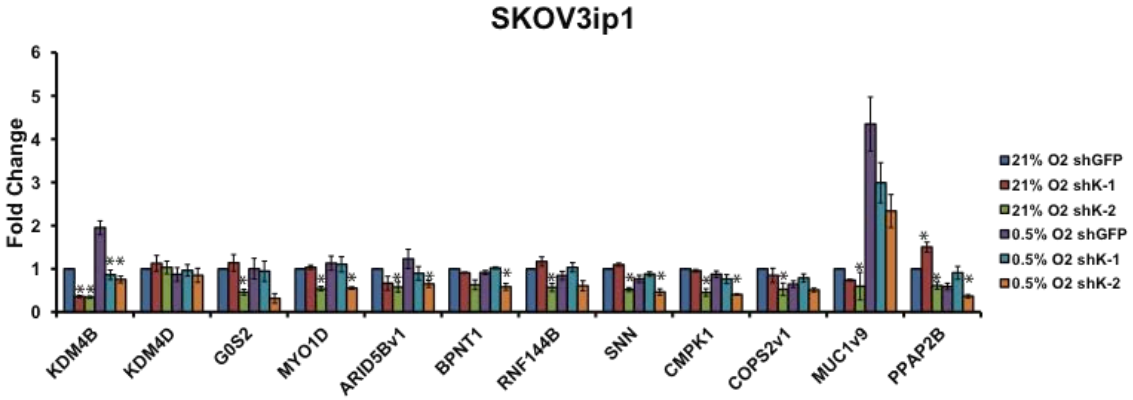
SKOV3ip1
Fold Change
0
1
2
3
4
5
6
KDM4B
KDM4D
G0S2
MYO1D
ARID5Bv1
BPNT1
RNF144B
SNN
CMPK1
COPS2v1
MUC1v9
PPAP2B
21% O2 shGFP
21% O2 shK-1
21% O2 shK-2
0.5% O2 shGFP
0.5% O2 shK-1
0.5% O2 shK-2

B.

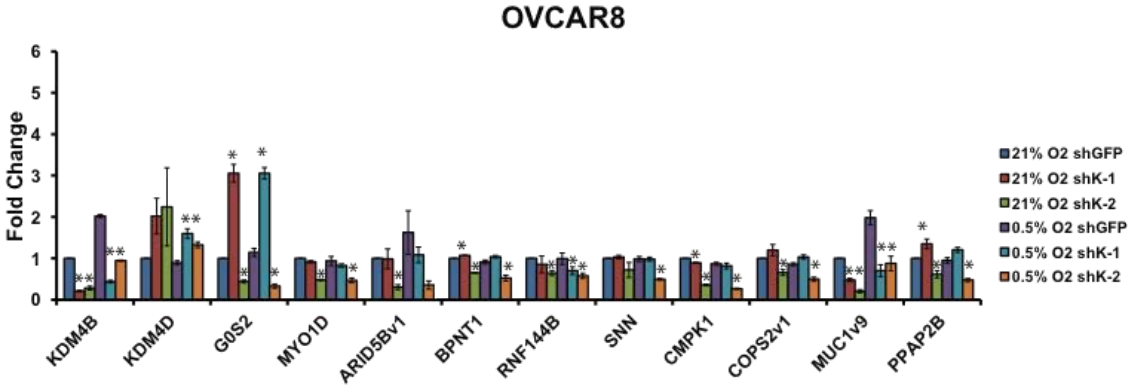
OVCAR8
Fold Change
0
1
2
3
4
5
6
KDM4B
KDM4D
G0S2
MYO1D
ARID5Bv1
BPNT1
RNF144B
SNN
CMPK1
COPS2v1
MUC1v9
PPAP2B
21% O2 shGFP
21% O2 shK-1
21% O2 shK-2
0.5% O2 shGFP
0.5% O2 shK-1
0.5% O2 shK-2

Figure 3.4. qPCR validation of 14 genes commonly down regulated under hypoxia and with shKDM4B knockdown in SKOV3ip.1 and OVCAR8 cell lines. A. qPCR validation of 14 commonly down regulated target genes; *KDM4B, KDM4D, G0S2, MYO1D, ARID5Bv1, BPNT1, RNF144B, SNN, CMPK1, COPS2v1, MUC1v9,* and *PPAP2B* expression in SKOV3ip.1 and OVCAR8 respectively (n=3) ($p<0.05$).

KDM4B May Regulate ARID5B Through PDGF Pathway Activation in Epithelial Ovarian Cancer. ARID5B-dependent migration is regulated by PDGF signaling, providing a novel link between KDM4B and its target gene *PDGFB* (Chapter 2) (Schmahl, Raymond et al. 2007). KDM4B was shown to regulate PDGFB expression in a demethylase dependent manner in previous studies (Chapter 2). KDM4B may activate expression of PDGFB, providing the appropriate ligand for PDGF Receptor Beta pathway activation (Fig 3.5A). ARID5B may be induced through different downstream signaling cascades activated by the PDGF receptor, including the PI3K/AKT pathway and MAPK (Mitogen activated protein kinase) pathway (Fig 3.5A). Relevant pathway components including KDM4B, PDGFB, PDGFRβ, and ARID5B showed down regulation of expression with loss of KDM4B in OVCAR8 cells in qPCR analysis (Fig 3.5B). The downstream target, ARID5B was also suppressed in a KDM4B dependent manner in OVCAR8 (Fig 3.5C). KDM4B expression dependent down regulation of ARID5B was conserved in SKOV3ip.1, a second representative cell line (Fig 3.5D). ARID5B was expressed in additional cell lines representing a range of EOC genotypic backgrounds (Fig 3.5E). HIO80, a non-transformed ovarian epithelial line, also displayed ARID5B expression suggesting a relevant normal cell function for this protein (Fig 3.5E). Increased ARID5B expression correlates with decreased survival in high-grade serous patients, demonstrating a strong clinical connection for this presumed KDM4B target gene (Fig 3.6; p=0.0017) (Cancer Genome Atlas Research 2011). This connection between PDGF signaling and ARID5B may explain invasive and migratory defects highlighted in loss of KDM4B studies *in vitro* and *in vivo* described in Chapter 2. Currently, ARID5B has not been investigated in the context of ovarian cancer progression and provides a novel link to explain KDM4B-dependent tumorigenic defects.

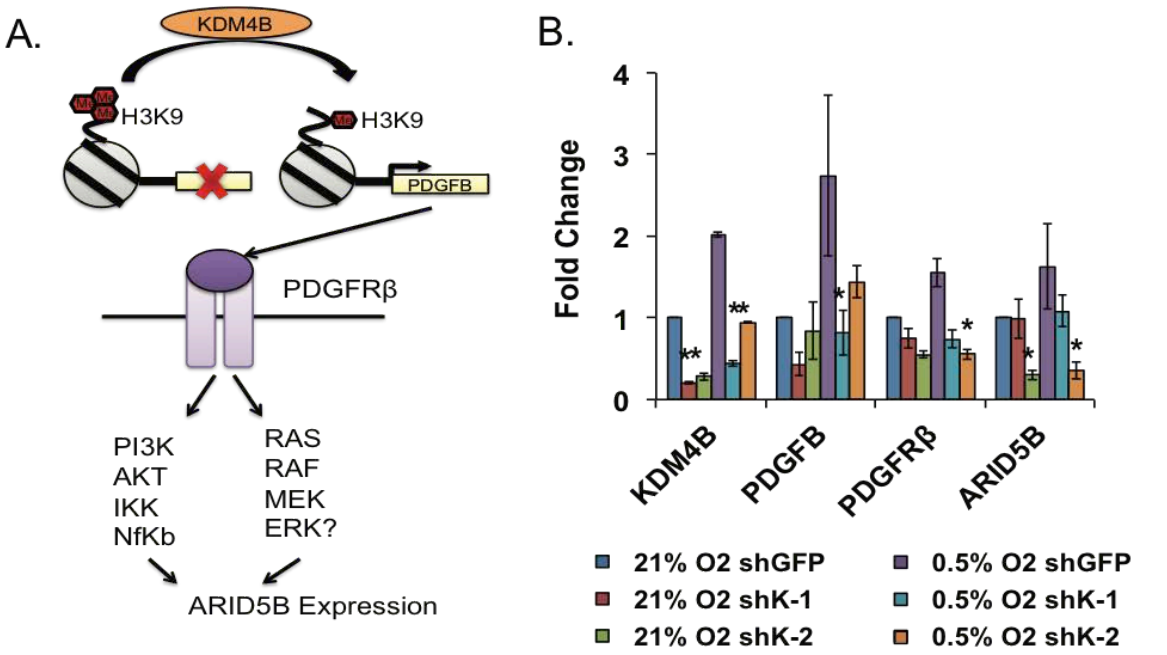
A.
KDM4B
H3K9
H3K9
PDGFB
PDGFRβ
PI3K
AKT
IKK
NfKb
RAS
RAF
MEK
ERK?
ARID5B Expression
B.
Fold Change
4
3
2
1
0
KDM4B
PDGFB
PDGFRβ
ARID5B
21% O2 shGFP
21% O2 shK-1
21% O2 shK-2
0.5% O2 shGFP
0.5% O2 shK-1
0.5% O2 shK-2

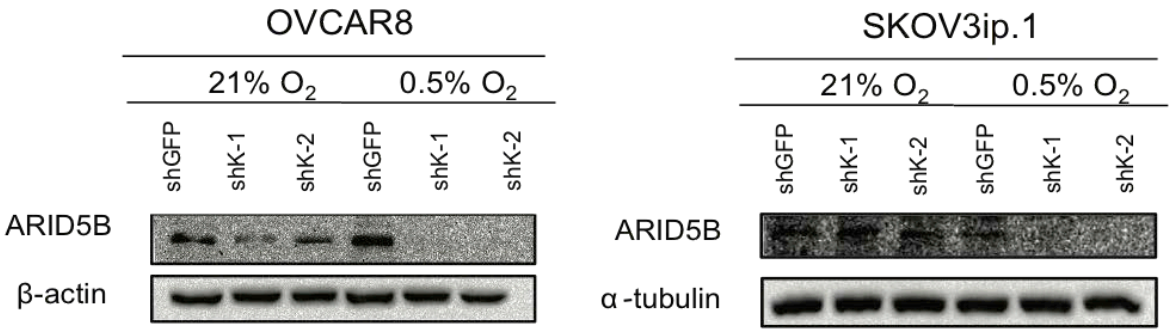
C.
OVCAR8
21% O2
0.5% O2
shGFP
shK-1
shK-2
shGFP
shK-1
shK-2
ARID5B
β-actin
D.
SKOV3ip.1
21% O2
0.5% O2
shGFP
shK-1
shK-2
shGFP
shK-1
shK-2
ARID5B
α-tubulin

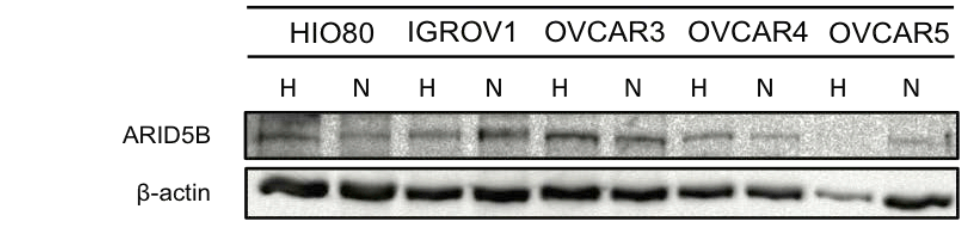
E.
HIO80
IGROV1
OVCAR3
OVCAR4
OVCAR5
H N H N H N H N H N
ARID5B
β-actin

Figure 3.5. KDM4B may regulate ARID5B expression through activation of the PDGF pathway. **A**. Diagram demonstrating the possible connection between KDM4B expression and ARID5B expression. This may occur through demethylation of H3K9, subsequent activation of the PDGF pathway, and activation of the PI_3K cascade or MAPK/ERK cascade. **B.** Immunoblot measurement of ARID5B expression in OVCAR8 cells expressing shRNA targeting KDM4B (shK-1 and shK-2) or GFP (control) in 21% and 0.5% O_2. β-actin serves as a loading control. **C.** Immunoblot measurement of ARID5B expression in SKOV3ip.1 cells expressing shRNA targeting KDM4B (shK-1 and shK-2) or GFP (control) in 21% and 0.5% O_2. α-tubulin serves as a loading control. **D**. Immunoblot detection of ARID5B in a panel of ovarian cancer cell lines in normoxia (N, 21% oxygen) and in hypoxia (H, 0.5% oxygen). HIO-80 cells serve as non-transformed OSE control. β-actin serves as loading control. **E.** qPCR validation of *KDM4B*, *PDGFB*, *PDGFRβ* and *ARID5Bv1* expression in OVCAR8 respectively (n=3).

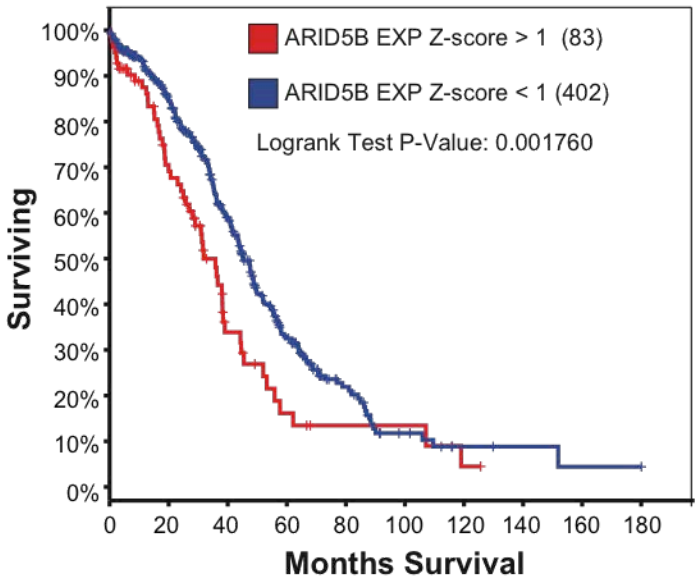
ARID5B EXP Z-score > 1 (83)
ARID5B EXP Z-score < 1 (402)
Logrank Test P-Value: 0.001760
Surviving
100%
90%
80%
70%
60%
50%
40%
30%
20%
10%
0%
0
20
40
60
80
100
120
140
160
180
Months Survival

Figure 3.6. Increased expression of ARID5B corresponds with decreased survival in high-grade serous patient tumors. TCGA analysis of high-grade serous tumors using CBIO showed decreased survival with alterations in *ARID5B*. (EXP<1) (P<0.05).

KDM4B Expression Associates with Differential Secretion of Factors Involved in Tumorigenesis in EOC Cell Lines. Angiogenesis and inflammation are key processes promoting tumor progression and invasiveness in EOC (Bast, Hennessy et al. 2009). Tumor cells communicate with the local microenvironment by secreting angiogenic factors to remodel the surrounding microenvironment and form new blood vessels (Matei, Kelich et al. 2007). KDM4B was shown to regulate PDGFB in Chapter 2, providing evidence that this enzyme plays a role in regulating this physiological process. In order to investigate the role of KDM4B in vascular and lymphatic remodeling, angiogenesis arrays were employed to identify key secreted factors in these processes. Using conditioned media collected from normoxia (21% O_2) and hypoxia (1% O_2) treated SKOV3ip.1 cells transduced with shGFP or shK-2, 11 secreted angiogenesis related proteins were identified on a set of angiogenesis arrays (Fig 3.7A and Fig 3.7B). KDM4B expression corresponds with secretion level changes for both pro angiogenic, anti angiogenic and other inflammatory factors (Fig 3.7A and Fig 3.7B). Identified pro-angiogenic proteins included: SERPINE1 (Serpin Family E Member 1), IGFBP1 (Insulin Growth Factor Binding Protein 1), uPA (Urinary-type Plasminogen Activator), ET-1 (Endothelin-1), IL-8 (Interleukin 8), and VEGF (Vascular Endothelial Growth Factor) (Fig 3.7A and Fig 3.7B). Identified anti-angiogenic secreted factors included: TIMP1 (Tissue Inhibitor of Metalloproteinase-1), TSP1 (Thrombospondin 1), IGFBP3 (Insulin Growth Factor Binding Protein 3), Activin A, and COL18A1 (Endostatin) (Fig 3.7A and Fig 3.7B). Secretion of both pro-angiogenic and anti-angiogenic factors was observed; however, results did not identify a relationship between KDM4B expression and a distinct angiogenic or inflammatory phenotype in SKOV3ip.1.

To verify if secreted factors were conserved between EOC cell lines, this set of experiments was replicated in a second model line, OVCAR8. Using conditioned media collected from normoxia (21% O_2) and hypoxia (1% O_2) treated OVCAR8 cells, 14 secreted angiogenesis related proteins were identified (Fig 3.8A and Fig 3.8B). Consistent with SKOV3ip.1, OVCAR8 cells displayed secretion level changes for both pro and anti angiogenic factors in a KDM4B-dependent manner (Fig 3.8A and Fig 3.8B). Among those identified were 8 proteins that overlapped between cell lines. Identified pro-angiogenic

proteins also secreted by SKOV3ip.1 included: SERPINE1, IGFBP1, uPA, ET-1, EG-VEGF (Fig 3.8A and Fig 3.8B). In addition to these, ANGTP2 (Angiopoetin-2), ARTM (Artemin), CD142 (Coagulation Factor III), and PDGF-AA were also identified (Fig 3.8A and Fig 3.8B). Identified overlapping anti-angiogenic secreted factors between SKOV3ip.1 and OVCAR8 included: TIMP1, TSP1, IGFBP3, and Activin A (Fig 3.8A and Fig 3.8B). Additionally, OVCAR8 cells secreted PTX3 (Pentraxin 3) and TSP2 (Thrombospondin 2) (Fig 3.8A and Fig 3.8B). KDM4B expression does not correspond with a specific type of angiogenic or inflammatory profile in OVCAR8 cell lines. However, the array results identify novel changes in many tumorigenic secreted factors including PDGF-AA and IGFBP1. Relevant protein secretions may be regulated by KDM4B via an upstream target or be indicative of a transcriptional mechanism regulated by KDM4B.

A.

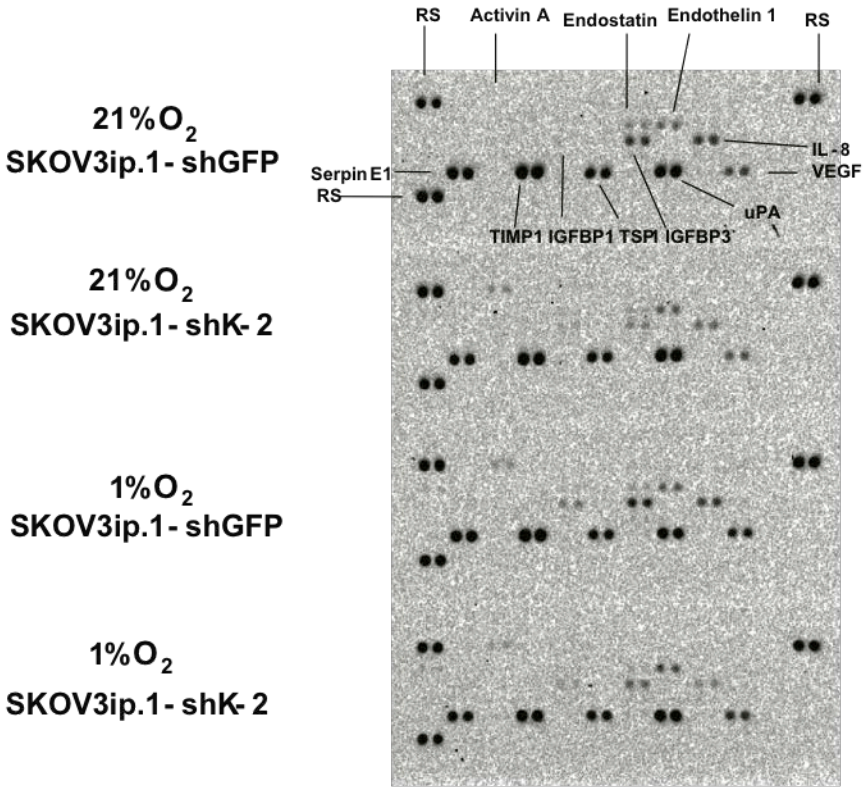
RS
Activin A
Endostatin
Endothelin 1
RS
21%O2
SKOV3ip.1- shGFP
21%O2
SKOV3ip.1- shK-2
1%O2
SKOV3ip.1- shGFP
1%O2
SKOV3ip.1- shK-2
Serpin E1
RS
IL-8
VEGF
uPA
TIMP1
IGFBP1
TSP1
IGFBP3

B.

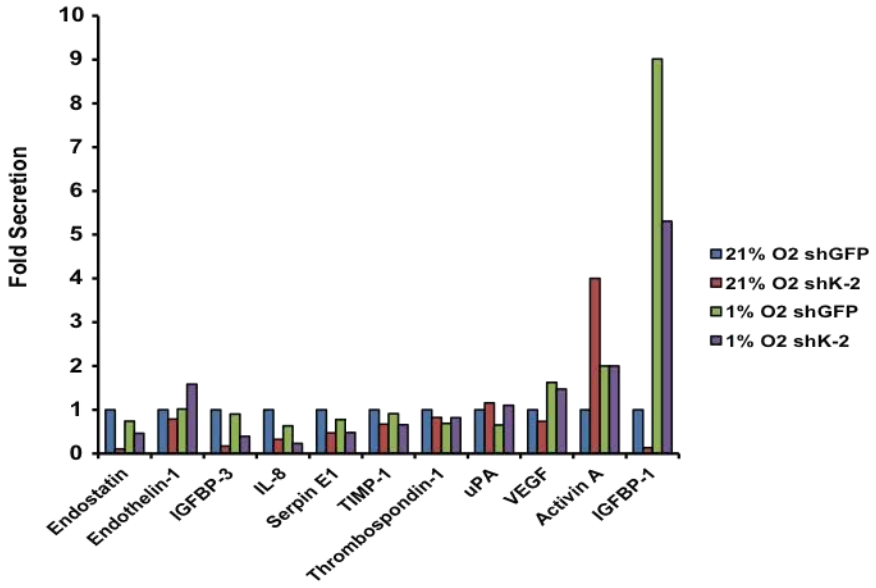
Fold Secretion
10
9
8
7
6
5
4
3
2
1
0
Endostatin
Endothelin-1
IGFBP-3
IL-8
Serpin E1
TIMP-1
Thrombospondin-1
uPA
VEGF
Activin A
IGFBP-1
21% O2 shGFP
21% O2 shK-2
1% O2 shGFP
1% O2 shK-2

Figure 3.7. Loss of KDM4B influences differential secretion of factors in the epithelial ovarian cancer line SKOV3ip.1. A. Conditioned media from SKOV3ip.1 cells expressing shRNA targeting KDM4B (shK-2) or GFP (control) in 21% and 1% O_2 showed differential expression of pro-angiogenic and anti-angiogenic factors on angiogenesis array blots (R and D) (n=1). Layout from top to bottom is as follows: 21% O_2 SKOV3ip.1-shGFP array, 21% O_2 SKOV3ip.1-shK-2 array, 1% O_2 SKOV3ip.1-shGFP array, and 1% O_2 SKOV3ip.1-shK-2 array. Differentially expressed proteins are labeled in the top array for reference. RS refers to built-in reference spots. **B.** Quantitation of protein expression changes is shown (n=1). Expression has been normalized to reference spots on arrays.

A.

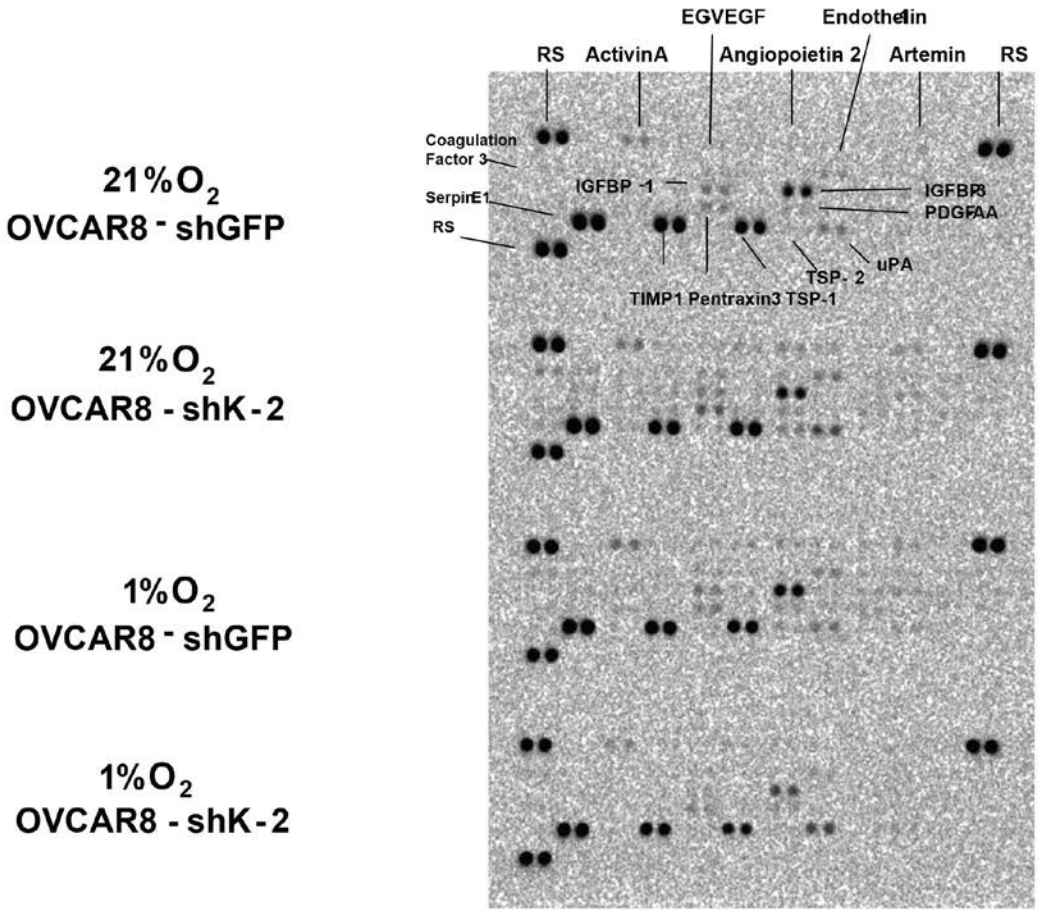
21%O2
OVCAR8 - shGFP
21%O2
OVCAR8 - shK-2
1%O2
OVCAR8 - shGFP
1%O2
OVCAR8 - shK-2
RS
ActivinA
EGVEGF
Angiopoietin 2
Endothelin
Artemin
RS
Coagulation Factor 3
SerpinE1
RS
IGFBP -1
IGFBP3
PDGFAA
uPA
TSP- 2
TIMP1 Pentraxin3 TSP-1

B.

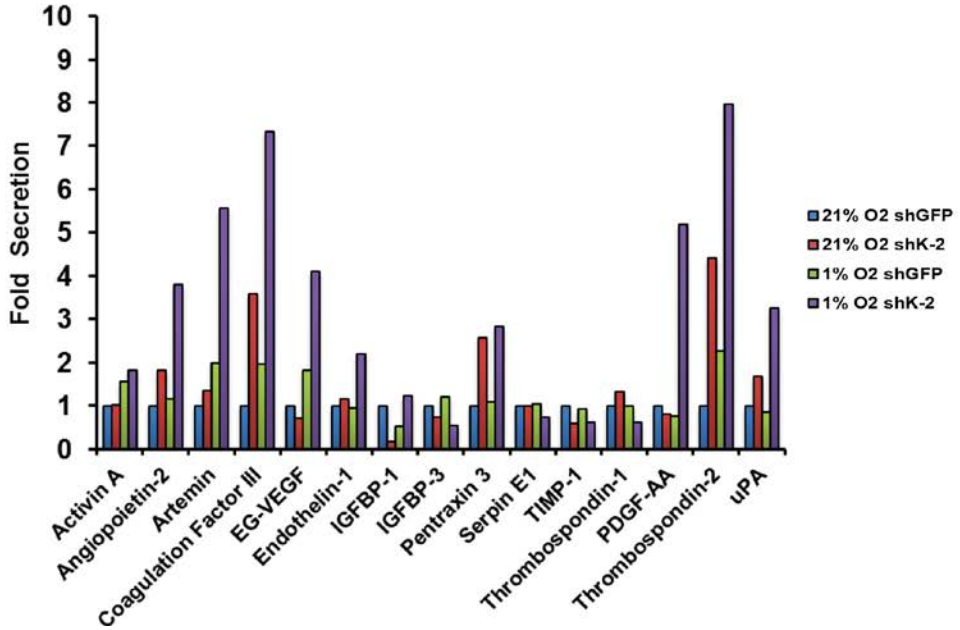
Fold Secretion
10
9
8
7
6
5
4
3
2
1
0
Activin A
Angiopoietin-2
Artemin
Coagulation Factor III
EG-VEGF
Endothelin-1
IGFBP-1
IGFBP-3
Pentraxin 3
Serpin E1
TIMP-1
Thrombospondin-1
PDGF-AA
Thrombospondin-2
uPA
21% O2 shGFP
21% O2 shK-2
1% O2 shGFP
1% O2 shK-2

Figure 3.8. Loss of KDM4B influences differential secretion of pro-angiogenic and anti-angiogenic factors in the epithelial ovarian cancer line OVCAR8. A. Conditioned media from OVCAR8 cells expressing shRNA targeting KDM4B (shK-2) or GFP (control) in 21% and 1% O_2 showed differential expression of pro-angiogenic and anti-angiogenic factors on angiogenesis array blots (R and D) (n=1). Layout from top to bottom is as follows: 21% O_2 OVCAR8-shGFP array, 21% O_2 OVCAR8-shK-2 array, 1% O_2 OVCAR8-shGFP array, and 1% O_2 OVCAR8-shK-2 array. Differentially expressed proteins are labeled in the top array for reference. RS refers to built-in reference spots. **B.** Quantitation of protein expression changes are shown (n=1). Expression has been normalized to reference spots on arrays.

Loss of KDM4B Expression Corresponds to Expression Changes in IL-8 and IGFBP-1. IL-8 and IGFBP-1 have established connections to epithelial ovarian cancer progression (Dal Maso, Augustin et al. 2004; Baxter 2014; Stronach, Cunnea et al. 2015). Secretion of these factors was identified using angiogenesis arrays (Fig 3.7 and Fig 3.8). SKOV3ip.1 showed decrease of *IL-8* and *IGFBP-1* secretion with loss of KDM4B (Fig 3.7A and Fig 3.8B). These changes corresponded to increased *IL-8* and no significant changes in *IGFBP-1* expression in SKOV3ip.1 cells (Fig 3.9A). Even though *IGFBP-1* and IL-8 showed no notable changes upon OVCAR8 angiogenesis array analysis, IL-8 increased while *IGFBP-1* expression decreased (Fig 3.9B). Considering the importance of angiogenesis and secreted factors in EOC metastasis, continued expression analysis of array targets will help establish functional contributions of KDM4B activity to this process.

A.

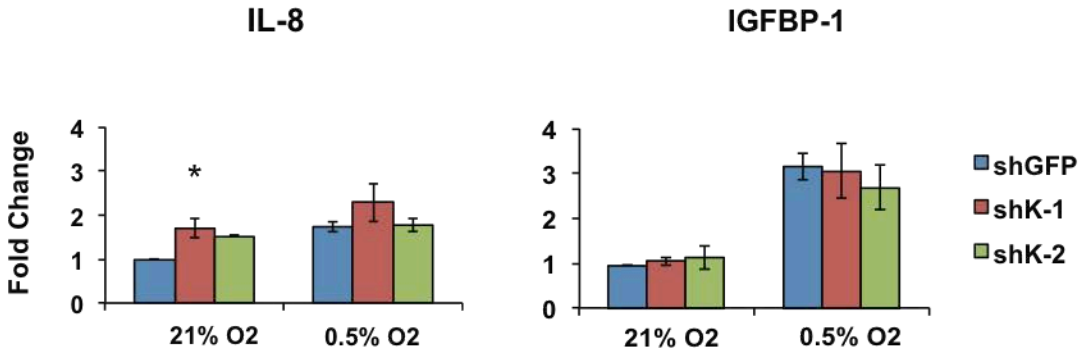
IL-8
IGFBP-1
Fold Change
4
3
2
1
0
*
21% O2
0.5% O2
shGFP
shK-1
shK-2

B.

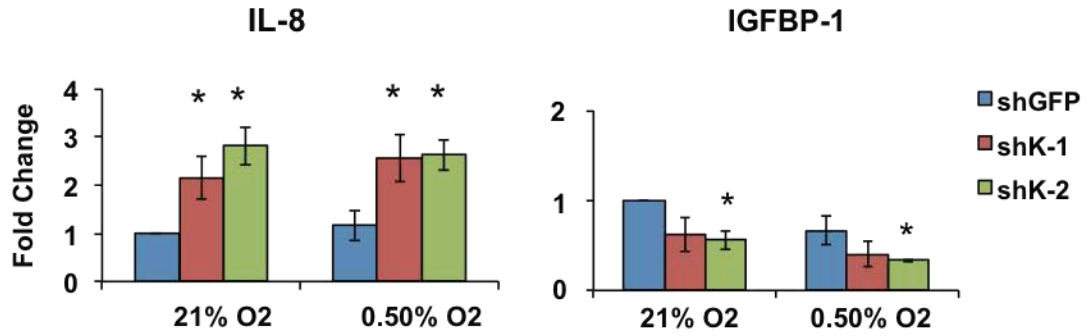
IL-8
IGFBP-1
Fold Change
4
3
2
1
0
* *
* *
21% O2
0.50% O2
2
1
0
*
*
shGFP
shK-1
shK-2

Figure 3.9. IL-8 and IGFBP-1 show differential regulation in the context of KDM4B expression between SKOV3ip.1 and OVCAR8 cell lines. A. qPCR validation of *IL-8* and *IGFBP-1* expression in SKOV3ip.1 with shRNA targeting *KDM4B* (shK-1 and shK-2) or GFP (control) in 21% and 0.5% O2 (n=3) ($p<0.05$). **B.** qPCR validation of *IL-8* and *IGFBP-1* expression in OVCAR8 with shRNA targeting *KDM4B* (shK-1 and shK-2) or GFP (control) in 21% and 0.5% O2 (n=3) ($p<0.05$).

Expression of KDM4B Increases Spheroid Invasion *in vitro*. Dissemination and metastasis of ovarian tumors involves the formation, invasion, and adhesion of cancer cell clusters called spheroids (Puiffe, Le Page et al. 2007). In patients, spheroids detach from the primary tumor and attach and invade at distant areas within the peritoneal cavity (Davidowitz, Selfors et al. 2014). Previous studies have shown KDM4B expression increases spheroid formation and maintenance *in vitro* and peritoneal dissemination *in vivo* (Chapter 2). Boyden chamber invasion through Matrigel and migration assays connect KDM4B to increased invasion (Chapter 2). These findings suggest increased KDM4B expression could drive spheroid invasion. In order to test this hypothesis, a novel 3D spheroid invasion assay was utilized. OVCAR8 spheroids were formed as indicated in previous studies (Chapter 2) and placed upon a polymerized ECM component, Type I collagen (Fig 3.10A and Fig 3.10B). Images were taken 7 and 14 days post spheroid addition to quantify invasive spheroid potential (Fig 3.10A). In order to quantify invasion distance, basic measurements were taken using ImageJ as indicated (Fig 3.10C). A central spheroid area and area of invasion were measured for all spheroid replicates in each condition at day 10 and day 17 as indicated (Fig 3.10A and Fig 3.10C). Representative images of OVCAR8 spheroid invasion assays from day 10 of this assay are shown (Fig 3.11A). OVCAR8 spheroids with loss of KDM4B show decreased invasion on this substrate at both 21% O_2 and 2% O_2 (Fig 3.11A). OVCAR8-shGFP control spheroids display increased disaggregation or budding from the main spheroid area (Fig 3.11A). The budding phenotype is not present in knockdown spheroids (Fig 3.11A). Invasion area quantification for 7 days of Type I Collagen invasion is included (Fig 3.11B). Even though these findings are not significant, they show a decreased quantification of invasion area (Fig 3.11B). In addition to *MUC1*, *ARID5B*, and *MYO1D* (Fig 3.4), additional target gene expression involved with invasion, migration, and epithelial-to-mesenchymal transitions were validated (Fig 3.11C). *CDH1* (E-cadherin), *CDH3* (P-cadherin), *ICAM6* (Intracellular Adhesion Molecule 6), *NCAM2* (Neural Cell Adhesion Molecule 2), *ITGA6* (Integrin Subunit Alpha 6), *ITGA7* (Integrin Subunit Alpha 7), *MMP15* (Matrix Metalloprotease 15), *ITGA2* (Integrin Subunit Alpha 2), *ITGA4* (Integrin Subunit Alpha 4), and *MMP1* (Matrix Metalloprotease 1) show KDM4B dependent decreases in expression in OVCAR8 (Fig 3.11C).

These target genes may be regulated downstream of KDM4B and influence spheroid invasion and migration.

A.

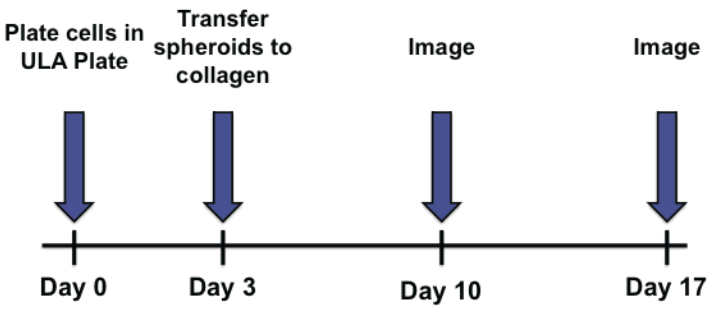
Plate cells in ULA Plate
Transfer spheroids to collagen
Image
Image
Day 0
Day 3
Day 10
Day 17

B.

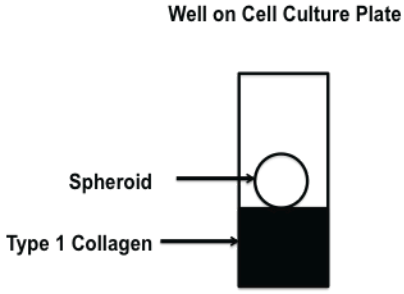
Well on Cell Culture Plate
Spheroid
Type 1 Collagen

C.

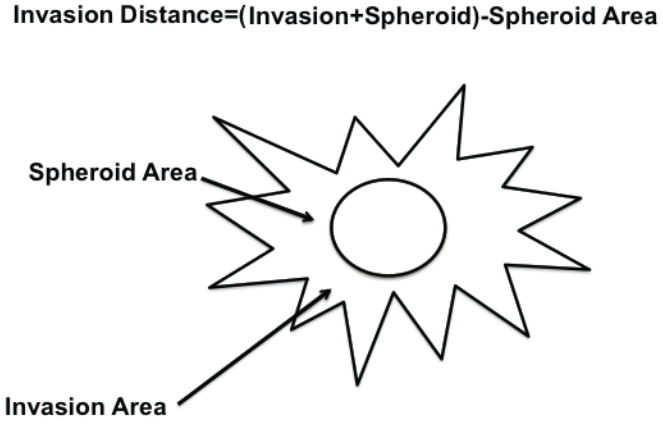
Invasion Distance=(Invasion+Spheroid)-Spheroid Area
Spheroid Area
Invasion Area

Figure 3.10. Development of 3-D spheroid invasion model for epithelial ovarian cancer. A. Timeline describes the process for spheroid invasion experiment. Spheroids were formed and the invasion assay set up as described in Materials and Methods and placed upon polymerized Type I Collagen. Images were taken after 7 and 10 days. **B.** Diagram shows representation of spheroid in relation to the polymerized Type I Collagen. **C.** Invasion distance was calculated as shown in the figure. Invasion area and spheroid area were measured as described using NIH software package ImageJ.

A.

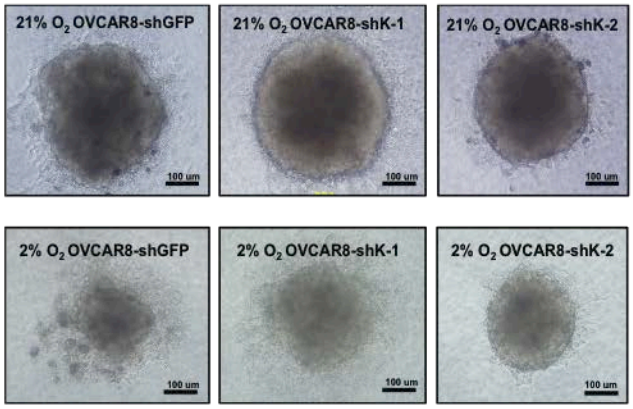
21% O2 OVCAR8-shGFP
21% O2 OVCAR8-shK-1
21% O2 OVCAR8-shK-2
2% O2 OVCAR8-shGFP
2% O2 OVCAR8-shK-1
2% O2 OVCAR8-shK-2
100 um

B.

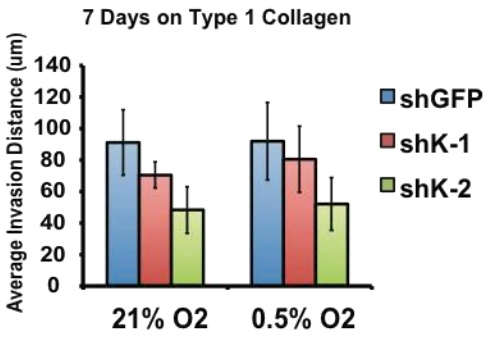
7 Days on Type 1 Collagen
Average Invasion Distance (um)
140
120
100
80
60
40
20
0
21% O2
0.5% O2
shGFP
shK-1
shK-2

C.

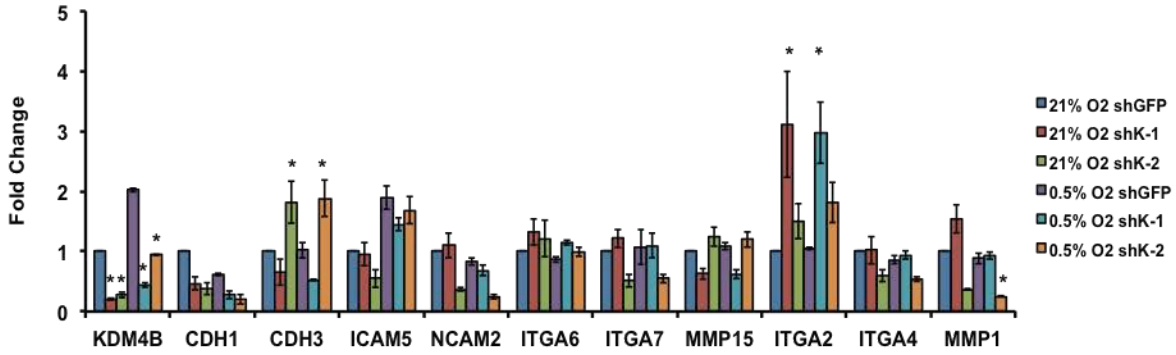
Fold Change
5
4
3
2
1
0
KDM4B
CDH1
CDH3
ICAM5
NCAM2
ITGA6
ITGA7
MMP15
ITGA2
ITGA4
MMP1
21% O2 shGFP
21% O2 shK-1
21% O2 shK-2
0.5% O2 shGFP
0.5% O2 shK-1
0.5% O2 shK-2

Figure 3.11. KDM4B expression increased invasion of OVCAR8 spheroids on Type I Collagen *in vitro* and differential gene expression of putative target genes involved with invasion and epithelial to mesenchymal transition. A. Images are from representative replicates from the invasion assay at the normoxic (21% O_2) and hypoxic treatment (1% O_2) following 7 days of specified oxygen tension treatment. (N=1; n=8) **B.** Quantification of OVCAR8 spheroid invasion area from experiment imaged in **A** is shown here. Error bars indicate standard deviation within technical replicates. **C.** qPCR validation of putative target genes with connections to regulation of invasion and EMT, including: *KDM4B*, *CDH1*, *CDH3*, *ICAM5*, *NCAM2*, *ITGA6*, *ITGA7*, *MMP15*, *ITGA2*, *ITGA4*, and *MMP1*. Expression analysis from OVCAR8 cells with shRNA targeting *KDM4B* (shK-1 and shK-2) or GFP (control) in 21% and 0.5% O2 (n=3) ($p<0.05$).

KDM4B Expression is Present in Patient Ascites Cells. In order to establish the clinical relevance of KDM4B in spheroid invasion and migration, patient ascites expression was explored. Patient ascites contains spheroids and other relevant factors secreted in the peritoneal fluid during metastasis (Puiffe, Le Page et al. 2007). Ascites cells were obtained from frozen stock cultures and maintained in ultra-low attachment cell culture dishes. Representative images of 4 separate patient samples are shown (Fig 3.12A-Fig 3.12B). Even though these were obtained from patients in different stages, there is no significant difference in appearance in culture conditions. KDM4B expression was present in various levels, not dependent on oxygen tension (Fig 3.12C). Loading control expression may very between epithelial ovarian cancer cell lines. This validated including both β-catenin and α-tubulin expression (Fig 3.12C). Since ascites contains a heterogeneous mix of cell types, EPCAM (Epithelial Cell Adhesion Molecule) was included to confirm the presence of epithelial cells (Fig 3.12C). The distinctive variation in expression of all proteins between the 4 patient lines may indicate a viability issue at protein lysis. However, the presence of KDM4B in patient ascites cells may identify a novel role for this protein in spheroid-driven peritoneal dissemination.

A.

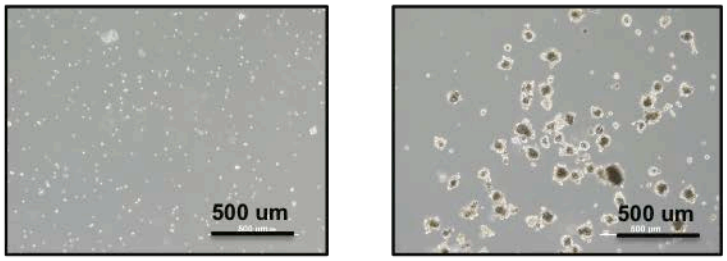

1129
Stage II

7500
Stage IIb

B.

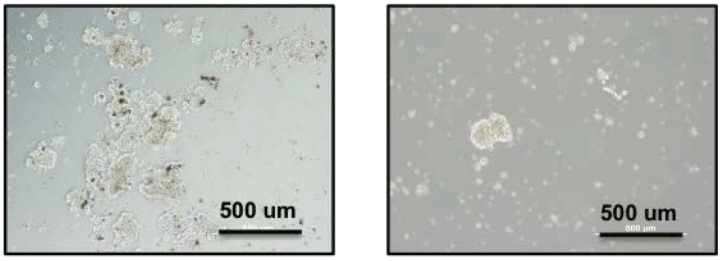

4203
Stage IIIc

7875
Stage IIIc

C.

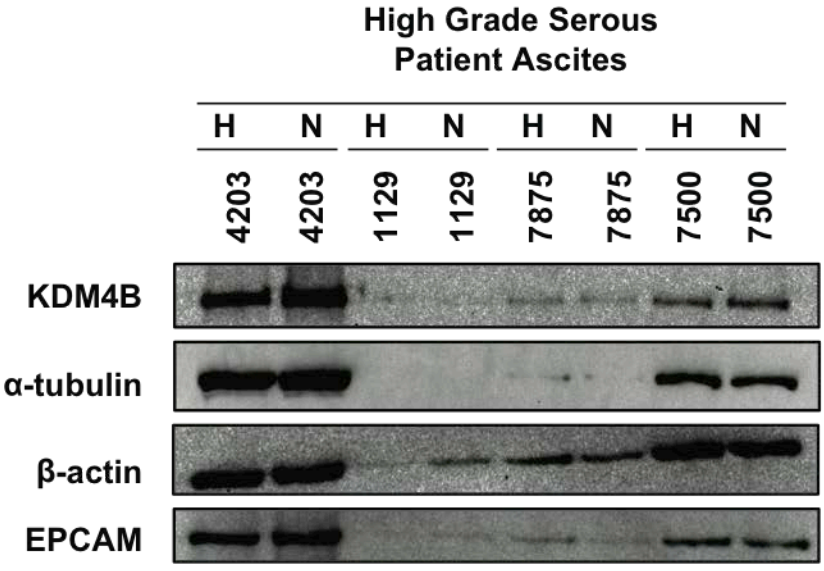

Figure 3.12. KDM4B is expressed in patient ascites maintained in ultra-low attachment conditions *in vitro*. A and B. Images of patient ascites maintained in ultra-low attachment cell culture plates are shown. De-identified patient codes are used to label ascites cell lines and FIGO staging for cell line is included. **C.** Immunoblot measurement of KDM4B expression in patient ascites lines maintained in ultra-low attachment cell culture at normoxic (N) condition or 21% O_2 and hypoxic (H) condition or 0.5% O_2. α-tubulin and β-actin serve as loading controls. EPCAM is included as a marker to identify tumor cells of epithelial origin.

DISCUSSION

Identifying the role of KDM4B in processes driving peritoneal dissemination and metastasis may provide novel therapeutic targets for consideration in EOC. Our previous experiments in Chapter 2 demonstrate a correlation between KDM4B expression and increased invasion, migration, and spheroid formation *in vitro* and *in vivo*. These findings suggest KDM4B influences vascular remodeling via differential secretion of factors and could affect inflammatory responses in the tumor microenvironment. The spheroid invasion assays also identifies a connection between KDM4B expression and EOC spheroid invasion, a detrimental component of advanced EOC progression (Chapter 3). RNA Sequencing identified a putative link between KDM4B, the KDM4B target gene *PDGFB*, and *ARID5B* expression. These proteins are established contributors to aspects driving metastasis including angiogenesis, inflammatory response, invasion, and cell motility and may impact the observations in these functional assays (Dong, Grunstein et al. 2004; Baba, Ohtake et al. 2011; Hata, Takashima et al. 2013; Emerenciano, Barbosa et al. 2014). Identifying how KDM4B regulates these aspects of tumorigenesis will explain another connection between this histone demethylase and EOC progression.

RNA Sequencing analysis between two representative cell models identified 14 commonly regulated target genes, including *MUC1*. This putative target gene provides compelling rationale for continued investigation and dissection in KDM4B-dependent EOC experimentation. MUC1 encodes an O-glycosylated membrane-bound protein that plays an essential role in forming protective mucous barriers on epithelial surfaces and lines mucosal surfaces of many different tissues (Budiu, Elishaev et al. 2013). Putative target genes, such as PDGFB, do not regulate MUC1 but previous studies indicate the utility in exploring the potential relationship between KDM4B and MUC1 in tumorigenic function. A previous EOC tumor microarray study by *Wang, et al.* identified high MUC1 expression in both primary epithelial ovarian cancers and in matched metastatic ovarian cancer tissue (> 90%), with MUC1 cytoplasmic expression correlating with poor overall survival and invasive capacity ($P<0.05$) (Wang, Ma et al. 2007). During tumor progression, MUC1 can become overexpressed and differentially glycosylate highlighting a role for MUC1 expression as a tumor associated antigen (Chauhan, Vannatta et al. 2009).

The extracellular domain of MUC1 may be cleaved and found in patient serum, suggesting its use as a prognostic biomarker (Engelstaedter, Heublein et al. 2012). These possible established links between MUC1 and EOC progression may implicate KDM4B in regulating invasion, migration, and attachment-free growth. However, MUC1 is a complex protein. Currently, there are 78 identified isoforms and numerous protein modifications possible on MUC1, potentially complicating the ability to effectively manipulate this gene *in vitro* and *in vivo* (Zhang, Vlad et al. 2013). ARID5B not only provides a potential link to the KDM4B target gene PDGFB, but a less complex target for mechanistic dissection.

The potential connection between KDM4B-dependent PDGFB expression and ARID5B provide provocative reasons to investigate their mechanistic relationship in regulating invasion and migration. ARID5B functions as a histone demethylase in combination with PHF2 to remove di-methyl marks from H3K9 (Baba, Ohtake et al. 2011). The PDGF pathway may also activate ARID5B expression (Schmahl, Raymond et al. 2007). Increased ARID5B expression correlates with decreased survival in high-grade serous patients, demonstrating a strong clinical connection for this presumed KDM4B target gene (Cancer Genome Atlas Research 2011). Mutations in ARID5B have been implicated in endometrial cancer and ALL, acute lymphoblastic leukemia (Cancer Genome Atlas Research, Kandoth et al. 2013; Emerenciano, Barbosa et al. 2014). Loss of ARID5B also decreases lipid metabolism, providing a potential link to ovarian cancer preferential omental targeting (Baba, Ohtake et al. 2011; Nieman, Kenny et al. 2011). Investigating the connection between KDM4B and ARID5B may provide another interesting link between KDM4B, another epigenetic modulator, and EOC progression.

In order to establish the tumorigenic functional role of the putative KDM4B target ARID5B, *in vitro* analysis to investigate proliferation, invasion, and migration and *in vivo* xenograft models would be pragmatic approaches. To demonstrate the effect of the loss of ARID5B on proliferation, a standard counting assay to estimate rate of proliferation could be performed. SKOV3ip.1 and OVCAR8 cells expressing shRNA to ARID5B or a GFP control would be seeded and treated with separate O_2 concentrations, 21% and 0.5% O_2. 2D scratch-wound assays would estimate the role of ARID5B in migration. Cells will be manipulated as indicated for the proliferation assay and seeded in scratch-would

assays at both 21% and 0.5% O_2. To estimate cell motility rate, imaging of the scratch would be performed every 4 hours until wound closure. NIH ImageJ measurements of the wound could be used to calculate rate of motility using the formula Rate=Distance/Time (R=D/T). In addition to 2D motility, defects on invasion and migration could be characterized using shRNA cell lines in 3D transwell Boyden Chamber Matrigel Assays at either 21% O_2 or 0.5% O_2. The ability of cells to invade through a Matrigel barrier could be estimated using CyQUANT® blue and correlated to the expression level of ARID5B and respective oxygen concentration. The *in vitro* contribution of ARID5B could be established using intraperitoneal xenograft models in nude mice using SKOV3ip.1 cells transduced with GFP or shARID5B constructs. Cells can be transduced with pLenti PGK V5-Luciferase Neo to allow for weekly bioluminescence imaging using the IVIS Spectrum *in vivo* imaging system. Post mortem analysis would determine: 1) overall tumor mass, 2) tumor nodule localization, and 3) ascites formation. Representative tumors will be harvested from each subject for RNA and protein analysis to verify ARID5B and KDM4B expression. To dissect the possible PDGFB dependent activation of ARID5B and invasion, the proposed 2D scratch and 3D transwell Boyden Chamber Assays could be completed using OVCAR8 and SKOV3ip.1 cell lines treated with PDGFB ligand. The findings from these proposed experiments would establish the functional and mechanistic roles of ARID5B in EOC tumorigenesis and establish a potential connection to PDGF pathway, a definite knowledge gap in this field.

The secreted proteome analyzed via the antibody arrays suggest KDM4B plays a role in secreting a myriad of factors involved with angiogenesis and inflammatory responses. KDM4B regulates secretion and expression of multiple factors, including IL-8 and IGFBP1 (Fig 3.7-3.9). IL-8 is a proinflammatory cytokine that promotes angiogenic and other tumorigenic effects (Stronach, Cunnea et al. 2015). IL-8 in EOC tumors corresponds with poor prognosis and advanced FIGO staging (Merritt, Lin et al. 2008). Overexpression of IL-8 in EOC has been shown to increase attachment-free growth, invasion, and vascular remodeling (Wang, Xu et al. 2012). IL-8 could provide a KDM4B target responsible for remodeling the tumor microenvironment in metastatic processes.

IGFBP1 was also identified as a differentially secreted protein in antibody array profiling (Fig 3.7-3.9). IGFBP1 is a protein secreted by the liver during inflammation to regulate IGF1(Rutkute and Nikolova-Karakashian 2007). IGFBP1 also has been shown to promote a pro angiogenic effect in tumor cell models (Rutkute and Nikolova-Karakashian 2007). IGFBP1 is a mitogen that has a demonstrated role in increasing cell proliferation and suppressing apoptosis (Terry, Tworoger et al. 2009). IGFBP1 has also been linked to increased ovarian cancer cell proliferation and invasion *in vitro*, suggesting a key role for this protein in these processes (Resnicoff, Ambrose et al. 1993). This connection between IGFBP1 and ovarian cancer tumorigenesis may indicate another tumorigenic pathway influenced by KDM4B activity.

Antibody array analysis used in these studies does not identify a particular KDM4B-dependent relationship between pro-angiogenic or anti-angiogenic factors. Secretion of different pro-angiogenic and anti-angiogenic factors varies between the cell lines used in proteome analysis (Fig. 3.7-3.9). Without further experimentation, these results can only suggest that loss of KDM4B effects protein secretion differently between cell lines. These unclear and complicated findings demonstrate the complexity of mechanisms regulating EOC angiogenesis. To further establish the role of KDM4B in angiogenesis, HUVEC (Human Umbilical Vein Endothelial Cell) *in vitro* assays using EOC cell lines containing an shRNA to KDM4B or a GFP control could be completed. This assay could pinpoint if KDM4B-dependent secretion of angiogenesis factors had a more pro-angiogenic or anti-angiogenic effect. Although chemotherapeutics targeting angiogenic factors show limited efficacy in EOC treatment, these types of experiments would identify additional tumorigenic pathways influenced by KDM4B expression (Della Pepa and Banerjee 2014; Li, Zhou et al. 2015; Petrillo, Nero et al. 2016).

Loss of KDM4B expression associated with decreased spheroid invasion (Fig 3.8-3.9). Spheroid formation and migration are indispensible factors driving the EOC metastatic cascade. The contribution of KDM4B in spheroid invasion assays matched earlier observations implicating KDM4B in increased invasion and migration in Boyden chamber assays (Chapter 2). In order to dissect how KDM4B influences spheroid invasion, this assay should be repeated using other components of the extracellular

matrix. Ovarian cancer cells can attach and spread on multiple ECM components, including: Type I Collagen, Type IV Collagen, Laminin, Vitronectin, and Fibronectin (Davidowitz, Selfors et al. 2014). Ovarian cancer cell lines also adhere and spread on mesothelial cells lining the peritoneal cavity. Complimenting additional ECM spheroid invasion assays with Mesothelial Clearance Assays would provide powerful insight into how KDM4B regulates the embedding and reattachments of invasive spheroids (Davidowitz, Selfors et al. 2014). At this time, the cellular mechanisms regulating mesothelial cell displacement by EOC spheroids are not well defined in previous research. KDM4B expression is associated with changes in numerous genes that regulate invasion, migration, and the epithelial to mesenchymal transition, including ITGA6, IL-8, IGFBP1, and CDH1 (Fig. 3.11). Further dissection using shRNA stable knockdown of these genes individually in spheroid invasion assays would identify their contribution to this spheroid property. Spheroid invasion assays should be completed using different extra cellular matrix components to identify their exact functional contribution to cellular movement. ChIP analysis of KDM4B binding would identify if these putative target genes are regulated directly or indirectly by this protein. Further investigation into this area may provide important insight into the KDM4B regulated mechanisms association with these cellular movement processes.

Presentation of ascites in advanced stages of EOC is a common finding at patient diagnoses (Cho and Shih Ie 2009). Ascites formation relies upon increased migratory and invasive potentials of spheroids (Davidowitz, Selfors et al. 2014). Utilizing ascites for experimentation is novel and highly relevant to EOC progression. KDM4B was differentially expressed in patient ascites cell lysates (Fig 3.10). However, ascites contains a myriad of cell types both neoplastic and normal from the surrounding tumor microenvironment (Smolle, Taucher et al. 2014). Further studies should be completed to appropriately sort cell types before immunoblotting or qPCR analysis. Follow-up assays using patient derived ascites cell lines would demonstrate the relevance of KDM4B activity in a representative *ex vivo* model.

This study demonstrates that the hypoxia-inducible histone demethylase KDM4B supports cellular adaptations influencing factors of the metastatic cascade, including invasion, migration, angiogenesis, and inflammation. Each aspect of metastasis drives disease pathogenesis and patient

mortality. The novel connection between KDM4B expression and the PDGF pathway may influence mechanistic or transcriptional regulation of these phenotypes. Future studies based on these observations would provide more extensive analysis into how KDM4B enzymatically regulates these pathways. Utilizing patient derived ascites cells for experimentation could provide observations in a highly clinically relevant model.

CHAPTER 4:

GENERAL DISCUSSION

Importance of this Project

Characterizing the roles of KDM4B in EOC provides novel epigenetic links between the hypoxic tumor microenvironment and histone methylation. Epigenetics and genetic aberrations work simultaneously in promoting tumorigenesis (Lund and van Lohuizen 2004). Delineating epigenetic and genetic changes establishes how they separately and synergistically drive tumorigenesis in EOC. This body of work is novel because it includes the first studies to investigate the role of KDM4B in EOC. Although not every aspect of KDM4B activity was explored, the data in this project connects KDM4B expression to aspects of the metastatic cascade, including: invasion, migration, and attachment-free growth *in vitro* (Chapter 2 and 3) (Naora and Montell 2005). In addition to *in vitro* observations, KDM4B expression corresponded to increased peritoneal dissemination and tumorigenesis in intraperitoneal xenograft models (Chapter 2). Identifying the functions regulated by KDM4B activity in EOC increases the understanding of the enzyme's activity and clarifies cell processes it may regulate. These observations establish KDM4B as an essential component influencing EOC progression, warranting further consideration and exploration by the field. At this time, no conserved KDM4B mechanisms and functions have been identified that are consistent between cell type and model system. Lack of a conserved mechanism dictates the necessity for continued KDM4B analysis.

Not only is KDM4B induced by HIF-1α, this project suggests another possible transcriptional link between HIF-1α and KDM4B activity (Beyer, Kristensen et al. 2008). These studies demonstrated possible interplay between KDM4B and HIF-1α activity. Commonly regulated targets, including *PDGFB* and *LOXL2* were identified in expression and ChIP analysis in SKOV3ip.1 and OVCAR8 (Chapter 2 and 3). This type of connection between KDM4B and HIF-1α has not been explored in the literature. HIF-1α recruits KDM3A to specific target genes, including *ADM* and *SERPINE1* (Krieg, Rankin et al. 2010; Perez-Perri, Acevedo et al. 2011). Considering the overlap between KDM4B and HIF-1α targets, it is possible this type of recruitment mechanism influences gene expression regulation in KDM4B EOC studies. This mechanism could only be established with further experimentation.

KDM4B expression is increased in EOC patient tumors and influences progression, presenting itself as a unique and novel target for therapeutic consideration and design (Chapter 2 and 3). Innovative therapeutic design will assist in combatting recurrent tumor formation and the late diagnoses plaguing effective EOC treatments (Giornelli 2016). Genomic expression and epigenetic abnormalities alter the background of each ovarian cancer cell and complicate the efficacy of standard therapies (Cho and Shih Ie 2009). . These contributing factors have slowed progress in improving therapeutics and increased tumor relapse in EOC (Mei, Chen et al. 2013). Ingenuity Pathway Analysis (IPA) identified KDM4B-dependent regulation of cell processes involved in EOC tumorigenesis, including cell death, cell movement, and DNA repair (Chapter 2). KDM4B dependent regulation of tumorigenic genes, including *PDGFB*, *LCN2*, and *LOXL2* was demonstrated using EOC models (Chapter 2 and 3). Targeting the enzymatic activity of KDM4B could provide genomic regulation of specific tumorigenic genes and cell processes regulating EOC. Positive outcomes from targeting KDM4B may establish KDM4B inhibition as a useful and progressive therapeutic option for treating other types of solid tumor cancers.

KDM4B expression may also be utilized as a novel EOC biomarker. At this time, biomarkers such as CA-125 are inconsistent and unreliable for adequate and early EOC diagnoses (Ueda, Enomoto et al. 2010). CA-125 expression varies between EOC stages and fluctuates during periods of tumor recurrence (Jacobs and Bast 1989). The unreliability of CA-125 justifies the exploration of using new biomarkers. KDM4B Tumor Microarray Analysis identified increased expression in primary, metastatic, and recurrent patient tumors (Chapter 2). KDM4B could also be used as an indicator of drug response. Given the relationship between KDM4B and PARP, PARP inhibitors like Niraparib may useful in EOC patients expressing KDM4B (Khoury-Haddad, Guttmann-Raviv et al. 2014; Hwang, Heo et al. 2015). Further pathological analysis of KDM4B expression in EOC could justify its utility as an EOC biomarker, prognostic indicator, or indicator of therapeutic efficacy.

KDM4B in Cancer

KDM4B expression has increased expression and established functional links to progression in numerous solid tumor cancers, including prostate, renal cell, breast, and gastric cancer (Kawazu, Saso et al. 2011; Coffey, Rogerson et al. 2013; Young, McDonald et al. 2013; Zhao, Li et al. 2013). In different cancer models, KDM4B expression has been linked to several aspects of tumorigenesis *in vitro* and *in vivo* including epithelial-to-mesenchymal transition, cell proliferation, apoptosis, DNA damage response, colony formation, cell survival, and metastasis (Kawazu, Saso et al. 2011; Tsai and Wu 2012; Young, McDonald et al. 2013; Berry, Kim et al. 2014; Hui, Yiling et al. 2015; Li, Wu et al. 2015). KDM4B activity has previously established connections to invasion, migration, and attachment-free growth *in vitro* and metastases *in vivo* (Kawazu, Saso et al. 2011; Li, Wu et al. 2015; Qiu, Fan et al. 2015). However, this body of work was the first to connect KDM4B expression on invasion, migration, and attachment-free growth *in vitro* using an EOC models.

Regulation of KDM4B expression and activity are important factors to consider while investigating KDM4B in cancer models. These control mechanisms are continuously being established in the literature. KDM4B may be regulated by a number of mechanisms in tumor models including, transcription factors, nuclear hormone receptors, tumor suppressors, or ubiquitin-dependent degradation (Palomera-Sanchez, Bucio-Mendez et al. 2010; Li, Zhao et al. 2011; Tsai and Wu 2012; Coffey, Rogerson et al. 2013; Ipenberg, Guttmann-Raviv et al. 2013; Zheng, Chen et al. 2014). KDM4B may be transcriptionally regulated by HIF-1α, β-catenin, and p53 (Beyer, Kristensen et al. 2008; Berry, Kim et al. 2014; Zheng, Chen et al. 2014). Nuclear hormone receptors such as Androgen Receptor (AR), Progesterone Receptor (PR), and Estrogen Receptor (ER) also influence expression of KDM4B (Yang, Jubb et al. 2010; Coffey, Rogerson et al. 2013). KDM4B can also be regulated by ubiquitination in response to DNA damage by RNF8 and RNF168 (Mallette, Mattiroli et al. 2012). Potential control mechanisms such as these are important to consider in future KDM4B studies. They could be directly regulating KDM4B or other targets, driving additional effects in different model systems. The significance of their role in disease pathogenesis will depend upon the model type and genetic background.

KDM4B regulates expression of many relevant cancer related targets across different tumor models, including *MYB*, *C-MYC*, and *CCND1* (Kawazu, Saso et al. 2011; Qiu, Fan et al. 2015). Proteins complexed with KDM4B, such as other transcription factors and nuclear hormone receptors help dictate and regulate these genetic changes. For instance, in gastric cancer models KDM4B binds the transcription activator β-catenin to induce expression of *JUN*, *MYC*, and *CCND1* (Zhao, Li et al. 2013). KDM4B activity has been connected to expression and activity of histone lysine methyltransferases. KDM4B works in concert with the methyltransferase MLL2 to regulate expression of ER+ target genes in breast cancer models, including *TFF1* (Trefoil Factor 1) and *EBAG9* (Estrogen Receptor Binding Site Associated, Antigen, 9) (Shi, Sun et al. 2011). Additional breast cancer studies have demonstrated KDM4B binds with ER and the SWI/SNF-B chromatin-remodeling complex to facilitate expression of MYC and MYB (Kawazu, Saso et al. 2011). Targets may be regulated through different mechanisms by the activity of KDM4B with different proteins.

The mechanisms driving KDM4B gene activation are not clearly characterized or conserved between cancer models. Some studies have shown KDM4B drives gene expression in a demethylation-dependent manner while others have not demonstrated this relationship (Kawazu, Saso et al. 2011; Coffey, Rogerson et al. 2013; Berry, Kim et al. 2014). This does not indicate genes in those studies were not expressed in a demethylation dependent manner. It is likely genomic variability influences KDM4B binding sites. Other proteins complexed with KDM4B may also dictate genomic targeting. KDM4B activity has also been linked to a variety of transcription factors, including HIF-1α and β-catenin (Berry and Janknecht 2013). Even though these are two demonstrated binding partners of KDM4B, it is likely other transcription factors or epigenetic remodelers could associate with KDM4B to influence activity and gene expression changes. These could include NF-kappa B (NF-kB) or STAT proteins, often implicated in the progression of tumorigenesis (Ling and Kumar 2012). KDM4B has also been shown to bind with the chromatin remodeling complex SWI/SNF-B to transition heterochromatic regions to a more euchromatic state, allowing accessibility to transcription factors to drive gene expression (Kawazu, Saso et al. 2011). A connection has been established between the methyltransferase MLL2 and KDM4B in

ER+ breast cancer models that effect chromatin compaction and subsequent gene expression (Kawazu, Saso et al. 2011). Combined, these mechanisms indicate the versatile nature of KDM4B in regulating tumorigenic gene expression in cancer models.

Relevance

KDM4B in Epithelial Ovarian Cancer

Demonstrating the role of KDM4B in ovarian cancer established a novel epigenetic link between the hypoxic tumor microenvironment and ovarian cancer progression. Epigenetic activity in ovarian cancer tumorigenesis remains an understudied aspect of EOC research (Marsh, Shah et al. 2014). Few studies have addressed identification of histone demethylase activity in gynecological cancers, let alone characterizing contributions from jumonji-domain containing proteins (Qiu, Fan et al. 2015; Wang, Mao et al. 2015). Hypoxia and HIF-1α activity are established contributors influencing tumor pathology and ovarian cancer progression (Osada, Horiuchi et al. 2007). However, little explanation for all HIF-1α regulated genetic and epigenetic changes within ovarian cancer tumor cells have been delineated.

KDM4B has well-established links to progression in many tumor models in the literature, except EOC. These sets of studies are highly unique, identifying the first connections between KDM4B expression and EOC tumorigenesis and peritoneal dissemination (Chapter 2 and 3) (Berry and Janknecht 2013). This project was the first to demonstrate the presence of KDM4B in epithelial ovarian cancer and pursue the purpose for its expression. The relevance of KDM4B was evident in patient samples and translated to significant effects in functional assays and expression analysis (Chapter 2 and 3). KDM4B expression was increased in primary, metastatic, and recurrent tumor sections (Chapter 2). KDM4B expression and activity was linked to tumorigenic gene expression and pathway changes, increased invasion, migration, attachment-free growth, and secreted factors *in vitro* (Chapter 2 and 3). The degree of KDM4B-dependent peritoneal dissemination was also increased using *in vitro* intraperitoneal xenograft models (Chapter 2). The data shows KDM4B is an essential enzyme for EOC progression and worthy of

consideration between other cancer models. Not every mechanistic question could be addressed in this body of work, leaving many areas for pursuit.

This body of work identified novel connections between KDM4B expression and invasion and migration *in vitro* and peritoneal dissemination *in vivo* (Chapter 2 and 3). The influence of KDM4B in regulating invasion and migration was shown using single cell Boyden chamber assays and multicellular spheroids (Chapter 2 and 3). These observations suggest KDM4B plays a conserved role in regulating SKOV3ip.1 and OVCAR8 single-cell and multi-cell motility, both problematic contributors to EOC progression and dissemination (Cho and Shih Ie 2009). Invasion and migration studies were conducted using matrigel, which contains multiple components of ECM, and Type 1 Collagen individually (Chapter 2 and 3). With this in mind, it is likely KDM4B regulates expression of cell adhesion factors or proteases responsible for invasion and migration through these types of substrates. *MUC1*, *LCN2*, and *LOXL2* were identified as possible contributors in these studies (Chapter 2 and 3).

MUC1 was identified through RNA Sequencing as a putative KDM4B target gene and may influence the results in invasion and migration experimentation (Chapter 3). MUC1 expression is linked to poor prognosis and highly metastatic EOC (Dong, Walsh et al. 1997; Horm and Schroeder 2013). Invasion through Matrigel is also increased by expression of this glycoprotein (Horn, Gaziel et al. 2009). Blocking MUC1 with the antibody C595 decreased tumor invasion and dissemination in EOC xenograft models (Wang, Chen et al. 2011). This possible connection between KDM4B and MUC1 may explain one aspect of how KDM4B regulates attachment-free growth, invasion, and migration.

LCN2, which processes MMP9 (Matrix Metallopeptidase 9), was also identified as a putative target gene regulated in these studies that influences tumor cell adhesion and invasion (Koh and Lee 2015). MMP9 has been established as a regulator of invasion and metastasis in ovarian cancer models (Kwon, Lee et al. 2014). LCN2 was shown to be upregulated in EOC tumors and correlated with tumor differentiation (Cho and Kim 2009). Targeting LCN2 has shown decreased angiogenesis and metastasis in breast cancer models, demonstrating its possible utility as an EOC target (Guo, Yang et al. 2016).

LCN2 provides a novel target for consideration in identification of KDM4B-dependent invasion and migration changes.

LOXL2 (Lysl Oxidase-like Protein-2) was also identified as a KDM4B target, regulated in a histone-demethylation dependent manner (Chapter 2 and 3). LOXL2, responsible for crosslinking Collagen Type IV, increases invasion and metastasis in a number of tumor models including breast and gastric cancers (Peng, Ran et al. 2009; Barker, Chang et al. 2011; Kim, Dong et al. 2014). The qPCR, ChIP analysis, and invasion and migration findings lend LOXL2 as an interesting possible link between KDM4B and increased invasion. Further pathological investigation may identify KDM4B as a useful biomarker for identifying more metastatic and invasion EOC diseases.

Shifting between an epithelial and mesenchymal state influences invasive and metastatic potentials of ovarian cancer cells as well as the ability of tumors to maintain attachment-free growth in spheroids (Deng, Wang et al. 2016). Some targets identified in this study could influence invasion and attachment-free growth like *CDH1* (E-cadherin). *CDH1* (E-cadherin) was shown to be downregulated with the loss of KDM4B expression (Chapter 3). Loss of E-cadherin shifts the tumor cell towards a more mesenchymal type, increasing its motility and ability to survive attachment free (Du and Shim 2016). KDM4B may be driving invasive potentials of tumor cells by influencing the transition from epithelial to mesenchymal type. A link between KDM4B and EMT has been shown in gastric and pancreatic cancers, indicating the possibility of this mechanism in EOC (Zhao, Li et al. 2013; Li, Wu et al. 2015).

Although increased angiogenesis was not indicated in a KDM4B dependent manner in patient or xenograft tumors (data not shown), a direct link between KDM4B and PDGFB was identified (Chapter 2 and 3). PDGFB is an established factor involved with angiogenesis and lymphangiogenesis, key aspects driving ovarian cancer metastasis and dissemination (Dong, Grunstein et al. 2004; Tejada, Yu et al. 2006). PDGFB may still influence increased invasion and peritoneal dissemination through other avenues besides vascular remodeling. PDGFB acts as a recruitment signal, initiating pericyte invasion and migration (Kelly, Haldeman et al. 1991). PDGFB was identified as a direct KDM4B target, regulated in a histone-demethylation dependent manner (Chapter 2 and 3). Aptamer targeting of PDGFB shows

reasonable efficacy in slowing angiogenesis in EOC (Lu, Shahzad et al. 2010). This connection between KDM4B and PDGFB is new to the KDM4B cancer field, potentially linking KDM4B to multiple aspects driving tumorigenesis.

This body of work showed KDM4B activates expression of *PDGFB*, *LOX*, *LOXL2*, and *LCN2* in a demethylation dependent manner on their respective promoters (Chapter 2). KDM4B does not regulate a genome wide effect on histone methylation. Loss of KDM4B did not increase global methylation of H3K9me3, H3K9me2, H3K9me, H3K36me3, H3K36me2 and H3K36me in EOC models (Chapter 2). This indicates that the demethylase activity of KDM4B at specific promoters may be the most important regulatory aspect of this enzyme at least for these genes.

Considering the functional importance of KDM4B and identified target genes, this protein is worth considering in therapeutic or combinatory treatment plans for EOC patients. At this time, inhibitors struggle with specificity of KDM4B. KDM4B is a member of a family of proteins sharing conserved domains, demethylase mechanism, and substrates for activity (Berry and Janknecht 2013). Targeting KDM4B may also cause secondary effects by disrupting functions that require its activity, such as ESC differentiation, driving other cell processes towards tumorigenic phenotypes (Das, Shao et al. 2014). Targeting of KDM4B regulated genes implicated in EOC tumorigenesis may provide another mode of EOC inhibition. Therapeutics are available that target PDGFB, LOX, LOXL2, and LCN2 are available and should be tested in appropriate EOC *in vitro* and *in vivo* models in the context of KDM4B dependent expression.

Expression of KDM4B was also identified for the first time in this study in EOC patient ascites lysates. Ascites spheroids provide a useful patient-derived model to test the contribution of KDM4B to these tumorigenic functions. Ascites fluid contains spheroids or multicellular groupings that are metastatic tumors formed during EOC progression (Puiffe, Le Page et al. 2007). This result suggests KDM4B is active and regulating gene expression in patient spheroids (Chapter 3). However, without further dissection its difficult to identify the mode of ascites spheroid formation KDM4B is regulating. Analysis of spheroid lysates provided a novel look into KDM4B dependent disease progression. Even

though this project addressed unknowns regarding KDM4B in EOC, many gaps still exist in the KDM4B field.

Knowledge Gaps in the KDM4B Field

This project answers questions regarding the previously unaddressed question of the role of KDM4B in EOC progression. These findings are innovative, but certain questions remain untouched by this body of work and available publications.

Several essential questions regarding histone demethylase transcriptional regulation and activity remain entirely unaddressed in regard to KDM4B function in any experimental model. The protein or signals responsible for recruiting KDM4B to specific sites for demethylation or transcriptional activation have not been clearly delineated in many models. Double strand breaks after γ-irradiation have been shown to recruit KDM4B to sites of DNA damage, supporting a role for the protein in the early DNA damage response in osteosarcoma models (Young, McDonald et al. 2013). Demethylation of H3K9me3 by KDM4B follows recruitment to these heterochromatic regions (Young, McDonald et al. 2013). However, this does not explain a conserved mode of recruitment for KDM4B in other cancer models.

There are likely additional signaling mechanisms directing KDM4B to bind and function at specific genomic loci. Not only is KDM4B induced by HIF-1α, it is possible this protein regulates its presence and activity within the cell (Beyer, Kristensen et al. 2008). HIF-1α is shown to recruit KDM3A to specific target genes (Krieg, Rankin et al. 2010; Perez-Perri, Acevedo et al. 2011). Considering the similar relationship between HIF-1α and KDM3A/KDM4B, it is a possible this recruitment mechanism also functions in KDM4B models. This potential HIF-1α/KDM4B connection could be addressed in future studies. This could be approached utilizing siRNA/shRNA for *in vitro* expression analysis, with binding profiled using ChIP assays. A conserved mode of recruitment by HIF-1α would be an innovative finding for the KDM4 research field.

KDM4B lysine residue and DNA targeting is not well characterized. KDM4B sequence-specific binding motifs have also not been identified. Loss of the Tudor and PHD domains has been shown to disrupt localization of KDM4B to heterochromatin during the DNA damage response (Young, McDonald et al. 2013). KDM4C also depends upon its Tudor domains for targeting to mitotic chromatin during mitosis (Kupershmit, Khoury-Haddad et al. 2014). There is also no identified KDM4B Response Element or conserved binding motif. Mutagenesis studies in EOC establishing the contributions of the Tudor and PHD domains in KDM4B binding would provide novel insight into targeting capacity of KDM4B.

The external (i.e.-ligand/receptor) and internal (i.e.-cellular cascade) signaling mechanisms that may contribute to KDM4B expression and activity should be identified and characterized. Transcription factors such as HIF-1α and β-catenin have been shown to regulate KDM4B expression (Beyer, Kristensen et al. 2008; Berry, Kim et al. 2014). The tumor suppressor p53 and nuclear hormone receptors such as AR and ER are also implicated in driving KDM4B expression (Palomera-Sanchez, Bucio-Mendez et al. 2010; Kawazu, Saso et al. 2011; Coffey, Rogerson et al. 2013). Because these signaling mechanisms are not universally conserved between cancer models, it is likely other factors are influencing induction of KDM4B expression and activity.

Specific relationships between certain histone methyltransferases and histone demethylases that regulate modification dynamics have not been identified. Dozens of histone lysine demethylases and histone lysine methyltransferases contribute to the regulation of histone methyl modifications at residues on H3K9 and H3K36 (Whetstine, Nottke et al. 2006; Kouzarides 2007). All histone lysine demethylases and methyltransferases as well as other epigenetic modifiers function in a genome-wide balance of chromatin modification writers and erasers. Establishing the connection between KDM4B and an H3K9 or H3K36 methyltransferase such as G9A, SUV39H1, or SET2 could explain KDM4B recruitment signals and epigenetic contributors regulation expression dynamics at specific genes (Fritsch, Robin et al. 2010; Jha and Strahl 2014).

Exploring possible compensatory relationships between KDM4 proteins would finer points of KDM4 activity regulation. This project suggested a compensatory role for KDM4A and KDM4D in lieu of silenced KDM4B expression in EOC (Chapter 2). This suggests that when the cancer cell lacks appropriate levels of KDM4B to maintain functions, KDM4A and KDM4D are increased to maintain gene activation or repression at H3K9 and H3K36 (Chapter 2) (Kouzarides 2007). Complete knockout of all KDM4 family proteins *in vitro* or *in vivo* may prove difficult because KDM4A and KDM4B are required for cell survival or apoptotic regulation in some models (Tsurumi, Dutta et al. 2013; Li and Dong 2015). It is also possible the cell may be programed to compensate for the loss of one KDM4 protein by increasing expression of another KDM4 or another jumonji protein. At this time, exploration of KDM4 compensation needs to be addressed.

Another innovative set of studies could identify non-histone substrates that may be modified by KDM4B. These types of questions may identify new roles for KDM4 histone demethylases and highlight new mechanisms for controlling chromatin condensation and gene transcription. Few studies have addressed KDM4 activity on non-histone substrates. At this point, KDM4C has been shown to modify Pc2 (Polycomb Repressive Complex 2) (Yang, Lin et al. 2011). KDM4B also has binding affinity for WIZ (Widely Interspaced Zinc Finger Motifs), CDYL1 (Chromodomain Protein Y-Like), CSB (DNA Excision Repair) and G9a (Euchromatic histone-lysine N-methyltransferase 2) (Ponnaluri, Vavilala et al. 2009). Investigating possible connections between KDM4B and these non-histone substrates could identify new enzymatic roles for this protein in transcription and DNA repair, and explain possible cooperation with histone methyltransferases like G9a. G9a expression is induced by hypoxia and is oncogenic in cancer, providing another interesting link to KDM4B (Chen, Yan et al. 2006; Lee, Kim et al. 2009; Chen, Hua et al. 2010). Establishing new connections to non-histone substrates could translate into relevant modes of gene expression regulation in other models.

Another area of KDM4B research with little success is drug targeting and development. At this point, specific inhibitors for this single enzyme are not available and advertised inhibitors should be considered with great scrutiny. Current available therapeutic inhibitors like ML324 and JIB-04, have

been marketed to target a specific class of enzymes but have broader effects (Rai, Kawamura et al. 2010; Chu, Wang et al. 2014). Developing specific inhibitors for individual jumonji proteins is difficult due to similarities between the structures of all members of the jumonji family (Whetstine, Nottke et al. 2006). These proteins contain JmjN and JmjC domains, use common cofactors for activity (Fe^{2+}, α-ketoglutarate, and oxygen), and bind similar histone and non-histone substrates (Whetstine, Nottke et al. 2006). These overlapping factors often prohibit specific inhibition and drives broad targeting of many jumonji family proteins. Investigations to conclusively identify specific diseases that would benefit from KDM4B targeting have also not been completed at this time. Unspecific inhibitors such as JIB-04 have shown an ability to decrease cell proliferation, cell viability *in vitro* and reduce tumor burden in xenograft models, but nothing has translated to usable patient therapies that specifically targets sole KDM4 family proteins (Wang, Chang et al. 2013; Chu, Wang et al. 2014).

Development and analysis of KDM4B knockout mice has been neglected in the KDM4B research field. At this time, there are few characterized transgenic KDM4B mouse models (Fujiwara, Fujita et al. 2016). Homozygous deletion of KDM4C results in embryonic lethality (Dambacher, Hahn et al. 2010; Pedersen and Helin 2010; Wang, Zhang et al. 2010). Incorporating loss of KDM4B models should be considered in other mutagenic mouse models. Even though heterozygous knockout mice lines have been developed and maintained, they have not been characterized. Conditional knockout or knock in mice could also answer tissue-specific questions regarding KDM4B in developmental and cancer promoting processes. Developing Tet-inducible models may also answer specific questions regarding timing of loss or gain of KDM4B expression in various cell processes or diseases.

The development of a tissue-specific KDM4B conditional knockout mouse would help answer relevant biological questions about the *in vivo* role of KDM4B in EOC tumorigenesis or other cancer models. At this time, these types of KDM4B models have not been developed and characterized. The only studied and published conditional KDM4B knockout mouse is a neuron-specific knockout, which may act as an *in vivo* model for neural development disorders (Fujiwara, Fujita et al. 2016). Parallel to KDM4B conditional knockout mice, it would be useful to incorporate the study of this gene into relevant

tumor models. Combining a KDM4B tissue specific knock in or knockout model with a spontaneous tumor-forming model may help answer some deeper questions regarding KDM4B dependent *in vivo* tumorigenesis. An example of a useful cross for EOC studies may be to combine a KDM4B knockin mouse with a spontaneous tumor-forming model like the p53/Rb1 ovarian surface epithelium knockout (Flesken-Nikitin, Choi et al. 2003). This type of transgenic model may give further insight into KDM4B-dependent EOC tumor formation from the ovarian surface epithelium.

Given the current depth of KDM4B research in cancer models, exploring its activity in other systems would be novel. The role of KDM4B in reproductive biology remains largely unstudied. Mining the RNA Sequencing Atlas, KDM4B displayed high expression in the ovary and the testes of normal human tissues (Yang, Imoto et al. 2000; Krupp, Marquardt et al. 2012; Labbe, Holowatyj et al. 2013). Little is known about the role of epigenetic regulators, including histone demethylases in ovarian biology. Another jumonji containing protein, KDM3B has recently been characterized in a knockout mouse model (Liu, Oyola et al. 2015). KDM3B is highly expressed in female reproductive organs including ovary, oviduct and uterus (Liu, Oyola et al. 2015). Knockout of KDM3B correlated with irregular estrous cycles, decreased ovulation capability, and fertilization rate (Liu, Oyola et al. 2015). These findings show the jumonji protein KDM3B plays an essential role in regulating gene expression during developmental processes (Liu, Chen et al. 2015). Considering the high expression of KDM4B in the ovary and testes, this enzyme may also contribute to reproductive processes (Labbe, Holowatyj et al. 2013). Each of these proteins may become induced and regulate different genes at separate times. Exploring the role of KDM4B in reproductive biology would provide answers to the uncharacterized role of epigenetics and histone demethylases in reproductive biology.

Future Directions for KDM4B Studies in Ovarian Cancer

Considering the observations from this project, further studies should start by addressing these main areas in the ovarian cancer model: *hypoxic connection to KDM4B activity, identification of a*

functional target gene, transcriptional mechanisms of KDM4B activity, contribution of specific domains to activity, and connections between KDM4B and EOC tumorigenesis from fallopian fimbrae. While there are other topics to address, these studies would provide the most powerful and applicable knowledge to the KDM4B field in the context of ovarian cancer. These follow-up studies would expand upon what we already know, without spending time revalidating previous research. As useful as it would be to revalidate known ideas, it may not drive novel discoveries.

Establish Function and Connections between Hypoxia and KDM4B in EOC Pathogenesis

KDM4B is a hypoxia-inducible enzyme; however, this project did not characterize the contribution of KDM4B to ovarian cancer progression in a hypoxia-dependent context (Beyer, Kristensen et al. 2008). Ovarian cancer has an established connection to a hypoxic tumor microenvironment and is an important component not to overlook in the study of a hypoxia-inducible enzyme (Osada, Horiuchi et al. 2007). KDM4B dependent target gene expression and *in vitro* assays were investigated using a hypoxic (0.5% O_2 – 2% O_2) and normoxic (21% O_2) treatment (Chapter 2 and 3). The role of hypoxia in driving KDM4B activity was not independently addressed in these experiments. Although loss of KDM4B decreases invasion, migration, proliferation, and spheroid formation *in vitro*, the lack of hypoxia driving these phenotypes in a KDM4B dependent manner was not explored (Chapter 2 and 3). This may be due to a variety of reasons, including enzyme dynamics or other internal cellular control mechanisms regulating KDM4B. It is possible under hypoxia during presumed maximum induction of KDM4B, this protein's binding may saturate its substrate binding sites and plateau. A substrate availability phenomenon could explain why KDM4B does not induce phenotypes further under hypoxia. It is also possible that too much expression of KDM4B is not healthy for the cell, offsetting the interdependent balance of other epigenetic regulators functioning to maintain cell processes. Internal cellular signaling mechanisms may also be controlling the expression and activity levels of KDM4B. KDM4B activity may be limited by necessary and available transcriptional cofactors for enzyme activity, such as c-Myc or Nanog (Yang, Jubb et al. 2010; Das, Shao et al. 2014).

In addition to the lack of exploration of hypoxia-driven, KDM4B-dependent functional assays, the sets of downstream suspected targets mined for expression and downstream target studies should also be reconsidered. KDM4B-dependent normoxic and hypoxic gene expression changes were identified (Chapter 2 and Chapter 3). This project focused on the commonly overlapping changes between the hypoxic and normoxic data sets. Overlapping target genes between oxygen tensions are likely the most robust and replicable targets. However, only considering the commonly regulated targets does not explain the role of hypoxia driven KDM4B activity in ovarian cancer. Additional ChIP and transcriptional analysis would clarify the contribution of hypoxia in this cancer model.

Identification of Functionally Relevant KDM4B Target Gene

Identification of a novel, functionally relevant KDM4B regulated target gene in the ovarian cancer model is another essential question that remains unanswered. In order to increase the power of KDM4B in ovarian cancer progression, it is essential to explain how it genetically regulates ovarian cancer tumorigenesis and demonstrate this *in vitro* and *in vivo*. This is one of the most important lingering questions but may not be the easiest aspect of KDM4B activity to answer. KDM4B research is complicated by the lack of conserved functions between cancer and developmental models. Identifying a functionally relevant downstream target gene may not be a simple question to answer because of the endless possibilities of KDM4B activity and interference from compensating proteins (Chapter 2). At this point, numerous putative target genes have been investigated in this research group's hands in ovarian cancer functional assays. These targets include *LOX*, *LCN2*, and *PDGFB* (Chapter 2 and 3). KDM4B-dependent expression and promoter binding can be shown using qPCR and in some cases ChIP, but the functional importance of the downstream target genes has not been demonstrated. ChIP of these commonly regulated target genes has also been difficult to replicate between ovarian cancer cell lines, only confounding the identification of putative downstream genes.

Investigation of putative target genes that are upregulated with loss of KDM4B expression may also help identify functionally relevant KDM4B target genes. Upregulated genes could be mined from

the microarray and RNA Sequencing analysis completed in this project. At this time, only downregulated genes with the loss of KDM4B expression have been explored. KDM4B could be controlled with indirect regulation of tumorigenic genes. Genes may be repressed upstream by another gene regulated by KDM4B expression and activity. Further *in silico* analysis of completed RNA Sequencing and microarray analysis would help develop the network of regulation regarding KDM4B. Connecting these molecular links will help explain the broad network of targets regulated by KDM4B.

In light of these issues, it seems necessary to rethink the philosophy and approaches used to address this lingering target gene question. Instead of "fishing" for specific target genes, it would be beneficial to start broad or genome wide with next-generation sequencing techniques. ChIP-Sequencing analysis of KDM4B binding and histone methylation profiles of 2-3 ovarian cancer cell models could pinpoint the most relevant and conserved KDM4B demethylase-dependent target genes. KDM4B ChIP-Sequencing has not been published for this cancer model type and would provide a useful resource for the field. Upon identification of the most conserved target genes, appropriate tumorigenic functional assays could be employed. Antibody specificity may also be an issue to consider when performing ChIP. Suspected target genes have not replicated well in ChIP experiments between the SKOV3ip.1 and OVCAR8 cell lines. This may be due to experimental conditions, including antibody specificity. In previous target gene identification attempts, it is also possible genetic manipulations of these genes using shRNA or siRNA were not completed appropriately and dampened experimental results. PDGFB remains one of the most consistent targets between ovarian cancer cell lines expressed in a KDM4B-dependent manner. In other experiments conducted by previous Krieg lab members, it is possible shPDGFB plasmid constructs were not titrated appropriately in preliminary experiments, effecting results in attachment-free growth assays. *LOX*, given its established connection to invasion, was investigated using Boyden Chambers and pooled siRNA. Experimental results were inconclusive and it is possible these were confounded by the use of siRNA instead of shRNA. Considering the rapid development of *in vitro* assays for invasion and migration in cancer research, it is realistic to consider that analysis of

invasion, migration, proliferation, or attachment-free growth may be better quantified using a different experimental technique.

Even though some of the major pathways of tumorigenesis were explored, it is possible that another important aspect regulating ovarian cancer tumorigenesis in a KDM4B-dependent manner was overlooked. Given the genome wide activity of KDM4B, it is likely that KDM4B regulates multiple tumorigenic pathways. The xenograft studies from Chapter 3 are the pinnacle and keystone experiments that demonstrate KDM4B expression is essential for ovarian cancer progression. It is obvious from these studies that KDM4B effects some tumor cell functions encompassed in the regarded "Hallmarks of Cancer" (Hanahan and Weinberg 2011). Invasion, migration, attachment-free growth, and proliferation have all been addressed and demonstrate KDM4B dependent roles in ovarian tumor progression. Resistance to apoptosis and increased angiogenesis should be investigated *in vitro*. Results from the proliferation counting assays showed loss of KDM4B decreased proliferation (Chapter 3). The proliferative defects could be due to a loss of the balance between proliferation and apoptosis, suggesting a role for KDM4B in regulating the activation of these processes (Hanahan and Weinberg 2011). It is possible that proliferation decreases while apoptosis is actually increasing. Breaking down the connection between KDM4B expression and cell cycle regulation could also clarifying the observation of decreased proliferation in the ovarian cancer model.

Clarification of KDM4B-dependent Transcriptional Mechanisms

Identification and clarification of KDM4B-dependent transcriptional mechanisms is the third component to address in future work. Current research shows KDM4B regulates gene expression in a demethylase dependent manner in many models, while working with a variety of transcriptional co-activators, including c-Myc, p300, and β-catenin (Berry and Janknecht 2013; Yang, AlTahan et al. 2015; Lee, Yu et al. 2016). Interaction between KDM4B and the methyltransferase MLL2 has also been established in ER+ breast cancer types (Coffey, Rogerson et al. 2013). The proteins involved with KDM4B in the transcriptional coactivation complex have not been investigated in ovarian cancer models.

Conversely, it is worth investigating if KDM4B activity has connection to transcriptional repressors. Given this topic is a virtual unknown; these questions could be approached with Co-IP and mass spectrometry. Understanding the complex KDM4B would answer questions not only on transcription and demethylase activity, but identify unknown binding partners for this protein. These types of experiments would help explain the behavior of KDM4B in ovarian cancer and possibly play a role in other models.

The transcriptional interplay between HIF-1α and KDM4B should also be explored. Hypoxia is one contributing factor in EOC tumorigenesis, driving invasion and metabolic adaptations (Osada, Horiuchi et al. 2007). HIF-1α nuclear expression has also been shown to promote tumorigenesis and correlates to poor prognosis in EOC (Osada, Horiuchi et al. 2007). HIF-1α also induces KDM4B expression, identifying an epigenetic link between tumor progression and a hypoxic tumor microenvironment (Beyer, Kristensen et al. 2008; Pollard, Loenarz et al. 2008; Yang, Jubb et al. 2010). This project demonstrates that KDM4B expression influences EOC progression. However, putative target genes regulated by KDM4B, including *PDGFB* and *MUC1*, are also induced by HIF-1α. This suggests a connection between KDM4B and HIF-1α targets. KDM4B could act as a recruitment signal for HIF-1α to a particular HRE. This recruitment hypothesis has been demonstrated in another jumonji protein, KDM3A (Pollard, Loenarz et al. 2008). Determining if KDM4B regulates gene expression in this model in a demethylase-dependent or independent manner becomes a fundamental question to answer. Genome-wide dissection of the connection between HIF-1α, KDM4B activity, and tumorigenic gene expression would further explain the connection between KDM4B and HIF-1α driven EOC progression.

Establishing the Contributions of KDM4B Domains to Enzymatic Targeting and Activity

Further investigation exploring the contribution of specific KDM4B domains to demethylase activity should be completed. At this time, this project does not adequately demonstrate if there are key roles of H3K9 demethylase activity through jmjC domains or histone binding activities through Tudor/PHD domain of KDM4B in the pathogenesis of epithelial ovarian cancer. H3K9me3 demethylation by KDM4B is dependent upon the jmjC domain in other models (Fodor, Kubicek et al.

2006). However, the role of the targeting Tudor/PHD domains has not been demonstrated well between many models (Coffey, Rogerson et al. 2013). Further studies on domain contribution would help understand how KDM4B binds and functions at certain genomic sites. Understanding the activity of the domains could provide useful knowledge for developing targeting therapies in ovarian cancer models.

Investigating the Connection between KDM4B and Fallopian EOC Tumorigenesis

In addition to further dissection of transcriptional and hypoxic mechanisms, KDM4B expression should be investigated in the fallopian tube fimbriae. The debate in the ovarian cancer field regarding the precursor tissue for ovarian cancer tumorigenesis is important and would be useful to explore (Auersperg 2013). Currently, this has not been addressed. KDM4B will likely be expressed in the fallopian tube, given its ubiquitous presence and activity in many normal tissues (Labbe, Holowatyj et al. 2013). If KDM4B were expressed in the fallopian fimbriae, this would not necessarily indicate that tumor progression always begins at this site. Increased KDM4B expression in the fimbrae would suggest that it might begin at this site. In the context of ovarian surface epithelium as site of origin, lack of KDM4B expression in normal ovarian surface epithelium suggests a transformative event may possibly induce this gene during cancer progression (Chapter 2) (Auersperg 2013). Further studies answering this question would help piece together different aspects influencing the "site of origin" debate.

Significance

This project is one of the first to demonstrate the relevant role of KDM4B in epithelial ovarian cancer progression. Demonstrating any connection between KDM4B and EOC progression is pioneering for the KDM4 and ovarian cancer fields. This project has provided clarity on many key aspects of KDM4B enzymatic activity and function in ovarian cancer tumorigenesis. In addition to showing that KDM4B expression is increased in primary and metastatic high-grade EOC patient tumors, this project has also completed novel dissection of the functional contribution and genetic activities dependent on KDM4B in ovarian cancer (Chapter 2 and 3). The manuscript in chapter 2 provides the first

demonstration of KDM4B's importance in facilitating invasion, migration, spheroid formation, and peritoneal dissemination *in vitro* and *in vivo* in EOC and shown these roles are conserved between two relevant EOC models. This work has established the first connections between KDM4B and any known genes contributing to ovarian cancer progression, including *PDGFB* and *LOX*. This project has also shown that KDM4B regulates these genes in a promoter specific, demethylase-dependent manner. These findings delineate clear and biologically relevant genetic and functional roles for KDM4B in EOC. Not only does this project fill a knowledge-gap on the functional contributions of jumonji domain-containing proteins in EOC progression, it also adds to the breadth of KDM4B mechanisms previously published in other cancer types.

Overall Conclusion

These novel investigations established the first mechanisms regarding KDM4B activity in epithelial ovarian cancer models. Most importantly, this project helped establish new links between the hypoxic tumor microenvironment and molecular changes in EOC tumorigenesis. The relevance of pursuing KDM4B was solidified by this work's analyzed patient tumor microarray study and observation of KDM4B expression in patient ascites lysates (Chapter 2 and 3). Staining analysis showed increased protein expression in primary, metastatic, and recurrent EOC patient tumors (Chapter 2). KDM4B expression corresponded to increased invasion, migration, and attachment-free growth *in vitro* (Chapter 2 and 3). KDM4B was shown to regulate tumorigenic gene expression in a promoter-specific, demethylase-dependent manner. These efforts help improve the understanding of KDM4B activity and establish portions of its mechanistic role in regulating EOC progression. Considering KDM4B is likely regulating expression genome-wide, future investigations will continue to characterize additional faucets of KDM4B activity and build upon these observations. Future studies will continue to unravel and establish the biological importance of this histone demethylase in driving EOC tumorigenesis and other cancer types.

References

Abarrategi, A., J. Tornin, L. Martinez-Cruzado, A. Hamilton, E. Martinez-Campos, J. P. Rodrigo, M. V. Gonzalez, N. Baldini, J. Garcia-Castro and R. Rodriguez (2016). "Osteosarcoma: Cells-of-Origin, Cancer Stem Cells, and Targeted Therapies." Stem Cells Int **2016**: 3631764.

Agarwal, R. and S. B. Kaye (2003). "Ovarian cancer: strategies for overcoming resistance to chemotherapy." Nat Rev Cancer **3**(7): 502-516.

Agger, K., S. Miyagi, M. T. Pedersen, S. M. Kooistra, J. V. Johansen and K. Helin (2016). "Jmjd2/Kdm4 demethylases are required for expression of Il3ra and survival of acute myeloid leukemia cells." Genes Dev **30**(11): 1278-1288.

Ai, Z., Y. Lu, S. Qiu and Z. Fan (2016). "Overcoming cisplatin resistance of ovarian cancer cells by targeting HIF-1-regulated cancer metabolism." Cancer Lett **373**(1): 36-44.

AlHilli, M. M., M. A. Becker, S. J. Weroha, K. S. Flatten, R. M. Hurley, M. I. Harrell, A. L. Oberg, M. J. Maurer, K. M. Hawthorne, X. Hou, S. C. Harrington, S. McKinstry, X. W. Meng, K. M. Wilcoxen, K. R. Kalli, E. M. Swisher, S. H. Kaufmann and P. Haluska (2016). "In vivo anti-tumor activity of the PARP inhibitor niraparib in homologous recombination deficient and proficient ovarian carcinoma." Gynecol Oncol.

Antony, J., F. Oback, L. W. Chamley, B. Oback and G. Laible (2013). "Transient JMJD2B-mediated reduction of H3K9me3 levels improves reprogramming of embryonic stem cells into cloned embryos." Mol Cell Biol **33**(5): 974-983.

Aoki, M., K. Nabeshima, K. Koga, M. Hamasaki, J. Suzumiya, K. Tamura and H. Iwasaki (2007). "Imatinib mesylate inhibits cell invasion of malignant peripheral nerve sheath tumor induced by platelet-derived growth factor-BB." Lab Invest **87**(8): 767-779.

Apte, S. M., C. D. Bucana, J. J. Killion, D. M. Gershenson and I. J. Fidler (2004). "Expression of platelet-derived growth factor and activated receptor in clinical specimens of epithelial ovarian cancer and ovarian carcinoma cell lines." Gynecol Oncol **93**(1): 78-86.

Armstrong, D. K. (2002). "Relapsed ovarian cancer: challenges and management strategies for a chronic disease." Oncologist **7 Suppl 5**: 20-28.

Auersperg, N. (2013). "The origin of ovarian cancers--hypotheses and controversies." Front Biosci (Schol Ed) **5**: 709-719.

Baba, A., F. Ohtake, Y. Okuno, K. Yokota, M. Okada, Y. Imai, M. Ni, C. A. Meyer, K. Igarashi, J. Kanno, M. Brown and S. Kato (2011). "PKA-dependent regulation of the histone lysine demethylase complex PHF2-ARID5B." Nat Cell Biol **13**(6): 668-675.

Balch, C., F. Fang, D. E. Matei, T. H. Huang and K. P. Nephew (2009). "Minireview: epigenetic changes in ovarian cancer." Endocrinology **150**(9): 4003-4011.

Barker, H. E., J. Chang, T. R. Cox, G. Lang, D. Bird, M. Nicolau, H. R. Evans, A. Gartland and J. T. Erler (2011). "LOXL2-mediated matrix remodeling in metastasis and mammary gland involution." Cancer Res **71**(5): 1561-1572.

Barker, H. E. and J. T. Erler (2011). "The potential for LOXL2 as a target for future cancer treatment." Future Oncol **7**(6): 707-710.

Bast, R. C., Jr. (2011). "Molecular approaches to personalizing management of ovarian cancer." Ann Oncol **22 Suppl 8**: viii5-viii15.

Bast, R. C., Jr., B. Hennessy and G. B. Mills (2009). "The biology of ovarian cancer: new opportunities for translation." Nat Rev Cancer **9**(6): 415-428.

Baxter, R. C. (2014). "IGF binding proteins in cancer: mechanistic and clinical insights." Nat Rev Cancer **14**(5): 329-341.

Berek, J. S., E. Chalas, M. Edelson, D. H. Moore, W. M. Burke, W. A. Cliby, A. Berchuck and C. Society of Gynecologic Oncologists Clinical Practice (2010). "Prophylactic and risk-reducing bilateral salpingo-oophorectomy: recommendations based on risk of ovarian cancer." Obstet Gynecol **116**(3): 733-743.

Berry, W. L. and R. Janknecht (2013). "KDM4/JMJD2 histone demethylases: epigenetic regulators in cancer cells." Cancer Res **73**(10): 2936-2942.

Berry, W. L., T. D. Kim and R. Janknecht (2014). "Stimulation of beta-catenin and colon cancer cell growth by the KDM4B histone demethylase." Int J Oncol **44**(4): 1341-1348.

Betsholtz, C., L. Karlsson and P. Lindahl (2001). "Developmental roles of platelet-derived growth factors." Bioessays **23**(6): 494-507.

Beyer, S., M. M. Kristensen, K. S. Jensen, J. V. Johansen and P. Staller (2008). "The histone demethylases JMJD1A and JMJD2B are transcriptional targets of hypoxia-inducible factor HIF." J Biol Chem **283**(52): 36542-36552.

Birner, P., M. Schindl, A. Obermair, G. Breitenecker and G. Oberhuber (2001). "Expression of hypoxia-inducible factor 1alpha in epithelial ovarian tumors: its impact on prognosis and on response to chemotherapy." Clin Cancer Res **7**(6): 1661-1668.

Black, J. C., E. Atabakhsh, J. Kim, K. M. Biette, C. Van Rechem, B. Ladd, P. D. Burrowes, C. Donado, H. Mattoo, B. P. Kleinstiver, B. Song, G. Andriani, J. K. Joung, O. Iliopoulos, C. Montagna, S. Pillai, G. Getz and J. R. Whetstine (2015). "Hypoxia drives transient site-specific copy gain and drug-resistant gene expression." Genes Dev **29**(10): 1018-1031.

Black, J. C., A. L. Manning, C. Van Rechem, J. Kim, B. Ladd, J. Cho, C. M. Pineda, N. Murphy, D. L. Daniels, C. Montagna, P. W. Lewis, K. Glass, C. D. Allis, N. J. Dyson, G. Getz and J. R. Whetstine (2013). "KDM4A Lysine Demethylase Induces Site-Specific Copy Gain and Rereplication of Regions Amplified in Tumors." Cell **154**(3): 541-555.

Black, J. C., C. Van Rechem and J. R. Whetstine (2012). "Histone lysine methylation dynamics: establishment, regulation, and biological impact." Mol Cell **48**(4): 491-507.

Bowtell, D. D. (2010). "The genesis and evolution of high-grade serous ovarian cancer." Nat Rev Cancer **10**(11): 803-808.

Budiu, R. A., E. Elishaev, J. Brozick, M. Lee, R. P. Edwards, P. Kalinski and A. M. Vlad (2013). "Immunobiology of human mucin 1 in a preclinical ovarian tumor model." Oncogene **32**(32): 3664-3675.

Burkman, R., J. J. Schlesselman and M. Zieman (2004). "Safety concerns and health benefits associated with oral contraception." Am J Obstet Gynecol **190**(4 Suppl): S5-22.

Burton, A., C. Azevedo, C. Andreassi, A. Riccio and A. Saiardi (2013). "Inositol pyrophosphates regulate JMJD2C-dependent histone demethylation." Proc Natl Acad Sci U S A **110**(47): 18970-18975.

Campeau, E., V. E. Ruhl, F. Rodier, C. L. Smith, B. L. Rahmberg, J. O. Fuss, J. Campisi, P. Yaswen, P. K. Cooper and P. D. Kaufman (2009). "A versatile viral system for expression and depletion of proteins in mammalian cells." PLoS One **4**(8): e6529.

Cancer Genome Atlas Research, N. (2011). "Integrated genomic analyses of ovarian carcinoma." Nature **474**(7353): 609-615.

Cancer Genome Atlas Research, N., C. Kandoth, N. Schultz, A. D. Cherniack, R. Akbani, Y. Liu, H. Shen, A. G. Robertson, I. Pashtan, R. Shen, C. C. Benz, C. Yau, P. W. Laird, L. Ding, W. Zhang, G. B. Mills, R. Kucherlapati, E. R. Mardis and D. A. Levine (2013). "Integrated genomic characterization of endometrial carcinoma." Nature **497**(7447): 67-73.

Cantuaria, G., A. Fagotti, G. Ferrandina, A. Magalhaes, M. Nadji, R. Angioli, M. Penalver, S. Mancuso and G. Scambia (2001). "GLUT-1 expression in ovarian carcinoma: association with survival and response to chemotherapy." Cancer **92**(5): 1144-1150.

Cerami, E., J. Gao, U. Dogrusoz, B. E. Gross, S. O. Sumer, B. A. Aksoy, A. Jacobsen, C. J. Byrne, M. L. Heuer, E. Larsson, Y. Antipin, B. Reva, A. P. Goldberg, C. Sander and N. Schultz (2012). "The cBio cancer genomics portal: an open platform for exploring multidimensional cancer genomics data." Cancer Discov **2**(5): 401-404.

Chan, K. K., N. Wei, S. S. Liu, L. Xiao-Yun, A. N. Cheung and H. Y. Ngan (2008). "Estrogen receptor subtypes in ovarian cancer: a clinical correlation." Obstet Gynecol **111**(1): 144-151.

Chauhan, S. C., K. Vannatta, M. C. Ebeling, N. Vinayek, A. Watanabe, K. K. Pandey, M. C. Bell, M. D. Koch, H. Aburatani, Y. Lio and M. Jaggi (2009). "Expression and functions of transmembrane mucin MUC13 in ovarian cancer." Cancer Res **69**(3): 765-774.

Chen, C., J. Ge, Q. Lu, G. Ping, C. Yang and X. Fang (2015). "Expression of Lysine-specific demethylase 1 in human epithelial ovarian cancer." J Ovarian Res **8**: 28.

Chen, H., Y. Yan, T. L. Davidson, Y. Shinkai and M. Costa (2006). "Hypoxic stress induces dimethylated histone H3 lysine 9 through histone methyltransferase G9a in mammalian cells." Cancer Res **66**(18): 9009-9016.

Chen, M. W., K. T. Hua, H. J. Kao, C. C. Chi, L. H. Wei, G. Johansson, S. G. Shiah, P. S. Chen, Y. M. Jeng, T. Y. Cheng, T. C. Lai, J. S. Chang, Y. H. Jan, M. H. Chien, C. J. Yang, M. S. Huang, M. Hsiao and M. L. Kuo (2010). "H3K9 histone methyltransferase G9a promotes lung cancer invasion and metastasis by silencing the cell adhesion molecule Ep-CAM." Cancer Res **70**(20): 7830-7840.

Cheng, J. C., C. Klausen and P. C. Leung (2013). "Hypoxia-inducible factor 1 alpha mediates epidermal growth factor-induced down-regulation of E-cadherin expression and cell invasion in human ovarian cancer cells." Cancer Lett **329**(2): 197-206.

Chi, J. T., Z. Wang, D. S. Nuyten, E. H. Rodriguez, M. E. Schaner, A. Salim, Y. Wang, G. B. Kristensen, A. Helland, A. L. Borresen-Dale, A. Giaccia, M. T. Longaker, T. Hastie, G. P. Yang, M. J. van de Vijver and P. O. Brown (2006). "Gene expression programs in response to hypoxia: cell type specificity and prognostic significance in human cancers." PLoS Med **3**(3): e47.

Chizuka, A., M. Suda, T. Shibata, E. Kusumi, A. Hori, T. Hamaki, Y. Kodama, K. Horigome, Y. Kishi, K. Kobayashi, T. Matsumura, K. Yuji, Y. Tanaka and M. Kami (2006). "Difference between hematological malignancy and solid tumor research articles published in four major medical journals." Leukemia **20**(10): 1655-1657.

Cho, H. and J. H. Kim (2009). "Lipocalin2 expressions correlate significantly with tumor differentiation in epithelial ovarian cancer." J Histochem Cytochem **57**(5): 513-521.

Cho, K. R. and M. Shih Ie (2009). "Ovarian cancer." Annu Rev Pathol **4**: 287-313.

Choi, J. H., Y. J. Song and H. Lee (2015). "The histone demethylase KDM4B interacts with MyoD to regulate myogenic differentiation in C2C12 myoblast cells." Biochem Biophys Res Commun **456**(4): 872-878.

Chu, C. H., L. Y. Wang, K. C. Hsu, C. C. Chen, H. H. Cheng, S. M. Wang, C. M. Wu, T. J. Chen, L. T. Li, R. Liu, C. L. Hung, J. M. Yang, H. J. Kung and W. C. Wang (2014). "KDM4B as a target for prostate cancer: structural analysis and selective inhibition by a novel inhibitor." J Med Chem **57**(14): 5975-5985.

Coffey, K., L. Rogerson, C. Ryan-Munden, D. Alkharaif, J. Stockley, R. Heer, K. Sahadevan, D. O'Neill, D. Jones, S. Darby, P. Staller, A. Mantilla, L. Gaughan and C. N. Robson (2013). "The lysine demethylase, KDM4B, is a key molecule in androgen receptor signalling and turnover." Nucleic Acids Res **41**(8): 4433-4446.

Cole, A. J., T. Dwight, A. J. Gill, K. A. Dickson, Y. Zhu, A. Clarkson, G. B. Gard, J. Maidens, S. Valmadre, R. Clifton-Bligh and D. J. Marsh (2016). "Assessing mutant p53 in primary high-grade serous ovarian cancer using immunohistochemistry and massively parallel sequencing." Sci Rep **6**: 26191.

Conley, S. J. and M. S. Wicha (2012). "Antiangiogenic agents: Fueling cancer's hypoxic roots." Cell Cycle **11**(7).

Crum, C. P., M. Herfs, G. Ning, J. G. Bijron, B. E. Howitt, C. A. Jimenez, S. Hanamornroongruang, F. D. McKeon and W. Xian (2013). "Through the glass darkly: intraepithelial neoplasia, top-down differentiation, and the road to ovarian cancer." J Pathol **231**(4): 402-412.

Cunat, S., P. Hoffmann and P. Pujol (2004). "Estrogens and epithelial ovarian cancer." Gynecol Oncol **94**(1): 25-32.

Dal Maso, L., L. S. Augustin, S. Franceschi, R. Talamini, J. Polesel, C. W. Kendall, D. J. Jenkins, E. Vidgen and C. La Vecchia (2004). "Association between components of the insulin-like growth factor system and epithelial ovarian cancer risk." Oncology **67**(3-4): 225-230.

Dambacher, S., M. Hahn and G. Schotta (2010). "Epigenetic regulation of development by histone lysine methylation." Heredity (Edinb) **105**(1): 24-37.

Dang, C. V. and G. L. Semenza (1999). "Oncogenic alterations of metabolism." Trends Biochem Sci **24**(2): 68-72.

Das, P. P., Z. Shao, S. Beyaz, E. Apostolou, L. Pinello, A. De Los Angeles, K. O'Brien, J. M. Atsma, Y. Fujiwara, M. Nguyen, D. Ljuboja, G. Guo, A. Woo, G. C. Yuan, T. Onder, G. Daley, K. Hochedlinger, J. Kim and S. H. Orkin (2014). "Distinct and combinatorial functions of Jmjd2b/Kdm4b and Jmjd2c/Kdm4c in mouse embryonic stem cell identity." Mol Cell **53**(1): 32-48.

Davidowitz, R. A., L. M. Selfors, M. P. Iwanicki, K. M. Elias, A. Karst, H. Piao, T. A. Ince, M. G. Drage, J. Dering, G. E. Konecny, U. Matulonis, G. B. Mills, D. J. Slamon, R. Drapkin and J. S. Brugge (2014). "Mesenchymal gene program-expressing ovarian cancer spheroids exhibit enhanced mesothelial clearance." J Clin Invest **124**(6): 2611-2625.

Della Pepa, C. and S. Banerjee (2014). "Bevacizumab in combination with chemotherapy in platinum-sensitive ovarian cancer." Onco Targets Ther **7**: 1025-1032.

Deng, J., L. Wang, H. Chen, J. Hao, J. Ni, L. Chang, W. Duan, P. Graham and Y. Li (2016). "Targeting epithelial-mesenchymal transition and cancer stem cells for chemoresistant ovarian cancer." Oncotarget.

Di Lorenzo, A. and M. T. Bedford (2011). "Histone arginine methylation." FEBS Lett **585**(13): 2024-2031.

Dong, J., J. Grunstein, M. Tejada, F. Peale, G. Frantz, W. C. Liang, W. Bai, L. Yu, J. Kowalski, X. Liang, G. Fuh, H. P. Gerber and N. Ferrara (2004). "VEGF-null cells require PDGFR alpha signaling-mediated stromal fibroblast recruitment for tumorigenesis." EMBO J **23**(14): 2800-2810.

Dong, Y., M. D. Walsh, M. C. Cummings, R. G. Wright, S. K. Khoo, P. G. Parsons and M. A. McGuckin (1997). "Expression of MUC1 and MUC2 mucins in epithelial ovarian tumours." J Pathol **183**(3): 311-317.

Du, B. and J. S. Shim (2016). "Targeting Epithelial-Mesenchymal Transition (EMT) to Overcome Drug Resistance in Cancer." Molecules **21**(7).

Dzal, Y. A., S. E. Jenkin, S. L. Lague, M. N. Reichert, J. M. York and M. E. Pamenter (2015). "Oxygen in demand: How oxygen has shaped vertebrate physiology." Comp Biochem Physiol A Mol Integr Physiol **186**: 4-26.

Edgar, R., M. Domrachev and A. E. Lash (2002). "Gene Expression Omnibus: NCBI gene expression and hybridization array data repository." Nucleic Acids Res **30**(1): 207-210.

Emerenciano, M., T. C. Barbosa, B. A. Lopes, C. B. Blunck, A. Faro, C. Andrade, C. Meyer, R. Marschalek, M. S. Pombo-de-Oliveira and L. Brazilian Collaborative Study Group of Infant Acute (2014). "ARID5B polymorphism confers an increased risk to acquire specific MLL rearrangements in early childhood leukemia." BMC Cancer **14**: 127.

Engelstaedter, V., S. Heublein, A. L. Schumacher, M. Lenhard, H. Engelstaedter, U. Andergassen, M. Guenthner-Biller, C. Kuhn, B. Rack, M. Kupka, D. Mayr and U. Jeschke (2012). "Mucin-1 and its relation to grade, stage and survival in ovarian carcinoma patients." BMC Cancer **12**: 600.

Erler, J. T., K. L. Bennewith, M. Nicolau, N. Dornhofer, C. Kong, Q. T. Le, J. T. Chi, S. S. Jeffrey and A. J. Giaccia (2006). "Lysyl oxidase is essential for hypoxia-induced metastasis." Nature **440**(7088): 1222-1226.

Fisher, S. A. and W. W. Burggren (2007). "Role of hypoxia in the evolution and development of the cardiovascular system." Antioxid Redox Signal **9**(9): 1339-1352.

Flesken-Nikitin, A., K. C. Choi, J. P. Eng, E. N. Shmidt and A. Y. Nikitin (2003). "Induction of carcinogenesis by concurrent inactivation of p53 and Rb1 in the mouse ovarian surface epithelium." Cancer Res **63**(13): 3459-3463.

Fodor, B. D., S. Kubicek, M. Yonezawa, R. J. O'Sullivan, R. Sengupta, L. Perez-Burgos, S. Opravil, K. Mechtler, G. Schotta and T. Jenuwein (2006). "Jmjd2b antagonizes H3K9 trimethylation at pericentric heterochromatin in mammalian cells." Genes Dev **20**(12): 1557-1562.

Fritsch, L., P. Robin, J. R. Mathieu, M. Souidi, H. Hinaux, C. Rougeulle, A. Harel-Bellan, M. Ameyar-Zazoua and S. Ait-Si-Ali (2010). "A subset of the histone H3 lysine 9 methyltransferases Suv39h1, G9a, GLP, and SETDB1 participate in a multimeric complex." Mol Cell **37**(1): 46-56.

Fujiwara, K., Y. Fujita, A. Kasai, Y. Onaka, H. Hashimoto, H. Okada and T. Yamashita (2016). "Deletion of JMJD2B in neurons leads to defective spine maturation, hyperactive behavior and memory deficits in mouse." Transl Psychiatry **6**: e766.

Gao, J., B. A. Aksoy, U. Dogrusoz, G. Dresdner, B. Gross, S. O. Sumer, Y. Sun, A. Jacobsen, R. Sinha, E. Larsson, E. Cerami, C. Sander and N. Schultz (2013). "Integrative analysis of complex cancer genomics and clinical profiles using the cBioPortal." Sci Signal **6**(269): pl1.

Giornelli, G. H. (2016). "Management of relapsed ovarian cancer: a review." Springerplus **5**(1): 1197.

Giri, N. C., L. Passantino, H. Sun, M. A. Zoroddu, M. Costa and M. J. Maroney (2013). "Structural investigations of the nickel-induced inhibition of truncated constructs of the JMJD2 family of histone demethylases using X-ray absorption spectroscopy." Biochemistry **52**(24): 4168-4183.

Gloss, B. S. and G. Samimi (2014). "Epigenetic biomarkers in epithelial ovarian cancer." Cancer Lett **342**(2): 257-263.

Goode, E. L., G. Chenevix-Trench, L. C. Hartmann, B. L. Fridley, K. R. Kalli, R. A. Vierkant, M. C. Larson, K. L. White, G. L. Keeney, T. N. Oberg, J. M. Cunningham, J. Beesley, S. E. Johnatty, X. Chen, K. E. Goodman, S. M. Armasu, D. N. Rider, H. Sicotte, M. M. Schmidt, E. A. Elliott, E. Hogdall, S. K. Kjaer, P. A. Fasching, A. B. Ekici, D. Lambrechts, E. Despierre, C. Hogdall, L. Lundvall, B. Y. Karlan, J. Gross, R. Brown, J. Chien, D. J. Duggan, Y. Y. Tsai, C. M. Phelan, L. E. Kelemen, P. P. Peethambaram, J. M. Schildkraut, V. Shridhar, R. Sutphen, F. J. Couch, T. A. Sellers and C. Ovarian Cancer Association (2011). "Assessment of hepatocyte growth factor in ovarian cancer mortality." Cancer Epidemiol Biomarkers Prev **20**(8): 1638-1648.

Gray, S. G., A. H. Iglesias, F. Lizcano, R. Villanueva, S. Camelo, H. Jingu, B. T. Teh, N. Koibuchi, W. W. Chin, E. Kokkotou and F. Dangond (2005). "Functional characterization of JMJD2A, a histone deacetylase- and retinoblastoma-binding protein." J Biol Chem **280**(31): 28507-28518.

Guo, L., X. Li, J. X. Huang, H. Y. Huang, Y. Y. Zhang, S. W. Qian, H. Zhu, Y. D. Zhang, Y. Liu, Y. Liu, K. K. Wang and Q. Q. Tang (2012). "Histone demethylase Kdm4b functions as a co-factor of C/EBPbeta to promote mitotic clonal expansion during differentiation of 3T3-L1 preadipocytes." Cell Death Differ **19**(12): 1917-1927.

Guo, P., J. Yang, D. Jia, M. A. Moses and D. T. Auguste (2016). "ICAM-1-Targeted, Lcn2 siRNA-Encapsulating Liposomes are Potent Anti-angiogenic Agents for Triple Negative Breast Cancer." Theranostics **6**(1): 1-13.

Gyorffy, B., A. Lanczky and Z. Szallasi (2012). "Implementing an online tool for genome-wide validation of survival-associated biomarkers in ovarian-cancer using microarray data from 1287 patients." Endocr Relat Cancer **19**(2): 197-208.

Han, F., J. Ren, J. Zhang, Y. Sun, F. Ma, Z. Liu, H. Yu, J. Jia and W. Li (2016). "JMJD2B is required for Helicobacter pylori-induced gastric carcinogenesis via regulating COX-2 expression." Oncotarget.

Hanahan, D. and R. A. Weinberg (2011). "Hallmarks of cancer: the next generation." Cell **144**(5): 646-674.

Hancock, R. L., K. Dunne, L. J. Walport, E. Flashman and A. Kawamura (2015). "Epigenetic regulation by histone demethylases in hypoxia." Epigenomics **7**(5): 791-811.

Harris, A. L. (2002). "Hypoxia--a key regulatory factor in tumour growth." Nat Rev Cancer **2**(1): 38-47.

Hart, W. R. (2005). "Mucinous tumors of the ovary: a review." Int J Gynecol Pathol **24**(1): 4-25.

Hata, K., R. Takashima, K. Amano, K. Ono, M. Nakanishi, M. Yoshida, M. Wakabayashi, A. Matsuda, Y. Maeda, Y. Suzuki, S. Sugano, R. H. Whitson, R. Nishimura and T. Yoneda (2013). "Arid5b facilitates chondrogenesis by recruiting the histone demethylase Phf2 to Sox9-regulated genes." Nat Commun **4**: 2850.

Heckmann, B. L., X. Zhang, X. Xie and J. Liu (2013). "The G0/G1 switch gene 2 (G0S2): regulating metabolism and beyond." Biochim Biophys Acta **1831**(2): 276-281.

Heinlein, C. A. and C. Chang (2004). "Androgen receptor in prostate cancer." Endocr Rev **25**(2): 276-308.

Helmlinger, G., F. Yuan, M. Dellian and R. K. Jain (1997). "Interstitial pH and pO2 gradients in solid tumors in vivo: high-resolution measurements reveal a lack of correlation." Nat Med **3**(2): 177-182.

Herlihy, N., M. Dogrusoz, T. H. van Essen, J. W. Harbour, P. A. van der Velden, M. C. van Eggermond, G. W. Haasnoot, P. J. van den Elsen and M. J. Jager (2015). "Skewed expression of the genes encoding epigenetic modifiers in high-risk uveal melanoma." Invest Ophthalmol Vis Sci **56**(3): 1447-1458.

Hielscher, A. and S. Gerecht (2015). "Hypoxia and free radicals: role in tumor progression and the use of engineering-based platforms to address these relationships." Free Radic Biol Med **79**: 281-291.

Hillringhaus, L., W. W. Yue, N. R. Rose, S. S. Ng, C. Gileadi, C. Loenarz, S. H. Bello, J. E. Bray, C. J. Schofield and U. Oppermann (2011). "Structural and evolutionary basis for the dual substrate selectivity of human KDM4 histone demethylase family." J Biol Chem **286**(48): 41616-41625.

Hoffmann, I., M. Roatsch, M. L. Schmitt, L. Carlino, M. Pippel, W. Sippl and M. Jung (2012). "The role of histone demethylases in cancer therapy." Mol Oncol **6**(6): 683-703.

Hojfeldt, J. W., K. Agger and K. Helin (2013). "Histone lysine demethylases as targets for anticancer therapy." Nat Rev Drug Discov **12**(12): 917-930.

Horiuchi, A., T. Imai, M. Shimizu, K. Oka, C. Wang, T. Nikaido and I. Konishi (2002). "Hypoxia-induced changes in the expression of VEGF, HIF-1 alpha and cell cycle-related molecules in ovarian cancer cells." Anticancer Res **22**(5): 2697-2702.

Horm, T. M. and J. A. Schroeder (2013). "MUC1 and metastatic cancer: expression, function and therapeutic targeting." Cell Adh Migr **7**(2): 187-198.

Horn, G., A. Gaziel, D. H. Wreschner, N. I. Smorodinsky and M. Ehrlich (2009). "ERK and PI3K regulate different aspects of the epithelial to mesenchymal transition of mammary tumor cells induced by truncated MUC1." Exp Cell Res **315**(8): 1490-1504.

Hui, Z., C. Yiling, Y. Wenting, H. XuQun, Z. ChuanYi and L. Hui (2015). "miR-491-5p functions as a tumor suppressor by targeting JMJD2B in ERalpha-positive breast cancer." FEBS Lett **589**(7): 812-821.

Hwang, S. Y., K. Heo, J. S. Kim, J. W. Im, S. M. Lee, M. Cho, D. H. Kang, J. Heo, J. W. Lee, C. W. Choi and K. Yang (2015). "Emodin attenuates radioresistance induced by hypoxia in HepG2 cells via the enhancement of PARP1 cleavage and inhibition of JMJD2B." Oncol Rep **33**(4): 1691-1698.

Ipenberg, I., N. Guttmann-Raviv, H. P. Khoury, I. Kupershmit and N. Ayoub (2013). "Heat shock protein 90 (Hsp90) selectively regulates the stability of KDM4B/JMJD2B histone demethylase." J Biol Chem **288**(21): 14681-14687.

Irizarry, R. A., B. Hobbs, F. Collin, Y. D. Beazer-Barclay, K. J. Antonellis, U. Scherf and T. P. Speed (2003). "Exploration, normalization, and summaries of high density oligonucleotide array probe level data." Biostatistics **4**(2): 249-264.

Iwamori, N., M. Zhao, M. L. Meistrich and M. M. Matzuk (2011). "The testis-enriched histone demethylase, KDM4D, regulates methylation of histone H3 lysine 9 during spermatogenesis in the mouse but is dispensable for fertility." Biol Reprod **84**(6): 1225-1234.

Jacobs, I. and R. C. Bast, Jr. (1989). "The CA 125 tumour-associated antigen: a review of the literature." Hum Reprod **4**(1): 1-12.

Jacobs, I. J. and U. Menon (2004). "Progress and challenges in screening for early detection of ovarian cancer." Mol Cell Proteomics **3**(4): 355-366.

Jha, D. K. and B. D. Strahl (2014). "An RNA polymerase II-coupled function for histone H3K36 methylation in checkpoint activation and DSB repair." Nat Commun **5**: 3965.

Ji, F., Y. Wang, L. Qiu, S. Li, J. Zhu, Z. Liang, Y. Wan and W. Di (2013). "Hypoxia inducible factor 1alpha-mediated LOX expression correlates with migration and invasion in epithelial ovarian cancer." Int J Oncol **42**(5): 1578-1588.

Joberty, G., M. Boesche, J. A. Brown, D. Eberhard, N. S. Garton, P. G. Humphreys, T. Mathieson, M. Muelbaier, N. G. Ramsden, V. Reader, A. Rueger, R. J. Sheppard, S. M. Westaway, M. Bantscheff, K. Lee, D. M. Wilson, R. K. Prinjha and G. Drewes (2016). "Interrogating the Druggability of the 2-Oxoglutarate-Dependent Dioxygenase Target Class by Chemical Proteomics." ACS Chem Biol.

Johmura, Y., J. Sun, K. Kitagawa, K. Nakanishi, T. Kuno, A. Naiki-Ito, Y. Sawada, T. Miyamoto, A. Okabe, H. Aburatani, S. Li, I. Miyoshi, S. Takahashi, M. Kitagawa and M. Nakanishi (2016).

"SCF(Fbxo22)-KDM4A targets methylated p53 for degradation and regulates senescence." Nat Commun **7**: 10574.

Katoh, M. and M. Katoh (2004). "Identification and characterization of JMJD2 family genes in silico." Int J Oncol **24**(6): 1623-1628.

Katoh, Y. and M. Katoh (2007). "Comparative integromics on JMJD2A, JMJD2B and JMJD2C: preferential expression of JMJD2C in undifferentiated ES cells." Int J Mol Med **20**(2): 269-273.

Kawazu, M., K. Saso, K. I. Tong, T. McQuire, K. Goto, D. O. Son, A. Wakeham, M. Miyagishi, T. W. Mak and H. Okada (2011). "Histone demethylase JMJD2B functions as a co-factor of estrogen receptor in breast cancer proliferation and mammary gland development." PLoS One **6**(3): e17830.

Keith, B., R. S. Johnson and M. C. Simon (2012). "HIF1alpha and HIF2alpha: sibling rivalry in hypoxic tumour growth and progression." Nat Rev Cancer **12**(1): 9-22.

Kelly, J. D., B. A. Haldeman, F. J. Grant, M. J. Murray, R. A. Seifert, D. F. Bowen-Pope, J. A. Cooper and A. Kazlauskas (1991). "Platelet-derived growth factor (PDGF) stimulates PDGF receptor subunit dimerization and intersubunit trans-phosphorylation." J Biol Chem **266**(14): 8987-8992.

Khoury-Haddad, H., N. Guttmann-Raviv, I. Ipenberg, D. Huggins, A. D. Jeyasekharan and N. Ayoub (2014). "PARP1-dependent recruitment of KDM4D histone demethylase to DNA damage sites promotes double-strand break repair." Proc Natl Acad Sci U S A **111**(7): E728-737.

Khoury-Haddad, H., P. T. Nadar-Ponniah, S. Awwad and N. Ayoub (2015). "The emerging role of lysine demethylases in DNA damage response: dissecting the recruitment mode of KDM4D/JMJD2D to DNA damage sites." Cell Cycle **14**(7): 950-958.

Kim, B. R., S. M. Dong, S. H. Seo, J. H. Lee, J. M. Lee, S. H. Lee and S. B. Rho (2014). "Lysyl oxidase-like 2 (LOXL2) controls tumor-associated cell proliferation through the interaction with MARCKSL1." Cell Signal **26**(9): 1765-1773.

Kim, T. D., S. Shin, W. L. Berry, S. Oh and R. Janknecht (2012). "The JMJD2A demethylase regulates apoptosis and proliferation in colon cancer cells." J Cell Biochem **113**(4): 1368-1376.

Kim, Y., Q. Lin, P. M. Glazer and Z. Yun (2009). "Hypoxic tumor microenvironment and cancer cell differentiation." Curr Mol Med **9**(4): 425-434.

Klipper-Aurbach, Y., M. Wasserman, N. Braunspiegel-Weintrob, D. Borstein, S. Peleg, S. Assa, M. Karp, Y. Benjamini, Y. Hochberg and Z. Laron (1995). "Mathematical formulae for the prediction of the residual beta cell function during the first two years of disease in children and adolescents with insulin-dependent diabetes mellitus." Med Hypotheses **45**(5): 486-490.

Klose, R. J., E. M. Kallin and Y. Zhang (2006). "JmjC-domain-containing proteins and histone demethylation." Nat Rev Genet **7**(9): 715-727.

Koh, S. A. and K. H. Lee (2015). "HGF mediated upregulation of lipocalin 2 regulates MMP9 through nuclear factor-kappaB activation." Oncol Rep **34**(4): 2179-2187.

Kouzarides, T. (2007). "Chromatin modifications and their function." Cell **128**(4): 693-705.

Krieg, A. J., E. B. Rankin, D. Chan, O. Razorenova, S. Fernandez and A. J. Giaccia (2010). "Regulation of the histone demethylase JMJD1A by hypoxia-inducible factor 1 alpha enhances hypoxic gene expression and tumor growth." Mol Cell Biol **30**(1): 344-353.

Krishnan, S. and R. C. Trievel (2013). "Structural and functional analysis of JMJD2D reveals molecular basis for site-specific demethylation among JMJD2 demethylases." Structure **21**(1): 98-108.

Kruidenier, L., C. W. Chung, Z. Cheng, J. Liddle, K. Che, G. Joberty, M. Bantscheff, C. Bountra, A. Bridges, H. Diallo, D. Eberhard, S. Hutchinson, E. Jones, R. Katso, M. Leveridge, P. K. Mander, J. Mosley, C. Ramirez-Molina, P. Rowland, C. J. Schofield, R. J. Sheppard, J. E. Smith, C. Swales, R. Tanner, P. Thomas, A. Tumber, G. Drewes, U. Oppermann, D. J. Patel, K. Lee and D. M. Wilson (2012). "A selective jumonji H3K27 demethylase inhibitor modulates the proinflammatory macrophage response." Nature **488**(7411): 404-408.

Krupp, M., J. U. Marquardt, U. Sahin, P. R. Galle, J. Castle and A. Teufel (2012). "RNA-Seq Atlas--a reference database for gene expression profiling in normal tissue by next-generation sequencing." Bioinformatics **28**(8): 1184-1185.

Kupershmit, I., H. Khoury-Haddad, S. W. Awwad, N. Guttmann-Raviv and N. Ayoub (2014). "KDM4C (GASC1) lysine demethylase is associated with mitotic chromatin and regulates chromosome segregation during mitosis." Nucleic Acids Res **42**(10): 6168-6182.

Kwon, M., S. J. Lee, Y. Wang, Y. Rybak, A. Luna, S. Reddy, A. Adem, B. T. Beaty, J. S. Condeelis and S. K. Libutti (2014). "Filamin A interacting protein 1-like inhibits WNT signaling and MMP expression to suppress cancer cell invasion and metastasis." Int J Cancer **135**(1): 48-60.

Labbe, R. M., A. Holowatyj and Z. Q. Yang (2013). "Histone lysine demethylase (KDM) subfamily 4: structures, functions and therapeutic potential." Am J Transl Res **6**(1): 1-15.

Langley, G. W., A. Brinko, M. Munzel, L. J. Walport, C. J. Schofield and R. J. Hopkinson (2016). "Analysis of JmjC Demethylase-Catalyzed Demethylation Using Geometrically-Constrained Lysine Analogues." ACS Chem Biol **11**(3): 755-762.

Lee, H. L., B. Yu, P. Deng, C. Y. Wang and C. Hong (2016). "Transforming Growth Factor-beta-Induced KDM4B Promotes Chondrogenic Differentiation of Human Mesenchymal Stem Cells." Stem Cells **34**(3): 711-719.

Lee, J., J. R. Thompson, M. V. Botuyan and G. Mer (2008). "Distinct binding modes specify the recognition of methylated histones H3K4 and H4K20 by JMJD2A-tudor." Nat Struct Mol Biol **15**(1): 109-111.

Lee, J. S., Y. Kim, I. S. Kim, B. Kim, H. J. Choi, J. M. Lee, H. J. Shin, J. H. Kim, J. Y. Kim, S. B. Seo, H. Lee, O. Binda, O. Gozani, G. L. Semenza, M. Kim, K. I. Kim, D. Hwang and S. H. Baek (2010). "Negative regulation of hypoxic responses via induced Reptin methylation." Mol Cell **39**(1): 71-85.

Lee, S. H., J. Kim, W. H. Kim and Y. M. Lee (2009). "Hypoxic silencing of tumor suppressor RUNX3 by histone modification in gastric cancer cells." Oncogene **28**(2): 184-194.

Leeper, K., R. Garcia, E. Swisher, B. Goff, B. Greer and P. Paley (2002). "Pathologic findings in prophylactic oophorectomy specimens in high-risk women." Gynecol Oncol **87**(1): 52-56.

Lengyel, E. (2010). "Ovarian cancer development and metastasis." Am J Pathol **177**(3): 1053-1064.

Li, J., L. Zhou, X. Chen and Y. Ba (2015). "Addition of bevacizumab to chemotherapy in patients with ovarian cancer: a systematic review and meta-analysis of randomized trials." Clin Transl Oncol.

Li, S., L. Wu, Q. Wang, Y. Li and X. Wang (2015). "KDM4B promotes epithelial-mesenchymal transition through up-regulation of ZEB1 in pancreatic cancer." Acta Biochim Biophys Sin (Shanghai) **47**(12): 997-1004.

Li, W., L. Zhao, W. Zang, Z. Liu, L. Chen, T. Liu, D. Xu and J. Jia (2011). "Histone demethylase JMJD2B is required for tumor cell proliferation and survival and is overexpressed in gastric cancer." Biochem Biophys Res Commun **416**(3-4): 372-378.

Li, X. and S. Dong (2015). "Histone demethylase JMJD2B and JMJD2C induce fibroblast growth factor 2: mediated tumorigenesis of osteosarcoma." Med Oncol **32**(3): 53.

Liao, J., F. Qian, N. Tchabo, P. Mhawech-Fauceglia, A. Beck, Z. Qian, X. Wang, W. J. Huss, S. B. Lele, C. D. Morrison and K. Odunsi (2014). "Ovarian cancer spheroid cells with stem cell-like properties contribute to tumor generation, metastasis and chemotherapy resistance through hypoxia-resistant metabolism." PLoS One **9**(1): e84941.

Ling, J. and R. Kumar (2012). "Crosstalk between NFkB and glucocorticoid signaling: a potential target of breast cancer therapy." Cancer Lett **322**(2): 119-126.

Liu, J. and U. A. Matulonis (2014). "New strategies in ovarian cancer: translating the molecular complexity of ovarian cancer into treatment advances." Clin Cancer Res **20**(20): 5150-5156.

Liu, L. and M. C. Simon (2004). "Regulation of transcription and translation by hypoxia." Cancer Biol Ther **3**(6): 492-497.

Liu, Z., X. Chen, S. Zhou, L. Liao, R. Jiang and J. Xu (2015). "The histone H3K9 demethylase Kdm3b is required for somatic growth and female reproductive function." Int J Biol Sci **11**(5): 494-507.

Liu, Z., M. G. Oyola, S. Zhou, X. Chen, L. Liao, J. C. Tien, S. K. Mani and J. Xu (2015). "Knockout of the Histone Demethylase Kdm3b Decreases Spermatogenesis and Impairs Male Sexual Behaviors." Int J Biol Sci **11**(12): 1447-1457.

Lu, C., M. M. Shahzad, M. Moreno-Smith, Y. G. Lin, N. B. Jennings, J. K. Allen, C. N. Landen, L. S. Mangala, G. N. Armaiz-Pena, R. Schmandt, A. M. Nick, R. L. Stone, R. B. Jaffe, R. L. Coleman and A. K. Sood (2010). "Targeting pericytes with a PDGF-B aptamer in human ovarian carcinoma models." Cancer Biol Ther **9**(3): 176-182.

Lu, C., P. H. Thaker, Y. G. Lin, W. Spannuth, C. N. Landen, W. M. Merritt, N. B. Jennings, R. R. Langley, D. M. Gershenson, G. D. Yancopoulos, L. M. Ellis, R. B. Jaffe, R. L. Coleman and A. K. Sood (2008). "Impact of vessel maturation on antiangiogenic therapy in ovarian cancer." Am J Obstet Gynecol **198**(4): 477 e471-479; discussion 477 e479-410.

Lu, J. W., Y. J. Ho, L. I. Lin, Y. C. Huang, K. T. Yeh, Y. H. Lin, Y. M. Lin and T. Y. Tzeng (2015). "JMJD2B as a potential diagnostic immunohistochemical marker for hepatocellular carcinoma: a tissue microarray-based study." Acta Histochem **117**(1): 14-19.

Lund, A. H. and M. van Lohuizen (2004). "Epigenetics and cancer." Genes Dev **18**(19): 2315-2335.

Luo, W., R. Chang, J. Zhong, A. Pandey and G. L. Semenza (2012). "Histone demethylase JMJD2C is a coactivator for hypoxia-inducible factor 1 that is required for breast cancer progression." Proc Natl Acad Sci U S A **109**(49): E3367-3376.

Luo, X., Y. Liu, S. Kubicek, J. Myllyharju, A. Tumber, S. Ng, K. H. Che, J. Podoll, T. D. Heightman, U. Oppermann, S. L. Schreiber and X. Wang (2011). "A selective inhibitor and probe of the cellular functions of Jumonji C domain-containing histone demethylases." J Am Chem Soc **133**(24): 9451-9456.

Madsen, C. V., K. D. Steffensen, D. A. Olsen, M. Waldstrom, C. H. Sogaard, I. Brandslund and A. Jakobsen (2012). "Serum platelet-derived growth factor and fibroblast growth factor in patients with benign and malignant ovarian tumors." Anticancer Res **32**(9): 3817-3825.

Maes, T., E. Carceller, J. Salas, A. Ortega and C. Buesa (2015). "Advances in the development of histone lysine demethylase inhibitors." Curr Opin Pharmacol **23**: 52-60.

Mallette, F. A., F. Mattiroli, G. Cui, L. C. Young, M. J. Hendzel, G. Mer, T. K. Sixma and S. Richard (2012). "RNF8- and RNF168-dependent degradation of KDM4A/JMJD2A triggers 53BP1 recruitment to DNA damage sites." EMBO J **31**(8): 1865-1878.

Marsh, D. J., J. S. Shah and A. J. Cole (2014). "Histones and their modifications in ovarian cancer - drivers of disease and therapeutic targets." Front Oncol **4**: 144.

Matei, D., S. Kelich, L. Cao, N. Menning, R. E. Emerson, J. Rao, M. H. Jeng and G. W. Sledge (2007). "PDGF BB induces VEGF secretion in ovarian cancer." Cancer Biol Ther **6**(12): 1951-1959.

McEvoy, L. M., S. A. O'Toole, C. D. Spillane, C. M. Martin, M. F. Gallagher, B. Stordal, G. Blackshields, O. Sheils and J. J. O'Leary (2015). "Identifying novel hypoxia-associated markers of chemoresistance in ovarian cancer." BMC Cancer **15**: 547.

Mei, L., H. Chen, D. M. Wei, F. Fang, G. J. Liu, H. Y. Xie, X. Wang, J. Zou, X. Han and D. Feng (2013). "Maintenance chemotherapy for ovarian cancer." Cochrane Database Syst Rev(6): CD007414.

Merritt, W. M., Y. G. Lin, W. A. Spannuth, M. S. Fletcher, A. A. Kamat, L. Y. Han, C. N. Landen, N. Jennings, K. De Geest, R. R. Langley, G. Villares, A. Sanguino, S. K. Lutgendorf, G. Lopez-Berestein, M. M. Bar-Eli and A. K. Sood (2008). "Effect of interleukin-8 gene silencing with liposome-encapsulated small interfering RNA on ovarian cancer cell growth." J Natl Cancer Inst **100**(5): 359-372.

Miyamoto, S., L. R. Ruhaak, C. Stroble, M. R. Salemi, B. Phinney, C. B. Lebrilla and G. S. Leiserowitz (2016). "Glycoproteomic Analysis of Malignant Ovarian Cancer Ascites Fluid Identifies Unusual Glycopeptides." J Proteome Res **15**(9): 3358-3376.

Mosammaparast, N. and Y. Shi (2010). "Reversal of histone methylation: biochemical and molecular mechanisms of histone demethylases." Annu Rev Biochem **79**: 155-179.

Mutch, D. G. and J. Prat (2014). "2014 FIGO staging for ovarian, fallopian tube and peritoneal cancer." Gynecol Oncol **133**(3): 401-404.

Naora, H. and D. J. Montell (2005). "Ovarian cancer metastasis: integrating insights from disparate model organisms." Nat Rev Cancer **5**(5): 355-366.

Ness, R. B. and C. Cottreau (1999). "Possible role of ovarian epithelial inflammation in ovarian cancer." J Natl Cancer Inst **91**(17): 1459-1467.

Nieman, K. M., H. A. Kenny, C. V. Penicka, A. Ladanyi, R. Buell-Gutbrod, M. R. Zillhardt, I. L. Romero, M. S. Carey, G. B. Mills, G. S. Hotamisligil, S. D. Yamada, M. E. Peter, K. Gwin and E. Lengyel (2011). "Adipocytes promote ovarian cancer metastasis and provide energy for rapid tumor growth." Nat Med **17**(11): 1498-1503.

Osada, R., A. Horiuchi, N. Kikuchi, J. Yoshida, A. Hayashi, M. Ota, Y. Katsuyama, G. Melillo and I. Konishi (2007). "Expression of hypoxia-inducible factor 1alpha, hypoxia-inducible factor 2alpha, and von Hippel-Lindau protein in epithelial ovarian neoplasms and allelic loss of von Hippel-Lindau gene: nuclear expression of hypoxia-inducible factor 1alpha is an independent prognostic factor in ovarian carcinoma." Hum Pathol **38**(9): 1310-1320.

Palomera-Sanchez, Z., A. Bucio-Mendez, V. Valadez-Graham, E. Reynaud and M. Zurita (2010). "Drosophila p53 is required to increase the levels of the dKDM4B demethylase after UV-induced DNA damage to demethylate histone H3 lysine 9." J Biol Chem **285**(41): 31370-31379.

Pawlus, M. R. and C. J. Hu (2013). "Enhanceosomes as integrators of hypoxia inducible factor (HIF) and other transcription factors in the hypoxic transcriptional response." Cell Signal **25**(9): 1895-1903.

Pedersen, M. T. and K. Helin (2010). "Histone demethylases in development and disease." Trends Cell Biol **20**(11): 662-671.

Peng, L., Y. L. Ran, H. Hu, L. Yu, Q. Liu, Z. Zhou, Y. M. Sun, L. C. Sun, J. Pan, L. X. Sun, P. Zhao and Z. H. Yang (2009). "Secreted LOXL2 is a novel therapeutic target that promotes gastric cancer metastasis via the Src/FAK pathway." Carcinogenesis **30**(10): 1660-1669.

Perez-Gracia, J. L. and E. M. Carrasco (2002). "Tamoxifen therapy for ovarian cancer in the adjuvant and advanced settings: systematic review of the literature and implications for future research." Gynecol Oncol **84**(2): 201-209.

Perez-Perri, J. I., J. M. Acevedo and P. Wappner (2011). "Epigenetics: new questions on the response to hypoxia." Int J Mol Sci **12**(7): 4705-4721.

Petrillo, M., C. Nero, G. Amadio, D. Gallo, A. Fagotti and G. Scambia (2016). "Targeting the hallmarks of ovarian cancer: The big picture." Gynecol Oncol **142**(1): 176-183.

Piek, J. M., P. J. van Diest, R. P. Zweemer, J. W. Jansen, R. J. Poort-Keesom, F. H. Menko, J. J. Gille, A. P. Jongsma, G. Pals, P. Kenemans and R. H. Verheijen (2001). "Dysplastic changes in prophylactically removed Fallopian tubes of women predisposed to developing ovarian cancer." J Pathol **195**(4): 451-456.

Pollard, P. J., C. Loenarz, D. R. Mole, M. A. McDonough, J. M. Gleadle, C. J. Schofield and P. J. Ratcliffe (2008). "Regulation of Jumonji-domain-containing histone demethylases by hypoxia-inducible factor (HIF)-1alpha." Biochem J **416**(3): 387-394.

Ponnaluri, V. K., D. T. Vavilala, S. Putty, W. G. Gutheil and M. Mukherji (2009). "Identification of non-histone substrates for JMJD2A-C histone demethylases." Biochem Biophys Res Commun **390**(2): 280-284.

Prat, J. (2012). "New insights into ovarian cancer pathology." Ann Oncol **23 Suppl 10**: x111-117.

Puiffe, M. L., C. Le Page, A. Filali-Mouhim, M. Zietarska, V. Ouellet, P. N. Tonin, M. Chevrette, D. M. Provencher and A. M. Mes-Masson (2007). "Characterization of ovarian cancer ascites on cell invasion, proliferation, spheroid formation, and gene expression in an in vitro model of epithelial ovarian cancer." Neoplasia **9**(10): 820-829.

Qiu, M. T., Q. Fan, Z. Zhu, S. Y. Kwan, L. Chen, J. H. Chen, Z. L. Ying, Y. Zhou, W. Gu, L. H. Wang, W. W. Cheng, J. Zeng, X. P. Wan, S. C. Mok, K. K. Wong and W. Bao (2015). "KDM4B and KDM4A promote endometrial cancer progression by regulating androgen receptor, c-myc, and p27kip1." Oncotarget **6**(31): 31702-31720.

Qu, B., O. Liu, X. Fang, H. Zhang, Y. Wang, H. Quan, J. Zhang, J. Zhou, J. Zuo, J. Tang and Z. Tang (2014). "Distal-less homeobox 2 promotes the osteogenic differentiation potential of stem cells from apical papilla." Cell Tissue Res **357**(1): 133-143.

Rai, G., A. Kawamura, A. Tumber, Y. Liang, J. L. Vogel, J. H. Arbuckle, N. R. Rose, T. S. Dexheimer, T. L. Foley, O. N. King, A. Quinn, B. T. Mott, C. J. Schofield, U. Oppermann, A. Jadhav, A. Simeonov, T. M. Kristie and D. J. Maloney (2010). Discovery of ML324, a JMJD2 demethylase inhibitor with demonstrated antiviral activity. Probe Reports from the NIH Molecular Libraries Program. Bethesda (MD).

Rankin, E. B., K. C. Fuh, T. E. Taylor, A. J. Krieg, M. Musser, J. Yuan, K. Wei, C. J. Kuo, T. A. Longacre and A. J. Giaccia (2010). "AXL is an essential factor and therapeutic target for metastatic ovarian cancer." Cancer Res **70**(19): 7570-7579.

Resnicoff, M., D. Ambrose, D. Coppola and R. Rubin (1993). "Insulin-like growth factor-1 and its receptor mediate the autocrine proliferation of human ovarian carcinoma cell lines." Lab Invest **69**(6): 756-760.

Rotili, D. and A. Mai (2011). "Targeting Histone Demethylases: A New Avenue for the Fight against Cancer." Genes Cancer **2**(6): 663-679.

Rutkute, K. and M. N. Nikolova-Karakashian (2007). "Regulation of insulin-like growth factor binding protein-1 expression during aging." Biochem Biophys Res Commun **361**(2): 263-269.

Sanchez-Fernandez, E. M., H. Tarhonskaya, K. Al-Qahtani, R. J. Hopkinson, J. S. McCullagh, C. J. Schofield and E. Flashman (2013). "Investigations on the oxygen dependence of a 2-oxoglutarate histone demethylase." Biochem J **449**(2): 491-496.

Sandhu, S. K., W. R. Schelman, G. Wilding, V. Moreno, R. D. Baird, S. Miranda, L. Hylands, R. Riisnaes, M. Forster, A. Omlin, N. Kreischer, K. Thway, H. Gevensleben, L. Sun, J. Loughney, M. Chatterjee, C. Toniatti, C. L. Carpenter, R. Iannone, S. B. Kaye, J. S. de Bono and R. M. Wenham (2013). "The poly(ADP-ribose) polymerase inhibitor niraparib (MK4827) in BRCA mutation carriers and patients with sporadic cancer: a phase 1 dose-escalation trial." Lancet Oncol **14**(9): 882-892.

Santin, A. D., F. Zhan, S. Bellone, M. Palmieri, S. Cane, E. Bignotti, S. Anfossi, M. Gokden, D. Dunn, J. J. Roman, T. J. O'Brien, E. Tian, M. J. Cannon, J. Shaughnessy, Jr. and S. Pecorelli (2004). "Gene expression profiles in primary ovarian serous papillary tumors and normal ovarian epithelium: identification of candidate molecular markers for ovarian cancer diagnosis and therapy." Int J Cancer **112**(1): 14-25.

Schito, L., S. Rey, M. Tafani, H. Zhang, C. C. Wong, A. Russo, M. A. Russo and G. L. Semenza (2012). "Hypoxia-inducible factor 1-dependent expression of platelet-derived growth factor B promotes lymphatic metastasis of hypoxic breast cancer cells." Proc Natl Acad Sci U S A **109**(40): E2707-2716.

Schmahl, J., C. S. Raymond and P. Soriano (2007). "PDGF signaling specificity is mediated through multiple immediate early genes." Nat Genet **39**(1): 52-60.

Schuebel, K., M. Gitik, K. Domschke and D. Goldman (2016). "Making Sense of Epigenetics." Int J Neuropsychopharmacol.

Schwartz, P. E., J. T. Chambers, E. I. Kohorn, S. K. Chambers, H. Weitzman, I. M. Voynick, N. MacLusky and F. Naftolin (1989). "Tamoxifen in combination with cytotoxic chemotherapy in advanced epithelial ovarian cancer. A prospective randomized trial." Cancer **63**(6): 1074-1078.

Seeber, L. M. and P. J. van Diest (2012). "Epigenetics in ovarian cancer." Methods Mol Biol **863**: 253-269.

Sekirnik, R., N. R. Rose, A. Thalhammer, P. T. Seden, J. Mecinovic and C. J. Schofield (2009). "Inhibition of the histone lysine demethylase JMJD2A by ejection of structural Zn(II)." Chem Commun (Camb)(42): 6376-6378.

Semenza, G. L. (2011). "Oxygen sensing, homeostasis, and disease." N Engl J Med **365**(6): 537-547.

Semenza, G. L. (2012). "Hypoxia-inducible factors: mediators of cancer progression and targets for cancer therapy." Trends Pharmacol Sci **33**(4): 207-214.

Shi, L., L. Sun, Q. Li, J. Liang, W. Yu, X. Yi, X. Yang, Y. Li, X. Han, Y. Zhang, C. Xuan, Z. Yao and Y. Shang (2011). "Histone demethylase JMJD2B coordinates H3K4/H3K9 methylation and promotes hormonally responsive breast carcinogenesis." Proc Natl Acad Sci U S A **108**(18): 7541-7546.

Shin, S. and R. Janknecht (2007). "Diversity within the JMJD2 histone demethylase family." Biochem Biophys Res Commun **353**(4): 973-977.

Shmakova, A., M. Batie, J. Druker and S. Rocha (2014). "Chromatin and oxygen sensing in the context of JmjC histone demethylases." Biochem J **462**(3): 385-395.

Siegel, R. L., K. D. Miller and A. Jemal (2015). "Cancer statistics, 2015." CA Cancer J Clin **65**(1): 5-29.

Simon, M. C. and B. Keith (2008). "The role of oxygen availability in embryonic development and stem cell function." Nat Rev Mol Cell Biol **9**(4): 285-296.

Sisley, K., D. W. Cottam, I. G. Rennie, M. A. Parsons, A. M. Potter, C. W. Potter and R. C. Rees (1992). "Non-random abnormalities of chromosomes 3, 6, and 8 associated with posterior uveal melanoma." Genes Chromosomes Cancer **5**(3): 197-200.

Smolle, E., V. Taucher and J. Haybaeck (2014). "Malignant ascites in ovarian cancer and the role of targeted therapeutics." Anticancer Res **34**(4): 1553-1561.

Span, P. N. and J. Bussink (2015). "Biology of hypoxia." Semin Nucl Med **45**(2): 101-109.

Stronach, E. A., P. Cunnea, C. Turner, T. Guney, R. Aiyappa, S. Jeyapalan, C. H. de Sousa, A. Browne, N. Magdy, J. B. Studd, R. Sriraksa, H. Gabra and M. El-Bahrawy (2015). "The role of interleukin-8 (IL-

8) and IL-8 receptors in platinum response in high grade serous ovarian carcinoma." Oncotarget **6**(31): 31593-31603.

Swenson-Fields, K. I., C. J. Vivian, S. M. Salah, J. D. Peda, B. M. Davis, N. van Rooijen, D. P. Wallace and T. A. Fields (2013). "Macrophages promote polycystic kidney disease progression." Kidney Int **83**(5): 855-864.

Takeuchi, T., Y. Yamazaki, Y. Katoh-Fukui, R. Tsuchiya, S. Kondo, J. Motoyama and T. Higashinakagawa (1995). "Gene trap capture of a novel mouse gene, jumonji, required for neural tube formation." Genes Dev **9**(10): 1211-1222.

Tan, M. K., H. J. Lim and J. W. Harper (2011). "SCF(FBXO22) regulates histone H3 lysine 9 and 36 methylation levels by targeting histone demethylase KDM4A for ubiquitin-mediated proteasomal degradation." Mol Cell Biol **31**(18): 3687-3699.

Tang, Q. Q., T. C. Otto and M. D. Lane (2003). "Mitotic clonal expansion: a synchronous process required for adipogenesis." Proc Natl Acad Sci U S A **100**(1): 44-49.

Tausendschon, M., N. Dehne and B. Brune (2011). "Hypoxia causes epigenetic gene regulation in macrophages by attenuating Jumonji histone demethylase activity." Cytokine **53**(2): 256-262.

Tejada, M. L., L. Yu, J. Dong, K. Jung, G. Meng, F. V. Peale, G. D. Frantz, L. Hall, X. Liang, H. P. Gerber and N. Ferrara (2006). "Tumor-driven paracrine platelet-derived growth factor receptor alpha signaling is a key determinant of stromal cell recruitment in a model of human lung carcinoma." Clin Cancer Res **12**(9): 2676-2688.

Terry, K. L., S. S. Tworoger, M. A. Gates, D. W. Cramer and S. E. Hankinson (2009). "Common genetic variation in IGF1, IGFBP1 and IGFBP3 and ovarian cancer risk." Carcinogenesis **30**(12): 2042-2046.

Thalhammer, A., J. Mecinovic, C. Loenarz, A. Tumber, N. R. Rose, T. D. Heightman and C. J. Schofield (2011). "Inhibition of the histone demethylase JMJD2E by 3-substituted pyridine 2,4-dicarboxylates." Org Biomol Chem **9**(1): 127-135.

Thinnes, C. C., K. S. England, A. Kawamura, R. Chowdhury, C. J. Schofield and R. J. Hopkinson (2014). "Targeting histone lysine demethylases - progress, challenges, and the future." Biochim Biophys Acta **1839**(12): 1416-1432.

Toyokawa, G., H. S. Cho, Y. Iwai, M. Yoshimatsu, M. Takawa, S. Hayami, K. Maejima, N. Shimizu, H. Tanaka, T. Tsunoda, H. I. Field, J. D. Kelly, D. E. Neal, B. A. Ponder, Y. Maehara, Y. Nakamura and R. Hamamoto (2011). "The histone demethylase JMJD2B plays an essential role in human carcinogenesis through positive regulation of cyclin-dependent kinase 6." Cancer Prev Res (Phila) **4**(12): 2051-2061.

Trojer, P., J. Zhang, M. Yonezawa, A. Schmidt, H. Zheng, T. Jenuwein and D. Reinberg (2009). "Dynamic Histone H1 Isotype 4 Methylation and Demethylation by Histone Lysine Methyltransferase G9a/KMT1C and the Jumonji Domain-containing JMJD2/KDM4 Proteins." J Biol Chem **284**(13): 8395-8405.

Tsai, Y. P. and K. J. Wu (2012). "Hypoxia-regulated target genes implicated in tumor metastasis." J Biomed Sci **19**: 102.

Tsurumi, A., P. Dutta, R. Shang, S. J. Yan and W. X. Li (2013). "Drosophila Kdm4 demethylases in histone H3 lysine 9 demethylation and ecdysteroid signaling." Sci Rep **3**: 2894.

Ueda, Y., T. Enomoto, T. Kimura, T. Miyatake, K. Yoshino, M. Fujita and T. Kimura (2010). "Serum biomarkers for early detection of gynecologic cancers." Cancers (Basel) **2**(2): 1312-1327.

Uribe, R. A., A. L. Buzzi, M. E. Bronner and P. H. Strobl-Mazzulla (2015). "Histone demethylase KDM4B regulates otic vesicle invagination via epigenetic control of Dlx3 expression." J Cell Biol **211**(4): 815-827.

Van Rechem, C., J. C. Black, T. Abbas, A. Allen, C. A. Rinehart, G. C. Yuan, A. Dutta and J. R. Whetstine (2011). "The SKP1-Cul1-F-box and leucine-rich repeat protein 4 (SCF-FbxL4) ubiquitin ligase regulates lysine demethylase 4A (KDM4A)/Jumonji domain-containing 2A (JMJD2A) protein." J Biol Chem **286**(35): 30462-30470.

Vang, R., M. Shih Ie and R. J. Kurman (2009). "Ovarian low-grade and high-grade serous carcinoma: pathogenesis, clinicopathologic and molecular biologic features, and diagnostic problems." Adv Anat Pathol **16**(5): 267-282.

Varier, R. A. and H. T. Timmers (2011). "Histone lysine methylation and demethylation pathways in cancer." Biochim Biophys Acta **1815**(1): 75-89.

Vaughan, S., J. I. Coward, R. C. Bast, Jr., A. Berchuck, J. S. Berek, J. D. Brenton, G. Coukos, C. C. Crum, R. Drapkin, D. Etemadmoghadam, M. Friedlander, H. Gabra, S. B. Kaye, C. J. Lord, E. Lengyel, D. A. Levine, I. A. McNeish, U. Menon, G. B. Mills, K. P. Nephew, A. M. Oza, A. K. Sood, E. A. Stronach, H. Walczak, D. D. Bowtell and F. R. Balkwill (2011). "Rethinking ovarian cancer: recommendations for improving outcomes." Nat Rev Cancer **11**(10): 719-725.

Vinci, M., S. Gowan, F. Boxall, L. Patterson, M. Zimmermann, W. Court, C. Lomas, M. Mendiola, D. Hardisson and S. A. Eccles (2012). "Advances in establishment and analysis of three-dimensional tumor spheroid-based functional assays for target validation and drug evaluation." BMC Biol **10**: 29.

Volarevic, V., S. Bojic, J. Nurkovic, A. Volarevic, B. Ljujic, N. Arsenijevic, M. Lako and M. Stojkovic (2014). "Stem cells as new agents for the treatment of infertility: current and future perspectives and challenges." Biomed Res Int **2014**: 507234.

Wagner, E. K., N. Nath, R. Flemming, J. B. Feltenberger and J. M. Denu (2012). "Identification and characterization of small molecule inhibitors of a plant homeodomain finger." Biochemistry **51**(41): 8293-8306.

Wang, J., M. Zhang, Y. Zhang, Z. Kou, Z. Han, D. Y. Chen, Q. Y. Sun and S. Gao (2010). "The histone demethylase JMJD2C is stage-specifically expressed in preimplantation mouse embryos and is required for embryonic development." Biol Reprod **82**(1): 105-111.

Wang, L., J. Chang, D. Varghese, M. Dellinger, S. Kumar, A. M. Best, J. Ruiz, R. Bruick, S. Pena-Llopis, J. Xu, D. J. Babinski, D. E. Frantz, R. A. Brekken, A. M. Quinn, A. Simeonov, J. Easmon and E. D. Martinez (2013). "A small molecule modulates Jumonji histone demethylase activity and selectively inhibits cancer growth." Nat Commun **4**: 2035.

Wang, L., H. Chen, M. H. Pourgholami, J. Beretov, J. Hao, H. Chao, A. C. Perkins, J. H. Kearsley and Y. Li (2011). "Anti-MUC1 monoclonal antibody (C595) and docetaxel markedly reduce tumor burden and ascites, and prolong survival in an in vivo ovarian cancer model." PLoS One **6**(9): e24405.

Wang, L., J. Ma, F. Liu, Q. Yu, G. Chu, A. C. Perkins and Y. Li (2007). "Expression of MUC1 in primary and metastatic human epithelial ovarian cancer and its therapeutic significance." Gynecol Oncol **105**(3): 695-702.

Wang, L., Y. Mao, G. Du, C. He and S. Han (2015). "Overexpression of JARID1B is associated with poor prognosis and chemotherapy resistance in epithelial ovarian cancer." Tumour Biol **36**(4): 2465-2472.

Wang, Y., R. C. Xu, X. L. Zhang, X. L. Niu, Y. Qu, L. Z. Li and X. Y. Meng (2012). "Interleukin-8 secretion by ovarian cancer cells increases anchorage-independent growth, proliferation, angiogenic potential, adhesion and invasion." Cytokine **59**(1): 145-155.

Weberpals, J. I., M. Koti and J. A. Squire (2011). "Targeting genetic and epigenetic alterations in the treatment of serous ovarian cancer." Cancer Genet **204**(10): 525-535.

Welford, S. M., B. Bedogni, K. Gradin, L. Poellinger, M. B. Powell and A. J. Giaccia (2006). "HIF1 alpha delays premature senescence through the activation of MIF." Genes & Development **20**(24): 3366-3371.

Welford, S. M. and A. J. Giaccia (2011). "Hypoxia and senescence: the impact of oxygenation on tumor suppression." Mol Cancer Res **9**(5): 538-544.

Wellmann, S., M. Bettkober, A. Zelmer, K. Seeger, M. Faigle, H. K. Eltzschig and C. Buhrer (2008). "Hypoxia upregulates the histone demethylase JMJD1A via HIF-1." Biochem Biophys Res Commun **372**(4): 892-897.

Wen, L., Y. Chen, L. L. Zeng, F. Zhao, R. Li, Y. Liu and C. Zhang (2012). "Triptolide induces cell-cycle arrest and apoptosis of human multiple myeloma cells in vitro via altering expression of histone demethylase LSD1 and JMJD2B." Acta Pharmacol Sin **33**(1): 109-119.

West, D. C., D. Pan, E. Y. Tonsing-Carter, K. M. Hernandez, C. F. Pierce, S. C. Styke, K. R. Bowie, T. I. Garcia, M. Kocherginsky and S. D. Conzen (2016). "GR and ER co-activation alters the expression of differentiation genes and associates with improved ER+ breast cancer outcome." Mol Cancer Res.

Whetstine, J. R., A. Nottke, F. Lan, M. Huarte, S. Smolikov, Z. Chen, E. Spooner, E. Li, G. Zhang, M. Colaiacovo and Y. Shi (2006). "Reversal of histone lysine trimethylation by the JMJD2 family of histone demethylases." Cell **125**(3): 467-481.

Woelber, L., V. Mueller, C. Eulenburg, J. Schwarz, W. Carney, F. Jaenicke, K. Milde-Langosch and S. Mahner (2010). "Serum carbonic anhydrase IX during first-line therapy of ovarian cancer." Gynecol Oncol **117**(2): 183-188.

Xia, X., M. E. Lemieux, W. Li, J. S. Carroll, M. Brown, X. S. Liu and A. L. Kung (2009). "Integrative analysis of HIF binding and transactivation reveals its role in maintaining histone methylation homeostasis." Proc Natl Acad Sci U S A **106**(11): 4260-4265.

Xia, Y., H. K. Choi and K. Lee (2012). "Recent advances in hypoxia-inducible factor (HIF)-1 inhibitors." Eur J Med Chem **49**: 24-40.

Xu, W., H. Yang, Y. Liu, Y. Yang, P. Wang, S. H. Kim, S. Ito, C. Yang, P. Wang, M. T. Xiao, L. X. Liu, W. Q. Jiang, J. Liu, J. Y. Zhang, B. Wang, S. Frye, Y. Zhang, Y. H. Xu, Q. Y. Lei, K. L. Guan, S. M. Zhao and Y. Xiong (2011). "Oncometabolite 2-hydroxyglutarate is a competitive inhibitor of alpha-ketoglutarate-dependent dioxygenases." Cancer Cell **19**(1): 17-30.

Yang, J., A. M. AlTahan, D. Hu, Y. Wang, P. H. Cheng, C. L. Morton, C. Qu, A. C. Nathwani, J. M. Shohet, T. Fotsis, J. Koster, R. Versteeg, H. Okada, A. L. Harris and A. M. Davidoff (2015). "The role of histone demethylase KDM4B in Myc signaling in neuroblastoma." J Natl Cancer Inst **107**(6): djv080.

Yang, J., A. M. Jubb, L. Pike, F. M. Buffa, H. Turley, D. Baban, R. Leek, K. C. Gatter, J. Ragoussis and A. L. Harris (2010). "The histone demethylase JMJD2B is regulated by estrogen receptor alpha and hypoxia, and is a key mediator of estrogen induced growth." Cancer Res **70**(16): 6456-6466.

Yang, L., C. Lin, W. Liu, J. Zhang, K. A. Ohgi, J. D. Grinstein, P. C. Dorrestein and M. G. Rosenfeld (2011). "ncRNA- and Pc2 methylation-dependent gene relocation between nuclear structures mediates gene activation programs." Cell **147**(4): 773-788.

Yang, Z. Q., I. Imoto, Y. Fukuda, A. Pimkhaokham, Y. Shimada, M. Imamura, S. Sugano, Y. Nakamura and J. Inazawa (2000). "Identification of a novel gene, GASC1, within an amplicon at 9p23-24 frequently detected in esophageal cancer cell lines." Cancer Res **60**(17): 4735-4739.

Ye, L., Z. Fan, B. Yu, J. Chang, K. Al Hezaimi, X. Zhou, N. H. Park and C. Y. Wang (2012). "Histone demethylases KDM4B and KDM6B promotes osteogenic differentiation of human MSCs." Cell Stem Cell **11**(1): 50-61.

Yin, L., F. Fang, X. Song, Y. Wang, G. Huang, J. Su, N. Hui and J. Lu (2016). "The pro-adhesive and pro-survival effects of glucocorticoid in human ovarian cancer cells." J Mol Endocrinol **57**(1): 61-72.

Yoneda, J., H. Kuniyasu, M. A. Crispens, J. E. Price, C. D. Bucana and I. J. Fidler (1998). "Expression of angiogenesis-related genes and progression of human ovarian carcinomas in nude mice." J Natl Cancer Inst **90**(6): 447-454.

Yoshioka, H., J. R. McCarrey and Y. Yamazaki (2009). "Dynamic nuclear organization of constitutive heterochromatin during fetal male germ cell development in mice." Biol Reprod **80**(4): 804-812.

Young, L. C., D. W. McDonald and M. J. Hendzel (2013). "Kdm4b histone demethylase is a DNA damage response protein and confers a survival advantage following gamma-irradiation." J Biol Chem **288**(29): 21376-21388.

Zhang, D., H. G. Yoon and J. Wong (2005). "JMJD2A is a novel N-CoR-interacting protein and is involved in repression of the human transcription factor achaete scute-like homologue 2 (ASCL2/Hash2)." Mol Cell Biol **25**(15): 6404-6414.

Zhang, L., A. Vlad, C. Milcarek and O. J. Finn (2013). "Human mucin MUC1 RNA undergoes different types of alternative splicing resulting in multiple isoforms." Cancer Immunol Immunother **62**(3): 423-435.

Zhang, W., P. Ni, C. Mou, Y. Zhang, H. Guo, T. Zhao, Y. H. Loh and L. Chen (2016). "Cops2 promotes pluripotency maintenance by Stabilizing Nanog Protein and Repressing Transcription." Sci Rep **6**: 26804.

Zhao, L., W. Li, W. Zang, Z. Liu, X. Xu, H. Yu, Q. Yang and J. Jia (2013). "JMJD2B Promotes Epithelial-Mesenchymal Transition by Cooperating with beta-Catenin and Enhances Gastric Cancer Metastasis." Clin Cancer Res.

Zhao, L., W. Li, W. Zang, Z. Liu, X. Xu, H. Yu, Q. Yang and J. Jia (2013). "JMJD2B promotes epithelial-mesenchymal transition by cooperating with beta-catenin and enhances gastric cancer metastasis." Clin Cancer Res **19**(23): 6419-6429.

Zheng, H., L. Chen, W. J. Pledger, J. Fang and J. Chen (2014). "p53 promotes repair of heterochromatin DNA by regulating JMJD2b and SUV39H1 expression." Oncogene **33**(6): 734-744.